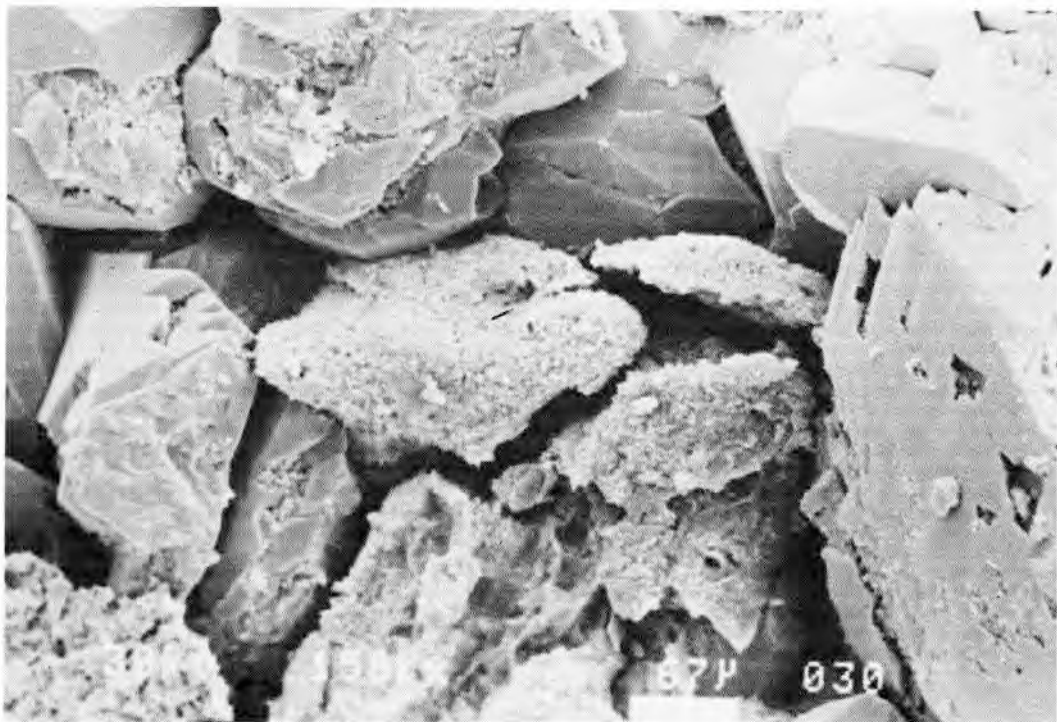


Volume 18 Number 1 June 1987

# GEOTECHNICAL ENGINEERING

*Journal of*  
SOUTHEAST ASIAN GEOTECHNICAL SOCIETY

*Sponsored by*  
ASIAN INSTITUTE OF TECHNOLOGY



# GEOTECHNICAL ENGINEERING

VOLUME 18 NUMBER 1 JUNE 1987

<b>Papers :</b>	<b>Page</b>
<b>Assessment of Singapore Rocks for Concrete Aggregate</b> M. A. AZIZ & S.D. RAMASWAMY . . . . .	1
<b>Theoretical Analysis of a Nonlinear Theory of Consolidation</b> R.M. ARENICZ & R.N. CHOWDHURY . . . . .	15
<b>Integrity and Uplift Testing of Piles in a Rock Filled Reclamation</b> G.L. EVANS, P.P. WONG & H. SANDERS . . . . .	43
<b>Improvement of Dispersive Soils by Mixing with Bangkok Clay or Bentonite</b> D.T. BERGADO & K.Y. KANG . . . . .	65
<b>Strength of Sandstone in Saturated and Partially Saturated Conditions</b> K.S. RAO, G. VENKATAPPA RAO & T. RAMAMURTHY . . . . .	99
<b>Closure :</b>	
<b>Erratum</b> . . . . .	129
<b>Conference News</b> . . . . .	131
<b>Announcements</b> . . . . .	135
<b>S.I. Units and Symbols</b> . . . . .	139

## CHAI MUKTABHANT

1917-1987



On 24th May 1987, Dr. Chai Muktabhant passed away in hospital after ailing for nearly a month under intensive care following surgery. His death comes as a tragic personal loss, not only to his family, but to the entire geotechnical community especially those in S.E. Asia and Thailand. For us he will remain as an example of goodness on, a man, a friend, an academic and a professional. Dr. Chai is survived by his wife, son and daughter.

The following excerpts have been taken from "Who is who in Thailand--1977" and the Citation of the Award of an Honorary

Doctorate Degree to him in 1986 as published in the June 1986 issue of the Geotechnical Engineering Journal.

Dr. Chai was born on 6th July 1917 in Bangkok. He was educated in Dhebsirindr School till 1934 and earned his Bachelors Degree in Civil Engineering from Chulalongkorn University in 1938, Master's degree in 1946 and an LL.B Degree in 1948. Dr. Chai earned another Master's Degree from Yale University in 1950 and a D.Sc. Degree from University of Michigan, Ann Arbor, Michigan, U.S.A. in 1953.

Dr. Chai is well known in Thailand and in the region as an expert in soil mechanics and foundation engineering, and, above all, the credit for introducing soil mechanics and foundation engineering in the undergraduate curriculum of the Chulalongkorn University and indeed in Thailand should go to Dr. Chai. He joined Chulalongkorn University in 1959 as an Assistant Professor and gradually worked up the ladder and became the Dean of Engineering in 1973. Dr. Chai received an honorary doctorate degree from

Chulalongkorn University in 1967 for his outstanding contribution as an educationist in engineering in Thailand.

As a founding Council Member of the Southeast Asian Geotechnical Society, Dr. Chai has always been unanimously elected to the Council from 1967 to date. His contribution and wisdom in maintaining the harmony among the members of the Society, and his personal contribution to the advancement of the subject, particularly in Thailand and in S.E. Asia in general, is worthy of praise.

In addition to his academic and professional contributions, Dr. Chai has also been very active in many spheres of community life and served as a member of the Task Group to preserve the Temple of Dawn and the Marble Temple. As a Fellow of Applied Science of the Royal Science Institute of Thailand, and as the President in the Engineering Field of the Industrial Research Division of the National Research Council of Thailand, Dr. Chai has often been requested to advise the Royal Thai government on numerous development projects.

Dr. Chai Muktabhant is one of the key persons in the earlier years of the establishment of the SEATO Graduate School of Engineering -- the predecessor institution of what is presently the Asian Institute of Technology (AIT). Dr. Chai Muktabhant received an Honorary Doctoral Degree from AIT in 1986 for his active involvement in planning the curriculum, and the staff in the difficult period of its formative years.

Those who knew Dr. Chai Muktabhant very closely always admired his extreme modesty, which displayed a total absence of pretension. Dr. Chai is a unique and respected educationist. In recognition of his outstanding contribution and services to the entire Thai community, Dr. Chai was awarded the Knight Grand Cordon (Special Class) of the Most Noble Order of the Crown of Thailand.

**(A.S. Balasubramaniam)**

**25th May 1987.**

**ASB : vc**



## ASSESSMENT OF SINGAPORE ROCKS FOR CONCRETE AGGREGATE

M.A. AZIZ\* and S.D. RAMASWAMY\*

### SYNOPSIS

Due to the increasing expansion of road systems, housing estates, commercial and industrial buildings, harbour facilities and other forms of concrete construction throughout Singapore, problems often arise concerning the supply of suitable rock aggregates for the production of good quality concrete. In view of this, the sensible and judicious selection of rock aggregates for the production of concrete is an economic necessity in Singapore. This paper presents the results of investigations carried out on various types of Singapore rocks in order to assess their suitability for making aggregates to produce good quality durable concrete for both onshore and offshore usage.

### INTRODUCTION

Proper selection of rock aggregates for use in concrete is of vital importance. Since the aggregate occupies about 60 to 70% of the volume of concrete, the aggregates in good quality concrete must be strong, sound and durable. But natural rock aggregates sometimes contain many deleterious substances which are very harmful to concrete structures (MCINTOSH, 1957; NEVILLE, 1975; JACKSON, 1977). Damage to concrete structures due to rock aggregates sensitive to alkalis is not uncommon. The variants of silica and silicate produced when siliceous rock aggregates react with alkalis inflict considerable damage to concrete. These alkali-aggregate reactions may cause damage to concrete even in the absence of external aggressive environmental media; the damage results purely from the use of unsound rock aggregates (NEVILLE, 1975; ORCHARD, 1976). Volume-unstable rock aggregates can cause concrete to expand and crack, and rock aggregates contaminated with sulphide, sulphate or organic contaminants can induce corrosion to both plain and reinforced concrete structures (BICZOK, 1972; NEVILLE, 1975).

Aggregate is generally viewed as an inert material dispersed throughout the cement paste, and used largely for economic reasons. But in fact, aggregate is not truly inert; its physical characteristics, and in some cases its chemical composition, affect to a varying degree the properties of concrete

---

\* Associate Professors, Department of Civil Engineering, National University of Singapore, Singapore.

in both plastic and hardened states, and thereby influence greatly the structural performance of concrete (NEVILLE, 1975; JACKSON, 1977; AZIZ & RAMASWAMY, 1970). Therefore, not only may the aggregate limit the strength of concrete, but it may also greatly affect the durability and structural performance of concrete. Aggregate is comparatively cheaper than cement, and it is therefore economical to use as much of the former and as little of the latter as possible. But economy is not the only reason for using aggregate in concrete; it confers considerable technical advantages on concrete, producing higher volume stability and better durability than cement paste alone.

In Singapore, problems are arising concerning the supply of suitable aggregates for use in concrete for various types of construction (AZIZ & RAMASWAMY, 1970). In view of this, proper selection of rocks for concrete aggregate is an economic necessity. The selection of rocks for concrete aggregate depends mainly upon the results of mechanical property tests (McINTOSH, 1957; HARTLEY, 1974). The criterion for good aggregate is that it should produce the desired properties in both the fresh and hardened concrete. In testing aggregates, it is important that a truly representative sample is used (BSI, 1975; ORCHARD, 1976). The properties of aggregate known to have a significant effect on concrete durability are its strength, deformation, toughness and hardness, volume change, porosity and absorption, specific gravity, shape and surface texture, grading, chemical reactivity, thermal behaviour, and resistance to attack by aggressive environmental factors (BICZOK, 1972; NEVILLE, 1975; JACKSON, 1977; and PITTS, 1984a, 1984b).

#### SINGAPORE ROCK TYPES

Rocks of Singapore primarily consist of four solid series, as shown in Figure 1 (PUBLIC WORKS DEPT. SINGAPORE, 1976; PITTS, 1984a, 1984b; RAMASWAMY, 1986). These are:

- Jurong Formation - Upper Triassic, Lower and Middle Jurassic
- Gombak Norite - Upper Palaeozoic
- Bukit Timah Granite - Lower and Middle Triassic
- Sajahat Formation - Lower Palaeozoic

A fair conception of the distribution and characteristics of rock types in Singapore has emerged from recent investigations by the authors and others (PITTS, 1984a, 1984b; and RAMASWAMY, 1986).

The Jurong formation consists of sedimentary rocks belonging to late Triassic and Lower to Middle Jurassic ages. The rock types consist of

## SINGAPORE AGGREGATES

conglomerates, sandstones and shales. The Sajahat formation is known to exist over a small area only. Rocks of basic composition forming the Gombak group have intruded into the Sajahat formation. These intrusions are primarily gabbroic and noritic rocks. Both these series are intruded in turn by a more acid sequence of granites. The plutonic rocks are intruded by small dykes of both doleritic and aplitic composition (PITTS, 1984a). These plutonic rocks are quarried extensively for use in construction. The granites in particular produce high class aggregates for use in road construction and concrete.

The basic geological deposits of Singapore, shown in Figure 1, are composed of igneous and sedimentary rocks and alluvium, both old and recent. Each group occurs in well defined areas in a distinct type of terrain. All sedimentary rocks (mainly shales) occur in the south, south-eastern and south-western parts of Singapore, Pulau Tekong and a group of southern islands. The term shale is normally used for all weak sedimentary rocks which encompass the central Singapore granite, lying west of the Pongol-Siglap line and the Changi-Pulau Ubin granite. The term granite is used in a general sense for the entire family of acid rocks including granite, adamellite, microgranite, and the acid and intermediate hybrids, mainly of granodioritic and dioritic composition, resulting from the assimilation of basic rocks. Other types of rocks such as norite, gabbro and noritic gabbro are also found to be exposed at Bukit Panjang and Bukit Gombak. Analysis of some Singapore rocks is given in Table 1 (PUBLIC WORKS DEPT. SINGAPORE, 1976).

### TESTING OF SINGAPORE ROCKS AND AGGREGATES

Rock samples were collected from various locations in Singapore, following the specifications laid down in BS 812:1975 (BSI, 1975). A summary of test results showing the physical properties of these rocks is given in Table 2.

It is observed from Table 2 that the physical properties of various acid rocks (granite, granodiorite, microgranite, dolerite and adamellite) are similar and equally acceptable. Basic rock types like norite, gabbro, and andesite exhibit distinctly inferior quality as compared to those of the acid group. Not surprisingly, the shale group exhibits relatively inferior physical properties.

Rock aggregate samples were also collected from different parts of Singapore, and their characteristic properties are shown in Table 3. All tests were carried out in accordance with BS 1881:1970 and BS 812:1975 (BSI, 1970, 1975).



SINGAPORE AGGREGATES

Table 3. Physical Properties of Aggregates from various Granite Sources in Singapore.

Source	Size (mm)	Percentage Passing				Specific Gravity	Compacted Bulk Density (kg/m <sup>3</sup> )	Water Absorption (%)	Aggregate Impact Value	Aggregate Abrasion Value	Polished Stone Coefficient
		B.S. Sieve									
		38 (mm)	19 (mm)	9.52 (mm)	4.76 (mm)						
Bukit Timah	19 down	75	25	9	0	2.67	1560	0.36	0.36	5.90	0.55
	19 down	88	18	10	0	2.71	1570	0.38	0.38	6.20	0.56
	38 down	93	12	2	1	0	1580	0.38	0.36	5.70	0.55
	38 down	90	18	3	1	0	1570	0.36	0.37	6.40	0.58
Bukit Mandai	19 down	86	23	3	0	2.70	1520	0.35	0.36	-	0.53
	19 down	85	31	10	0	2.69	1440	0.43	-	5.80	0.50
	38 down	98	3	0	0	2.70	1520	0.24	0.33	6.30	0.54
	38 down	94	7	2	0	0	1490	0.35	-	6.10	0.51
Bukit Gombak	19 down	89	25	4	0	2.69	1520	0.30	0.30	-	0.52
	19 down	87	20	4	0	2.70	1490	0.43	0.33	4.80	0.48
	38 down	94	8	1	1	0	1440	0.22	-	5.70	0.54
	38 down	97	3	1	0	0	1450	0.36	0.36	-	0.46
Pulau Ubin	19 down	83	18	2	1	2.64	1460	0.41	0.32	6.20	0.49
	19 down	78	2	1	1	2.47	1430	0.52	0.38	5.40	0.54
	38 down	93	10	3	1	0	1430	0.46	0.29	-	0.48
	38 down	95	8	3	0	0	1450	0.38	-	5.90	0.52

Table 2. Summary of Physical Properties of Various Singapore Rocks.

Rock Type	Specific Gravity	Bulk Density (kg/m <sup>3</sup> )	Porosity (%)	Water Absorption (%)	Compressive Strength (N/mm <sup>2</sup> )	Aggregate Abrasion Value	Polished Stone Coefficient
Granite	2.73-2.85	2,600-2,880	0.20- 0.85	0.50-0.80	130-220	6.0-7.6	0.56-0.65
Granodiorite	2.68-2.74	2,560-2,850	0.10- 0.60	0.65-1.10	120-215	5.0-6.4	0.54-0.63
Microgranite	2.74-2.83	2,610-2,820	0.15- 0.65	0.60-0.90	125-220	6.5-7.4	0.55-0.58
Adamellite	2.69-2.82	2,580-2,900	0.20- 0.90	0.80-1.34	120-210	5.8-6.2	0.52-0.59
Dolerite	2.68-2.77	2,530-2,670	0.25- 0.85	0.96-1.26	100-180	4.3-6.1	0.50-0.56
Gabbro	2.65-2.72	2,580-2,900	0.2 - 0.80	1.35-2.35	90-170	4.4-5.7	0.42-0.46
Norite	2.64-2.70	2,350-2,600	-	1.40-2.40	60-150	3.0-3.8	0.38-0.42
Andesite	2.63-2.68	2,500-2,600	-	1.30-2.25	65-165	3.5-4.8	0.40-0.45
Shale	2.32-2.62	2,000-2,450	8.00-12.50	2.20-5.60	15-80	1.2-4.0	0.15-0.29



SINGAPORE AGGREGATES

Table 3. Physical Properties of Aggregates from various Granite Sources in Singapore.

Source	Size (mm)	Percentage Passing				Specific Gravity	Compacted Bulk Density (kg/m <sup>3</sup> )	Water Absorption (%)	Aggregate Impact Value	Aggregate Abrasion Value	Polished Stone Coefficient
		B.S. Sieve									
		38 (mm)	19 (mm)	9.52 (mm)	4.76 (mm)						
Bukit Timah	19 down	75	25	9	0	2.67	1560	0.36	0.36	5.90	0.55
	19 down	88	18	10	0	2.71	1570	0.38	0.38	6.20	0.56
	38 down	93	12	2	1	0	1580	0.38	0.36	5.70	0.55
	38 down	90	18	3	1	0	1570	0.36	0.37	6.40	0.58
Bukit Mandai	19 down	86	23	3	0	2.70	1520	0.35	0.36	-	0.53
	19 down	85	31	10	0	2.69	1440	0.43	-	5.80	0.50
	38 down	98	3	0	0	2.70	1520	0.24	0.33	6.30	0.54
	38 down	94	7	2	0	0	1490	0.35	-	6.10	0.51
Bukit Gombak	19 down	89	25	4	0	2.69	1520	0.30	0.30	-	0.52
	19 down	87	20	4	0	2.70	1490	0.43	0.33	4.80	0.48
	38 down	94	8	1	1	0	1440	0.22	-	5.70	0.54
	38 down	97	3	1	0	0	1450	0.36	0.36	-	0.46
Pulau Ubin	19 down	83	18	2	1	2.64	1460	0.41	0.32	6.20	0.49
	19 down	78	2	1	1	2.47	1430	0.52	0.38	5.40	0.54
	38 down	93	10	3	1	0	1430	0.46	0.29	-	0.48
	38 down	95	8	3	0	0	1450	0.38	-	5.90	0.52

From the test results of rock aggregates from various granite sources (Table 3), it is observed that the physical properties of the aggregates from Bukit Timah are comparatively superior to those from Bukit Mandai, Bukit Gombak and Pulau Ubin. In addition to the physical tests mentioned, other special tests were also carried out on the aggregate samples in order to determine the impurities present, alkali reactivity, and soundness. The tests for organic impurities were carried out in accordance with ASTM Standard C40-66 (ASTM, 1966), and the results are presented in Table 4.

**Table 4. Results of Colorimetric Tests for Organic Impurities (ASTM Standard C40-66).**

Aggregate Type	Observed Colour of Solution	Remarks
Acid rock aggregates (granite family)	Yellowish	Low organic content
Basic rock aggregates (norite, gabbro, andesite, etc.)	Light Brown	Low organic content
Shale aggregate	Dark Brown	High organic content

It is seen that the acid rock aggregates do not contain any organic impurities, but the basic rock aggregates contain a low amount of organic matter and the organic content of the shale aggregates is very high.

Table 5 shows test results for both acid and basic rock aggregates for silt, clay and fine dust (BS 812: 1967 & ASTM Standard C117-69). It is observed that basic rock aggregates contain higher silt, clay and fine dust content than those from acid rocks.

**Table 5. Results of Testing for Silt, Clay and Fine Dust (BS 812: 1967 and ASTM Standard C117-69).**

Aggregate Type	Combined Percentage of Silt, Clay and Fine Dust	Remarks
Acid rock aggregates	0.2 to 0.8	Not harmful
Basic rock aggregates	1.4 to 3.6	Slightly harmful

An alkali - reactivity test was carried out as per ASTM Standard C227-71 (Mortar Bar Test), and the results are presented in Table 6. Potential alkali-

## SINGAPORE AGGREGATES

reactivity for acid rock aggregates was insignificant, whereas for shale aggregates the potential was found to be high.

**Table 6. Results of Alkali-Reactivity Tests (ASTM Standard C 227-71 : Mortar Bar Test).**

Aggregate Type	Expansion (%)		Potential Alkali Attack
	after 3 months	after 6 months	
Acid rock aggregates	Less than 0.05	Less than 0.1	Insignificant
Basic rock aggregates	0.06 to 0.95	0.13 to 0.24	Medium
Shale aggregates	0.15 to 0.25	0.24 to 0.45	High

The potential alkali-reactivity for basic rock aggregates was tolerably low.

Sodium sulphate soundness tests were carried out in accordance with ASTM Standard C88-73, and the results are presented in Table 7. Summarizing all the test results reported in Tables 3 to 7, it is observed that the acid rock aggregates exhibit good to excellent durability and the basic rock aggregates satisfactory durability, while shale aggregates exhibit poor durability.

**Table 7. Results of Sodium Sulphate Soundness Tests (ASTM Standard C88-73).**

Aggregate Type	Reduction in Size of Particles	Remarks
Acid rock aggregates	No reduction	Highly sound
Basic rock aggregates	Moderate reduction	Medium sound
Shale aggregates	High reduction	Unsound

## THERMAL PROPERTIES OF ROCK AGGREGATES

The main thermal properties of rock aggregates that are considered significant for the performance of concrete include the coefficient of thermal expansion, specific heat and conductivity. The coefficient of thermal expansion has significance in normal structural concrete, especially for rigid pavements. Specific heat and conductivity are important in mass concrete, or where the insulation property of concrete is desirable.

Since the use of exposed mass concrete is limited in Singapore, these studies were confined to the linear coefficient of thermal expansion of aggregates and the concrete made with those aggregates, from the structural concrete point of view.

The coefficient of thermal expansion of aggregate influences the value of the coefficient of thermal expansion of concrete containing the given aggregate. The two main constituents of concrete - cement paste and aggregate - have dissimilar thermal coefficients, and the coefficient of concrete is the resultant of the two values. The higher the coefficient of thermal expansion of the aggregate, the higher is the coefficient of thermal expansion of the concrete, but the latter also depends on the aggregate content in the mix and on the mix proportions in general (WALKER et al, 1952; BONNEL & HARPER, 1951; HANNANT, 1964). If the coefficient of thermal expansion of aggregate differs too much from that of the cement paste, a large variation in temperature may introduce differential movement and break the bond between the aggregate particles and the surrounding paste (WALKER et al, 1950).

The linear coefficient of thermal expansion of rocks from various Singapore sources, as shown in Table 8, was determined by the dilatometer test devised by VERBECK & HASS (1951). From Table 8, it is seen that the linear coefficient of thermal expansion of most of the Singapore granitic aggregates varies between 7 and  $14 \times 10^{-6}$  per °C. Table 9 shows the linear coefficients of thermal expansion of cement-sand paste, granitic aggregate and concrete made with the particular granitic aggregate. It is evident from Table 9 that the linear coefficients of thermal expansion of the various concrete specimens are not much different from those of the aggregates. The variation of placement temperature and the recorded daily maximum temperature difference that can be expected in Singapore is in the order of 3 to 4 °C only. In view of the above, granitic aggregates in Singapore do not seem to pose any problem to the production of durable concrete from the thermal expansion view point.

**Table 8. Linear Coefficient of Thermal Expansion of various of Singapore Rocks.**

Source	Rock Type	Linear Coefficient of Thermal Expansion ( $10^{-6}$ per °C)
Mandai	Granite	7.50 - 9.80
Bukit Timah	Granodiorite	8.60 - 11.50
Bukit Gombak	Microgranite	8.80 - 13.60
Pulau Ubin	Microgranite	7.40 - 12.60

SINGAPORE AGGREGATES

Table 9. Linear Coefficients of Thermal Expansion of Concrete made with Singapore Granitic Aggregates.

Test Samples/Specimens	Linear Coefficient of Thermal Expansion ( $10^{-6}$ per $^{\circ}\text{C}$ )		
	Cement Paste* (1:2)	Granitic Aggregate	Concrete** (1:2:4)
1	12.35	9.86	10.68
2	11.48	10.32	11.54
3	12.66	9.64	10.87
4	11.83	10.26	11.35
5	13.47	10.63	11.76
6	12.23	9.75	11.33

\*sand used from Tampinese sand quarry (Figure 1)

\*\*water - cement ratio = 0.45

PHYSICAL PROPERTIES OF CRUSHED GRANITE FINE AGGREGATES

Due to heavy development works, Singapore is already running short of good quality sand (fine aggregate). Therefore, granitic rocks machine-crushed to produce fine aggregates were investigated for their suitability (KOH, 1983). The fine aggregates so produced consisted of particles having rough and angular surfaces compared with those of locally available natural sand, with grain size distributions as shown in Figure 2.

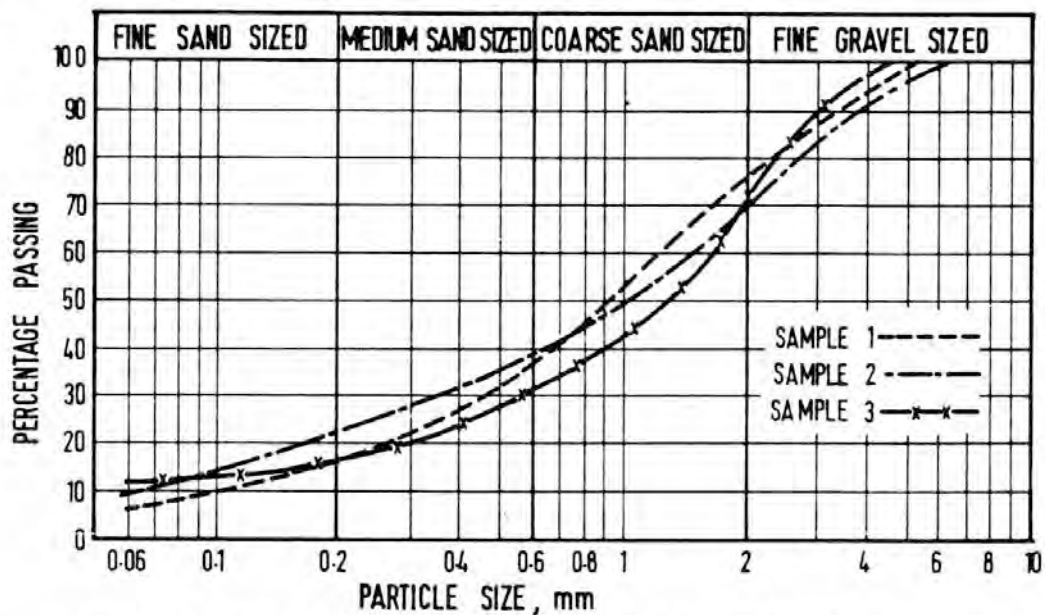


Fig. 2. Grain Size Distribution Curves of Crushed Granite Fine Aggregates.

Standard cube specimens of 1:2:4 concrete with a fixed water-cement ratio of 0.5 were made with coarse granitic aggregates and locally available natural sand and granitic sand as fine aggregates (in accordance with BS 1881 : 1970, Part 3) and tested for 28 day strength (in accordance with BS 1881 : 1970, Part 4). The results are presented in Table 10. It can be readily seen from this table that the crushed granite fine aggregates can be conveniently used to produce high quality durable concrete having characteristic compressive strengths of around 40 MPa or even higher.

**Table 10. Compressive Strengths of Concrete Utilising Natural Sand and / or Crushed Granite Fine Aggregates.**

Specimen Series*	28-day Compressive Strength (MPa)
A : Concrete made with locally available natural sand	22 to 25
B : Concrete made with both locally available sand and crushed granite fine aggregate in equal proportion	28 to 33
C : Concrete made with crushed granite fine aggregate	37 to 42

\*Ordinary Portland Cement and granitic coarse aggregates were used in all specimens.

#### ASSESSMENT OF AGGREGATES

The parameters considered in the assessment of durability of aggregates were specific gravity and density, porosity and water absorption, compressive strength, aggregate impact value, aggregate abrasion, absorption, polished stone coefficient, sodium sulphate soundness, alkali-reactivity, and impurities. From all the test results reported herein (Tables 2 to 7), sedimentary rocks (shale materials) were found to be weak and hence not suitable for making durable concrete. The basic rocks comprising gabbro, norite, and andesite were found to be moderately strong and are suitable for making medium strength concrete having satisfactory durability. The acid rocks comprising the granite family were found to be very strong and hence produce strong and durable concrete. Granitic coarse aggregates and crushed granite fine aggregates (manufactured sand) can be recommended where high strength concrete is required for special structures.



## SINGAPORE AGGREGATES

### CONCLUSIONS

Singapore rocks can be grouped into three main categories from a strength point of view: weak rocks consisting of shale materials, medium strong rocks consisting of gabbro, norite, and andesite, and very strong rocks consisting of granite, granodiorite, microgranite, adamellite and dolerite.

Durability of concrete depends upon many factors, but from the view point of aggregate type, granitic rocks are the best. For important concrete structures, careful distinction must be made between the medium strong basic rocks and strong acid (granitic) rocks for judicious selection of aggregates. Very strong and durable concrete can be made using both coarse and fine aggregates made from granitic rocks.

These conclusions are based on limited studies carried out on aggregates obtained from only a few sources. Therefore, any individual aggregate source being considered for use in concrete production requires its own test programme before final acceptance.

### REFERENCES

- ASTM (1966). Standard C 40-66, Test for organic materials. American Society for Testing and Materials, Philadelphia, USA.
- ASTM (1969). Standard C 117-69, Test for materials finer than no. 200 sieve in mineral aggregates by washing. American Society for Testing and Materials, Philadelphia, USA.
- ASTM (1971). Standard C 277-71, Test for potential alkali reactivity of cement-aggregate combination (mortar-bar method). American Society for Testing and Materials, Philadelphia, USA.
- ASTM (1971). Standard C 289-71, Test for potential reactivity of aggregate (chemical method). American Society for Testing and Materials, Philadelphia, USA.
- ASTM (1973). Standard C 88-73, Test for soundness of aggregates by use of sodium sulphate or magnesium sulphate. American Society for Testing and Materials, Philadelphia, USA.
- AZIZ, M.A. & RAMASWAMY, S.D. (1978). Some geotechnical properties of Singapore shale and its potential use in road construction. *Proc. 3rd Reg. Conf. on Geol. & Min. Res. SEA*, Bangkok, pp. 201-204.
- BICZOK, I. (1972). Concrete corrosion-concrete protection. *Akademiai Kiado*, Budapest, pp. 393-398.
- BONNEL, D.G.R. & HARPER, F.C. (1951). The thermal expansion of concrete. *Tech. Paper No. 7*, National Building Studies, HMSO, London.
- BSI (1967). British Standard BS 812:1967, Test for silt, clay and fine dusts. British Standards Institution, London.
- BSI (1970). British Standard BS 1881 : Part 3 : 1970, Methods of making and curing test specimens. British Standards Institution, London.
- BSI (1970). British Standard BS 1881: Part 4: 1970, Methods of testing concrete for strength. British Standards Institution, London.

AZIZ & RAMASWAMY

- BSI (1975). British Standard BS 812: 1975, Methods for the sampling and testing of mineral aggregates, sand and fillers. British Standards Institution, London.
- DOLAR-MANTUANI, L. (1983). *Handbook of Concrete Aggregates*. Noyes Pub. p. 345.
- GEOLOGICAL SOCIETY OF LONDON (1986). *Sand, Gravel and Crushed Rock Aggregates*.
- HANNANT, D.J. (1954). Effect of heat on concrete strength. *Engineering*, London, vol. 197, pp. 302-308.
- HARTLEY, A. (1974). A review of the geological factors influencing the mechanical properties of road surface aggregates. *Q. Jl. Eng. Geol.*, London, vol. 7, pp. 69-100.
- JACKSON, N. Ed. (1977). *Civil Engineering Materials*. ELBS and Macmillan, London.
- KOH, T.L. (1983). Study into the feasibility of using granite fine aggregates for concrete mixes. *Jl. Inst. Engrs.*, Singapore, vol. 24, no. 2, pp. 41-47.
- McINTOSH, J.D. (1957). The selection of natural aggregates for various types of concrete works. *Reinf. Concr. Rev.*, London, vol. 4, no. 5, pp. 281-305.
- NEVILLE, A.M. (1975). *Properties of Concrete*. ELBS and Pitman, London, pp. 103-178.
- ORCHARD, D.F. (1976). *Concrete Technology, Vol. 3: Properties and Testing of Aggregates*. Applied Science Publishers, London.
- PITTS, J. (1984a). A review of geology and engineering geology of Singapore. *Q. Jl. Eng. Geol.*, London, vol. 17, pp. 93-101.
- PITTS, J. (1984b). A Survey of engineering geology of Singapore. *Geotechnical Engineering*, vol. 15, no. 1, pp. 1-20.
- PUBLIC WORKS DEPARTMENT OF SINGAPORE (1976). *Geology of the Republic of Singapore*.
- RAMASWAMY, S. D. & AZIZ, M.A. (1977). Identification and excavatability of weak rocks in Singapore. *Jl. Inst. Engrs.*, Singapore, vol. 17, no. 2, pp. 51-67.
- RAMASWAMY, S.D. & AZIZ, M.A. (1981). Importance of polished stone coefficient in the choice of stones for road surfaces in Singapore. *Proc. 3rd Conf. Road Eng. Assoc. Asia & Australasia*, Taipei, vol. 1, pp. 461-473.
- RAMASWAMY, S.D. (1986). Distribution and characteristics of rock types of Singapore. *Proc. 5th Int. Congress IAEG*, Buenos Aires, pp. 153-158.
- VERBECK, F.J. & HASS, W.E. (1951). Dilatometer method for determination of thermal coefficient of expansion of fine and coarse aggregates. *Proc. Highway Res. Bd.*, vol. 30, pp. 187-193.
- WALKER, S., BLOEM, D.L. & MULLEN, W.G. (1952). Effects of temperature changes on concrete as influenced by aggregates. *J. Amer. Concr. Inst.*, vol. 48, pp. 661-79.

## **THEORETICAL ANALYSIS OF A NONLINEAR THEORY OF CONSOLIDATION**

R.M. ARENICZ\* and R.N. CHOWDHURY\*

### **SYNOPSIS**

A general nonlinear theory of consolidation is compared with existing theories. The theory, proposed by G. Szefer in 1977, allows for various assumptions concerning stress-strain behaviour, seepage law, and properties of the soil. For purposes of comparison with other theories, the nonlinear system of equations describing the consolidation process has been linearized and solved numerically. The analysis has been done for one-dimensional boundary problems assuming either Darcy or non-Darcy flow. If there is no threshold gradient and Darcy's law is assumed to be valid, the results are found to be in accordance with those from the Terzaghi and Biot theories. However, the Szefer theory gives a better insight into the changes of porosity during the process of consolidation. Moreover, for non-Darcy conditions (assuming the validity of a threshold hydraulic gradient) the theory gives results which agree with those obtained by Parlange, who considered a non-Darcian consolidation process in clay soils.

### **INTRODUCTION**

There are many existing theories of consolidation, the Terzaghi and Biot theories being the most widely known. Both these theories are based on the validity of Darcy's law of seepage, and have many other common features. The Terzaghi theory has been found useful for most practical applications and, in fact, the original one-dimensional theory has been extended for two and three-dimensional situations. Considering its mathematical formulation, the Biot theory is an advance on the Terzaghi theory, as the system of equations describing the consolidation process is coupled in a realistic way for the two and three-dimensional cases. Consequently, it reflects the behaviour of soil better than the original Terzaghi theory. On the other hand, the Biot theory has the disadvantage that physical parameters are not as easy to obtain as those required for the Terzaghi theory. Nevertheless, because of the insight it offers, geotechnical engineers have shown significant interest in the Biot theory, even though it may not be used so frequently as the Terzaghi theory. For any engineering problem, it is most desirable to consider and analyse theories which are general in nature so that the accuracy and the relevance of the simpler and more direct approaches can be considered in perspective.

---

\* Lecturer, \*\* Reader, Department of Civil and Mining Engineering, University of Wollongong, Wollongong, N.S.W., Australia.

The main aim of this paper is to consider the general theory of consolidation proposed by SZEFER (1977). Only general assumptions are made in this theory about the flow law, stress-strain behaviour, variations of porosity, and other features of the consolidation process. Consequently, a wide range of natural soils can be accommodated within its framework. Moreover, certain aspects of soil behaviour which are not considered in the well known theories can be described. For example, a given relationship between porosity and permeability can be assumed. A nonlinear relationship between porosity and effective stress can be considered. A non-Darcy flow law can be introduced, with or without a threshold gradient, so that there is no seepage below such a hydraulic gradient. The assumption of small deformation theory is not essential, and large deformation can be handled if necessary. As such, it is an interesting theory which needs to be assessed in relation to the widely accepted theories. Such an assessment has not been done previously.

This paper offers numerical solutions of the nonlinear system of equations describing the consolidation process. The analysis has been done for one-dimensional boundary problems assuming either a Darcy flow law or a non-Darcy flow law with a threshold gradient. The results are compared to existing theories based on the linear or Darcy flow law (eg, Terzaghi, Biot) and the results obtained by PARLANGE (1973) for one-dimensional consolidation with a non-Darcy flow law. Before the presentation of the analysis, there is a brief review of previous research on soil behaviour during consolidation and development of nonlinear theories of consolidation.

#### BRIEF REVIEW OF CONSOLIDATION THEORIES

According to many well known results from experimental and field investigations of the soil consolidation process, there are important physical phenomena which are not described by either Terzaghi's or Biot's consolidation theories:

1. The value of porosity depends upon the present stress state. Investigations done by RAYMOND (1969), DAVIS & RAYMOND (1955) and POSKITT (1969, 1971) indicate a logarithmic dependence between porosity and effective stress in clays.
2. The value of the permeability coefficient depends upon the present porosity. There is, again, a logarithmic dependence between permeability and porosity, according to results obtained by RAYMOND (1969), POSKITT (1970) and BERRY & WILKINSON (1969). Therefore,

### NONLINEAR CONSOLIDATION

permeability depends upon the present stress/strain state in a mass of soil.

3. A progressive development of research in the field of liquid movement through porous media also indicates substantial deviations from Darcy's flow law, especially for cohesive soils. The results, obtained by many investigators, have been compared and analysed by SWARTZENDRUBER (1962a, 1962b, 1968), SCHMIDT & WESTMANN (1973) and others. These analyses have generally pointed out nonlinearity in the law of liquid flow through soil.
4. The density of the soil skeleton varies during the time of consolidation.
5. In many cases (and not only in soft soils) it is essential to take into account the large deformations of the soil skeleton because of the relationship existing between the physical and geometrical parameters of porous media.
6. Certain kinds of soil (eg, peat) show nonlinear rheological properties. The results of such observations have been analysed and published by BERRY & POSKITT (1972), BARDEN (1965), CHRISTENSEN & WU (1964) and others.
7. A permanent deformation and a sensitivity to the rapidity of loading, stated by OHTA & HATA (1973) and POOROOSHASB et al (1973), seem to be the important factors in the consolidation process.

All the physical effects mentioned above lead, naturally, to a nonlinear theory of consolidation. In recent years, a growing number of such theories have been published. Variable permeability has been considered by McNABB (1960) and POSKITT (1969, 1970, 1971). Large deformations have been calculated by GIBSON et al (1967). Nonlinear stress-strain relationships have been taken into account by JANBU (1965) and SHAPIRO (1970). Nonlinear rheological behaviour of the soil skeleton has been considered by BARDEN (1965) and SHIRINKULOV & DASIBIEKOV (1966). Non-Darcy flow has been the subject of papers by SCHMIDT & WESTMANN (1973), ELNAGGAR et al (1972, 1973) and ARENICZ (1981).

### SZEFER'S GENERAL THEORY

One of the interesting efforts in this area has been made by SZEFER (1977), who published a complete theory of three-dimensional nonlinear consolidation, based on the mixture theory and considering:



- changes of density, porosity, and permeability;
- large deformations;
- nonlinear properties of constituents;
- interaction between phases and supply of phases in balance equations;
- coupling between density, porosity, deformation tensor, velocity, stress tensor, and effective liquid pressure.

A statement of Szefer's theory is not widely available and, therefore, its main equations and features are presented in Appendix B. Appendix B also outlines the linearization of Szefer's basic equations.

ANALYSIS OF SZEFER'S EQUATIONS FOR ONE DIMENSIONAL PROBLEMS

As is shown in Appendix B, Szefer's theory describes the one-dimensional consolidation process by the following set of equations:

$$\left(2N_1 - A_1 + \frac{Q_1 Q_2}{R_1}\right) \frac{\partial^2 w}{\partial z^2} + \left(\frac{Q_1}{R_1} - \frac{n_R}{1-n_R}\right) \frac{\partial p}{\partial z} = 0 \dots\dots\dots (1)$$

$$kH \frac{\partial^2 p}{\partial z^2} = \frac{b-1}{n_R R} \frac{\partial p}{\partial t} + \left(\frac{1+a}{n_R} - \frac{n_R-b}{n_R} \frac{Q_2}{R_1}\right) \frac{\partial^2 w}{\partial z \partial t} \dots\dots\dots (2)$$

$$\sigma_{zz} = \left(2N_1 - A_1 + \frac{Q_1 Q_2}{R_1}\right) \frac{\partial w}{\partial z} + \frac{Q_1}{R_1} p \dots\dots\dots (3)$$

$$\Xi = -\frac{1}{R_1} p - \frac{Q_2}{R_1} \frac{\partial w}{\partial z} \dots\dots\dots (4)$$

$$\beta = \frac{b}{R_1} p + \left(a + b \frac{Q_2}{R_1}\right) \frac{\partial w}{\partial z} \dots\dots\dots (5)$$

where:

$$H = \begin{cases} 0 & \text{for } \frac{\partial p}{\partial z} \leq i_0 \\ 1 & \text{for } \frac{\partial p}{\partial z} > i_0 \end{cases} \dots\dots\dots (6)$$

and the other quantities are as shown in Appendix A.

It is now possible to compare the governing equations 1 to 5 with the corresponding equations of both the Biot and Terzaghi theories. Firstly, it is evident that even after linearization and considering the simplest one-



*NONLINEAR CONSOLIDATION*

dimensional problems, Szefer's theory still describes changes in soil porosity during consolidation, a feature which is lacking in the Biot and Terzaghi theories. Secondly, liquid density can also vary during consolidation, although for real liquids (which are practically incompressible) this is not a very important consideration. Thirdly, the filtration law includes a possible threshold gradient ( $i_0$ ) and it can be reduced to Darcy's law in the particular case of  $i_0 = 0$ . Therefore, this system of equations seems to describe the real behaviour of soils more closely than either the Biot or Terzaghi theories.

**ANALYSIS OF BOUNDARY CONDITIONS FOR ONE-DIMENSIONAL PROBLEMS**

Consider a porous, liquid-saturated layer of homogeneous medium resting on a undeformable foundation. The layer of thickness  $h$  is consolidated by an external uniformly distributed load  $g(t)$ . Initial conditions are assumed to be homogeneous. The top edge of the layer is permeable, while the bottom one is impermeable. Such a set of conditions will henceforth be called basic, because considering all the other combinations of the boundary conditions it can be noticed that:

- (a) the assumption of two impermeable edges leads immediately to the simple and trivial case of an elastic layer without flow of liquid, and the solution of equations 1 to 5 is given in Appendix C;
- (b) because the forces of gravity are neglected, the distribution of pore water pressure in the case wherein only the bottom edge is permeable must be inverse in comparison to its distribution under basic conditions as defined above (in which the top edge only is permeable);
- (c) distribution of pore water pressure in the case of two permeable edges is, for the same reason, symmetrical in relation to the midpoint and can be obtained by combination of the basic and inverse solutions each for a layer of  $h/2$  thickness.

Therefore, only the basic set of boundary conditions has to be considered. These are:

$$p(z = 0,t) = 0 \quad \dots\dots\dots (7)$$

$$\left(2N_1 - A_1 + \frac{Q_1 Q_2}{R_1} \frac{\partial w}{\partial z}\right)_{z=0,t} + \left(\frac{Q_1}{R_1} - \frac{n_R}{r-n_R}\right) p(z=0,t) = -g(t) \quad \dots\dots (8)$$

$$w(z = h,t) = 0 \quad \dots\dots\dots (9)$$

$$\begin{aligned}
 p(z = h, t) &= \\
 &= \frac{\left(1 + a + \frac{b-1}{R_1} Q_2\right) \frac{g(t)}{1-n_R}}{\frac{b-1}{R_1} \left(2N_1 - A_1 + \frac{Q_1 Q_2}{R_1}\right) - \left(\frac{Q_1}{R_1} - \frac{n_R}{1-n_R}\right) \left(1 + a + \frac{b-1}{R_1} Q_2\right)} \\
 &\quad \text{for } H(z = h) = 0 \quad \dots\dots\dots (10)
 \end{aligned}$$

$$\left. \frac{\partial p}{\partial z} \right|_{z=h, t} = i_0, \text{ for } H(z = h) = 1 \quad \dots\dots\dots (11)$$

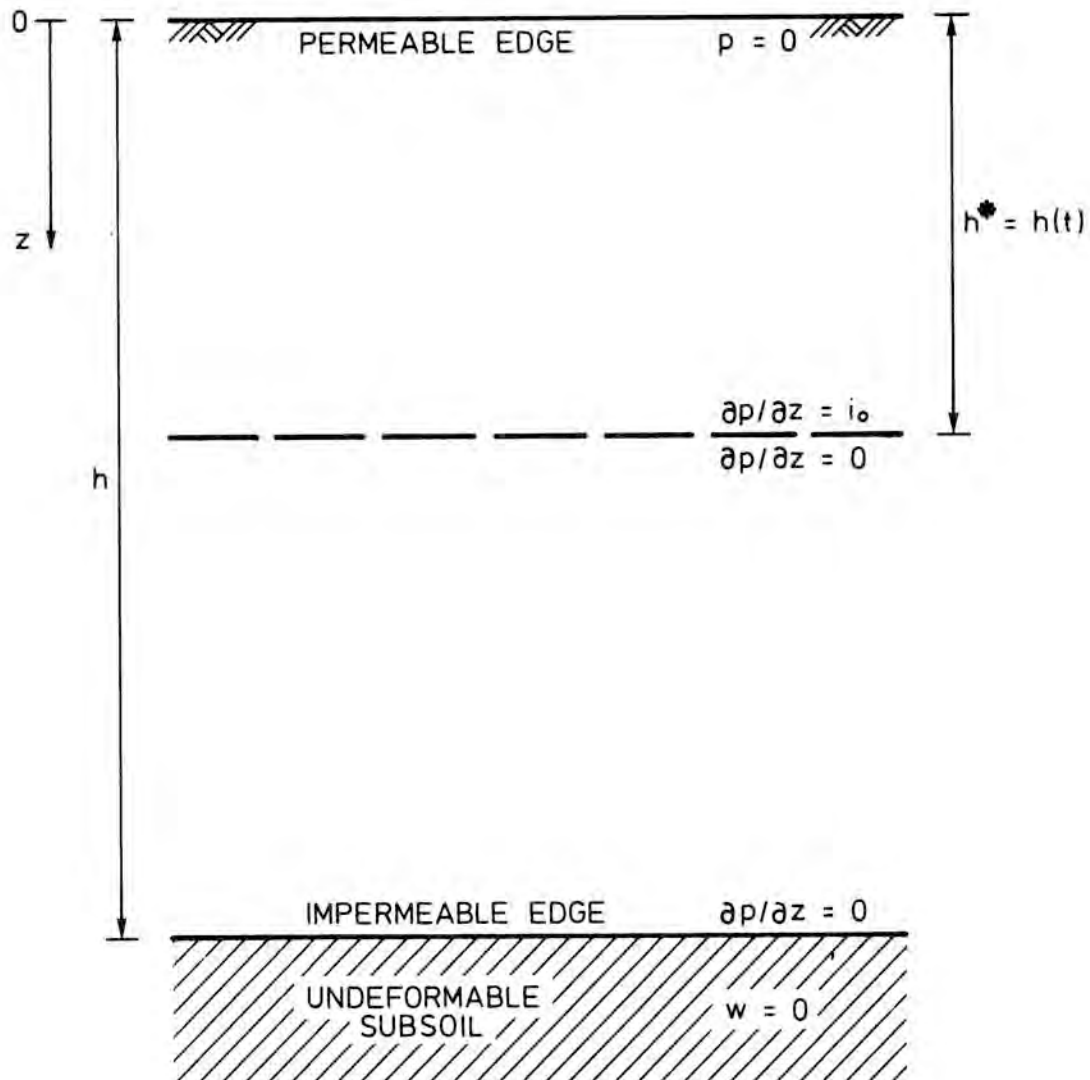


Fig. 1. Boundary Conditions of Consolidating Layer.

*NONLINEAR CONSOLIDATION*

The double condition for  $p$  (equations 10 and 11) requires some explanation. The form of the function  $H$  (equation 6) permits the existence of two time-dependent zones in the layer under consideration. These zones are separated by a line  $\frac{\partial p}{\partial z} = i_0$ . The first zone is adjacent to the permeable edge, and liquid flow occurs inside; in the second, adjacent to the impermeable edge, flow does not occur. As shown in Figure 1, if the flow zone includes only a part of the layer, the area without liquid flow ( $H = 0$ ) is adjacent to the impermeable edge. Hence, the value of  $p$  in this whole zone (particularly for  $z=h$ ) is equal to that from the solution (equation C1 of Appendix C). The flow zone may include the whole layer however, since its range is a function of time, in which case the condition of the impermeable edge should not be taken from equation C1; rather, it should be changed into  $\frac{\partial p}{\partial z} = i_0$ , because the dividing line between the two zones becomes the bottom edge of the layer.

**SOLUTION OF SZEFER'S EQUATIONS FOR A ONE-DIMENSIONAL PROBLEM**

As is shown in Appendix D, the system of equations 1 to 5 can be transformed to the following dimensionless form:

$$H^* \frac{\partial^2 \Psi}{\partial \xi^2} = \frac{\partial \Psi}{\partial T} + C_1 \frac{\partial q}{\partial T} \dots\dots\dots (12)$$

$$\frac{\partial \omega}{\partial \xi} = D_1 \Psi + M_1 q \dots\dots\dots (13)$$

$$\Psi_{zz} = D_2 \Psi - q \dots\dots\dots (14)$$

$$\Xi = D_3 \Psi + M_3 q \dots\dots\dots (15)$$

$$\beta = D_4 \Psi + M_4 q \dots\dots\dots (16)$$

together with the boundary conditions:

$$\Psi (\xi = 0, T) = 0 \dots\dots\dots (17)$$

$$\omega (\xi = 1, T) = 0 \dots\dots\dots (18)$$

$$\Psi (\xi = 1, T) = -Cq, \text{ for } H^*(\xi = 1, T) = 0 \dots\dots\dots (19)$$

$$\frac{\partial \Psi}{\partial \xi} \Big|_{\xi=1, T} = \mu, \text{ for } H^*(\xi = 1, T) = 1 \dots\dots\dots (20)$$

where:

$$H^* = 0 \text{ for } \frac{\partial \Psi}{\partial \xi} < \mu \dots\dots\dots (21)$$

$$H^* = 1 \text{ for } \frac{\partial \Psi}{\partial \xi} \geq \mu \quad \dots\dots\dots (22)$$

and notation is as shown in Appendix A.

The solution of the above system (equations 12 to 16) can easily be found after solving the nonlinear heterogeneous parabolic equation of the second order (equation 12), which can only be done numerically.

From among commonly known and used numerical methods of solving parabolic equations, the method of finite differences by Crank-Nicholson (POTTER, 1973) has been chosen. It consists of averaging the spatial derivatives and gives an absolute stability of the solution as well as accuracy of the second order regarding the time and space steps. This method has been successfully used by PARLANGE (1973) for a numerical solution of a consolidation problem including the nonlinear flow law, formulated on the basis of Terzaghi's theory. The details of the method used for numerical solution are presented in Appendix E.

As stated earlier, the general solution of the equations 12 to 16 for any time T can only be done numerically. However, it is possible to find the exact solution of the above equations for  $T = \infty$  (ie,  $t = \infty$ , end of consolidation process). Assuming that the consolidating external load  $g(t)$  is a non-decreasing function, the following formulae can be obtained:

- (a) maximum depth of liquid flow zone (consolidating zone)

$$\chi_{end} = \begin{cases} -Cq_o/\mu & \text{for } -Cq_o/\mu \leq 1 \\ 1 & \text{for } -Cq_o/\mu \geq 1 \end{cases} \quad \dots\dots\dots (23)$$

- (b) final effective liquid pressure

$$\Psi_{end} = \begin{cases} \mu\xi & \text{for } \xi \leq \chi_{end} \\ -Cq_o & \text{for } \xi > \chi_{end} \end{cases} \quad \dots\dots\dots (24)$$

- (c) final skeleton displacement

$$\omega_{end} = \begin{cases} \frac{D_1\mu}{2} (\xi^2 - \chi_{end}^2) - M_1q_o(1 - \xi) + D_1Cq_o(1 - \chi_{end}), & \text{for } \xi \leq \chi_{end} \\ (D_1C - M_1)q_o(1 - \xi), & \text{for } \xi \geq \chi_{end} \end{cases} \quad \dots\dots\dots (25)$$

and for the upper edge particularly

$$\omega_{end} (\xi = 0) = \frac{-D_1\mu}{2} \chi_{end}^2 - M_1q_o + D_1Cq_o(1 - \chi_{end}) \quad \dots\dots\dots (26)$$

NONLINEAR CONSOLIDATION

(d) final vertical stress

$$\Psi_{zz}^{\text{end}} = \begin{cases} D_2\mu\xi - q_o, & \text{for } \xi \leq \chi_{\text{end}} \\ (-D_2C + 1)q_o, & \text{for } \xi > \chi_{\text{end}} \end{cases} \dots\dots\dots (27)$$

(e) final relative change of fluid density

$$\Xi_{\text{end}} = \begin{cases} D_3\mu\xi + M_3q_o, & \text{for } \xi \leq \chi_{\text{end}} \\ (-D_3C + M_3)q_o, & \text{for } \xi > \chi_{\text{end}} \end{cases} \dots\dots\dots (28)$$

(f) final relative change of soil porosity

$$\beta_{\text{end}} = \begin{cases} D_4\mu\xi + M_4q_o, & \text{for } \xi \leq \chi_{\text{end}} \\ (-D_4C + M_4)q_o, & \text{for } \xi > \chi_{\text{end}} \end{cases} \dots\dots\dots (29)$$

DISCUSSION OF RESULTS

Using the numerical technique discussed in Appendix E, the solutions for a series of one-dimensional problems were obtained on the basis of Szefer's theory. A flow chart and computer program were first prepared to conform to equations E5 to E10. The numerical solutions were then obtained using a CDC CYBER-72 computer. The details of input data are given in Appendix E. The numerical solution for  $t = 100,000$  days was found to correspond very closely to the exact solution given by Equations 23 and 29 for the case  $t = \infty$ .

Figure 2 shows the variation of dimensionless pore water pressure  $\Psi$  with dimensionless depth  $\xi$  within the soil layer for different values of dimensionless time  $T$ . These changes relate to the loading stage only, which according to the input data in Appendix E, takes a period of  $t=100$  days ( $T=0.00058$ ). The upper part of the diagram, Figure 2a, corresponds to the case with zero threshold gradient ( $i_o = 0$ ) and hence, parameter  $\mu = 0$  (assuming Darcy's law to be valid at all values of the gradient). The results obtained on the basis of Szefer's theory correspond to the well known Terzaghi and Biot solutions in which the formulation does not include a threshold gradient.

Numerical solutions were also obtained for a number of non-zero values of the threshold gradient  $i_o$  as stated in Appendix E. One set of such results is presented in Figure 2b for the value of dimensionless threshold gradient  $\mu = 0.33$ . No direct comparisons with the Terzaghi and Biot theories can be made because solutions for a non-zero  $i_o$  (and hence non-zero  $\mu_o$ ) cannot be obtained from the original theories. However, it is interesting to note some features of the results. The curves indicate an abrupt change in hydraulic gradient at some depth. This discontinuity is expected because of the assumption of a non-zero threshold gradient as part of the flow law. As time increases, the depth at which the discontinuity occurs also increases.



### NONLINEAR CONSOLIDATION

The soil layer may be visualised as two sections, the upper one consolidating and the lower one with no flow and no consolidation. (Note that the base of the layer has been taken as impermeable, and hence undrained.) As time increases, the thickness of the consolidating portion increases. During the loading process of 100 days ( $T = 0.00058$ ), it is obvious from Figure 2b that less than 20% of the layer thickness participates in the consolidation process. The pore pressure is constant with depth in the lower, non-consolidating part of the soil layer and all the curves in Figure 2b become vertical. The corresponding curves in Figure 2a have some inclination to the vertical, indicating that the whole of the soil layer is undergoing consolidation at all times if  $\mu = 0$  ( $i_0 = 0$ ).

The tangent (dotted) lines in Figure 2b are all parallel to each other because in each case the break or discontinuity occurs when the hydraulic gradient drops to the threshold gradient.

After  $t = 100$  days, the load remains constant and consolidation of the clay layer continues with the same boundary drainage conditions as before, ie, top drained and bottom undrained. The numerical calculations were made for a number of time steps finishing at  $t = 100,000$  days, ie,  $t$  or  $T$  approaching infinity. As expected under constant load, the pore water pressure at any depth decreases with increasing time. The results for  $\mu = 0$  ( $i_0 = 0$ ) are presented in Figure 3a and one set of results for non-zero threshold gradient  $i_0$  (dimensionless value  $\mu = 0.33$ ) are presented in Figure 3b. The lower boundary of the consolidating part of the soil layer moves downward with increasing time in Figure 3b. Moreover, even for  $t = \infty$  there is a residual pore water pressure in the soil. On the other hand, the results shown in Figure 3a correspond to those based on the Biot and Terzaghi theories because the threshold gradient is assumed to be zero. The whole of the soil layer is consolidating at any given time, and at  $t = \infty$ , there is zero pore water pressure throughout the soil layer.

The type of results shown in Figures 2b and 3b correspond closely with the results based on the work of PARLANGE (1973), who presented a solution of a one-dimensional problem based on Terzaghi's theory extended to include a non-zero threshold gradient. However, it should be noted that equations 1 to 5 based on Szefer's theory include provision for changes in porosity and fluid density during the consolidation process, which is not a feature of Parlange's work. Despite different origins, the two formulations may be reduced to the same type of equation if fluid density and soil porosity are assumed to be constant during the consolidation process.



ARENICZ & CHOWDHURY

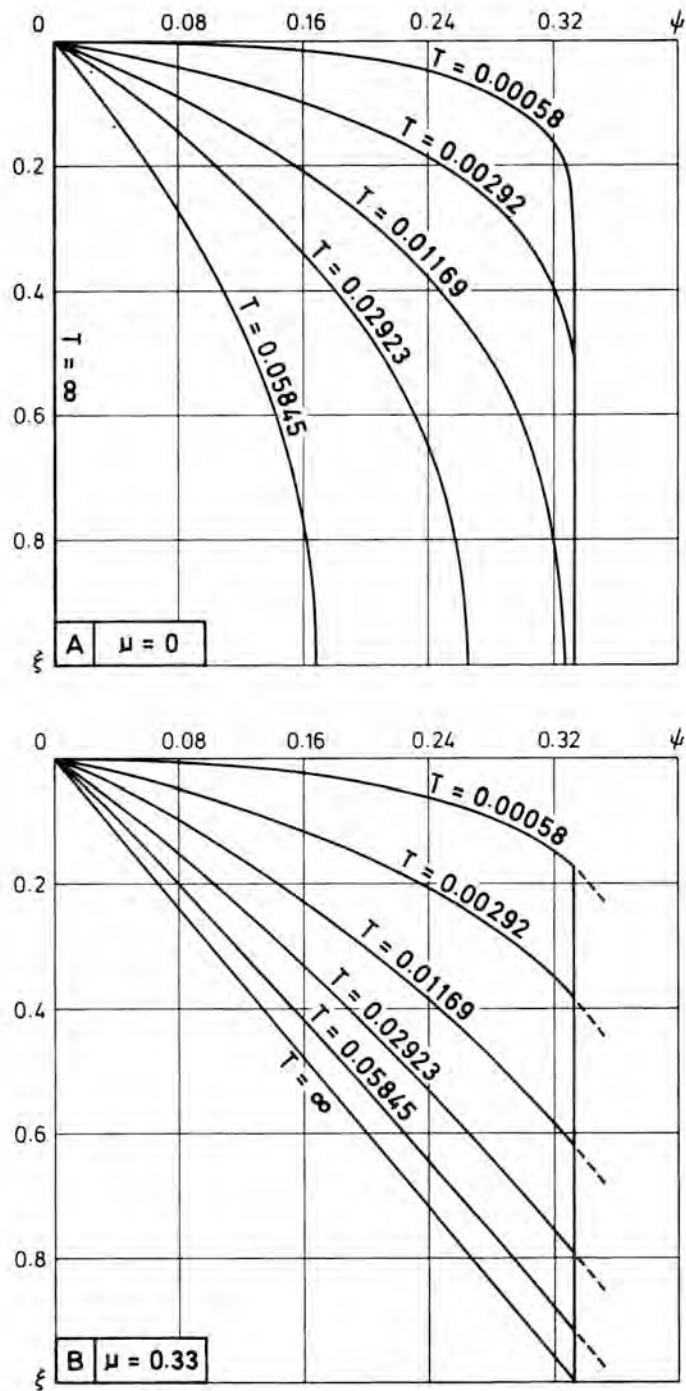
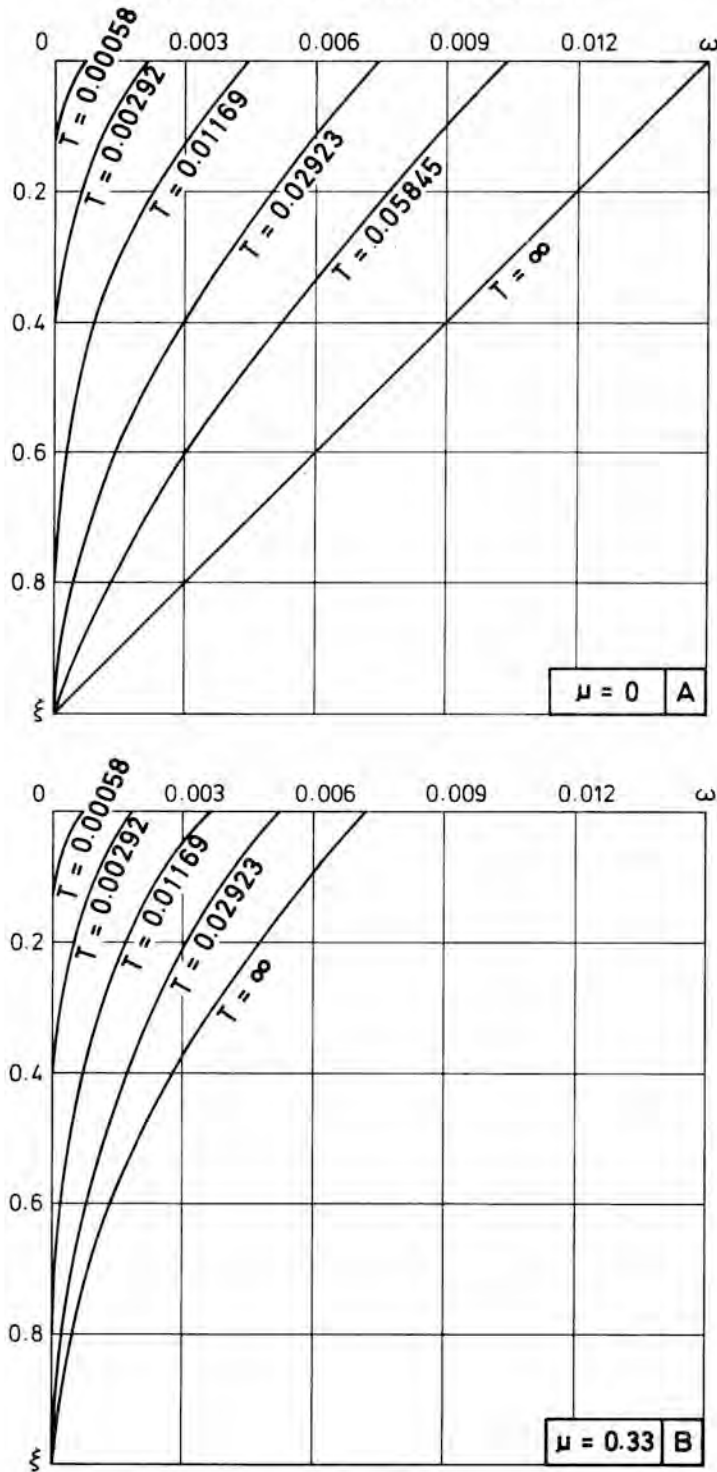


Fig. 3. Changes of Pore Pressure during Consolidation under Steady Load : (a) Both Szefer's and Biot's Theories,  $\mu = 0$ ; (b) Szefer's Theory,  $\mu = 0.33$ . Note  $\psi$ ,  $\xi$ ,  $\mu$  are dimensionless forms of pore pressure, vertical coordinate and threshold gradient, respectively.

**NONLINEAR CONSOLIDATION**



**Fig. 4. Vertical Displacement of Soil Skeleton during Consolidation under Steady Load :**  
 (a) Both Szefer's and Biot's Theories,  $\mu = 0$ ; (b) Szefer's Theory,  $\mu = 0.33$ .  
 Note  $\omega$ ,  $\xi$ ,  $\mu$  are dimensionless forms of displacement, vertical coordinate and threshold gradient, respectively.

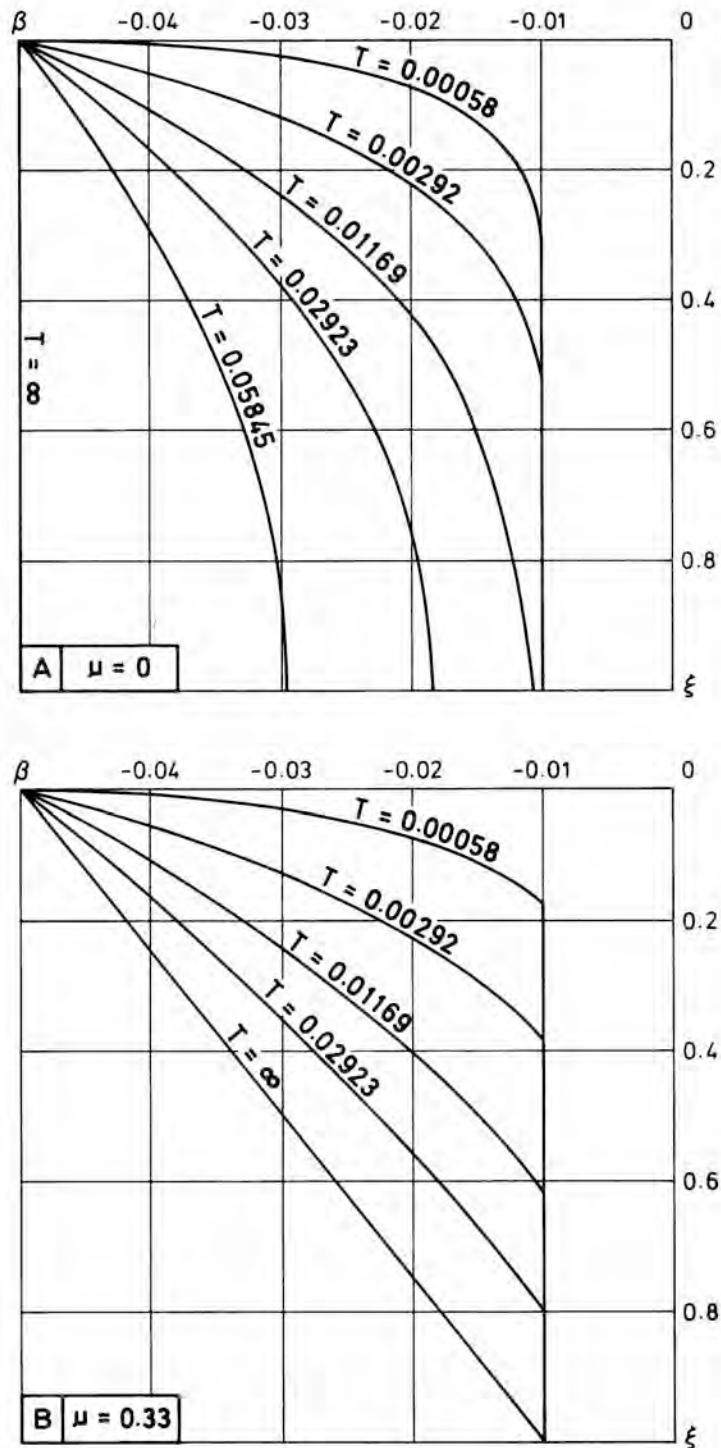


Fig. 5. Relative Changes of Soil Porosity during Consolidation under Steady Load, Szefer's Theory : (a)  $\mu = 0$ ; (b)  $\mu = 0.33$ . Note  $\beta$ ,  $\xi$ ,  $\mu$  are dimensionless forms of change of soil porosity, vertical coordinate and threshold gradient, respectively.

## NONLINEAR CONSOLIDATION

The results for vertical displacement (dimensionless parameter  $\omega$ ) for  $\mu = 0$  and  $\mu = 0.33$  are shown in Figures 4a and 4b respectively. These results correspond to consolidation under constant load, ie, for the period  $100 \text{ days} \leq t \leq 100,000 \text{ days}$  ( $0.00058 \leq T \leq \infty$ ). The results are reasonable and, as expected, the displacement at a given depth decreases as time increases. There are significant differences, however, between corresponding curves for  $\mu = 0$  and  $\mu = 0.33$  which shows the importance of the threshold gradient, if such a gradient is a feature of the particular soil undergoing consolidation. Again the displacement for  $\mu = 0$  corresponds to the Terzaghi and Biot theories.

Relative changes of soil porosity at different depths in the soil layer and at different times under steady load are shown in Figure 5. For  $\mu=0$ , the results are shown in Figure 5a and for  $\mu = 0.33$  the results are shown in Figure 5b; once again, differences in the corresponding figures are evident. These differences become marked as time  $t$  approaches infinity.

Relative changes in fluid density were also calculated, and the trend in the results was reasonable during the loading process. However, the density should approach its initial value at  $t = \infty$  and this does not happen. Thus, the particular relationship obtained by Szefer (shown at equation B26) requires modification, and consequently equation B31 also requires modification. Fortunately this equation is not coupled to the other equations of the system, and therefore can be considered separately.

## CONCLUSIONS

Szefer's general theory of consolidation is found to provide a fresh insight into the consolidation process and to enable the study of a number of changes in a soil layer as consolidation proceeds. Even for a relatively simple one-dimensional problem, the results are interesting from a cognitive point of view. The theory has been shown to compare well with others (where comparisons are possible) and it would, therefore, be worthwhile to make further investigation of the theory for more complex situations and for a variety of drainage conditions. An analysis of the constitutive equation B26 and its physical significance requires examination. Further research should also include a thermodynamic analysis of the consolidation process described by Szefer's equations. Attention should also be given to investigations which would be required in order to obtain the physical parameters for Szefer's theory.

The following main conclusions relate to the present study:

*ARENICZ & CHOWDHURY*

- (1) For a specific problem with specified drainage conditions, numerical solutions based on the general theory are in accord with the exact solutions for  $t = \infty$ .
- (2) For any arbitrary value of threshold gradient  $i_0 \neq 0$  and of time  $t \neq \infty$ , exact solutions cannot be obtained. However, the results on the basis of zero threshold gradient are in accord with the Terzaghi and Biot theories, both for the increasing load stage and the constant load stage.
- (3) The influence of non-zero value of the threshold gradient on the results (pore water pressure and skeleton displacement) was found to be completely in accordance with the results obtained by PARLANGE (1973), as also discussed in ARENICZ (1981).
- (4) In the case of a non-zero value of the initial hydraulic gradient, two adjacent zones occur in the porous medium-- a consolidating zone (with a liquid flow) and a zone without flow. The thickness of the consolidating zone increases with time. The maximal range of the consolidating zone does not necessarily extend through the whole layer. Its thickness is inversely proportional to the value of the initial hydraulic gradient for  $\mu \geq -Cq_0$ , or is equal to the layer's thickness for  $0 \leq \mu \leq -Cq_0$  (where  $\mu$  is the dimensionless hydraulic gradient and  $q_0$  is initial value of the dimensionless load function). The final ( $t = \infty$ ) values of the pore water pressure, its density, and the porosity of the soil are proportional to both the value of the initial hydraulic gradient and the thickness of the consolidating zone. For a certain instant of time and for a certain depth, the values of pore water pressure are always greater than the values obtained assuming Darcy's flow law ( $i_0 = 0$ ) and Biot's theory, whereas the value of skeleton displacement is always less.
- (5) As the external load increases, the porosity of the whole layer decreases. A decrease in the pore water pressure under constant external load causes a further decrease in the porosity, but only in the zone of flow. The final ( $t = \infty$ ) value of the soil porosity is less than its initial value.

ACKNOWLEDGEMENT

The work described herein was carried out at the Cracow Technical University and at the University of Wollongong and the authors wish to acknowledge the Department of Civil and Mining Engineering, University of Wollongong.

*ARENICZ & CHOWDHURY*

- (1) For a specific problem with specified drainage conditions, numerical solutions based on the general theory are in accord with the exact solutions for  $t = \infty$ .
- (2) For any arbitrary value of threshold gradient  $i_0 \neq 0$  and of time  $t \neq \infty$ , exact solutions cannot be obtained. However, the results on the basis of zero threshold gradient are in accord with the Terzaghi and Biot theories, both for the increasing load stage and the constant load stage.
- (3) The influence of non-zero value of the threshold gradient on the results (pore water pressure and skeleton displacement) was found to be completely in accordance with the results obtained by PARLANGE (1973), as also discussed in ARENICZ (1981).
- (4) In the case of a non-zero value of the initial hydraulic gradient, two adjacent zones occur in the porous medium-- a consolidating zone (with a liquid flow) and a zone without flow. The thickness of the consolidating zone increases with time. The maximal range of the consolidating zone does not necessarily extend through the whole layer. Its thickness is inversely proportional to the value of the initial hydraulic gradient for  $\mu \geq -Cq_0$ , or is equal to the layer's thickness for  $0 \leq \mu \leq -Cq_0$  (where  $\mu$  is the dimensionless hydraulic gradient and  $q_0$  is initial value of the dimensionless load function). The final ( $t = \infty$ ) values of the pore water pressure, its density, and the porosity of the soil are proportional to both the value of the initial hydraulic gradient and the thickness of the consolidating zone. For a certain instant of time and for a certain depth, the values of pore water pressure are always greater than the values obtained assuming Darcy's flow law ( $i_0 = 0$ ) and Biot's theory, whereas the value of skeleton displacement is always less.
- (5) As the external load increases, the porosity of the whole layer decreases. A decrease in the pore water pressure under constant external load causes a further decrease in the porosity, but only in the zone of flow. The final ( $t = \infty$ ) value of the soil porosity is less than its initial value.

ACKNOWLEDGEMENT

The work described herein was carried out at the Cracow Technical University and at the University of Wollongong and the authors wish to acknowledge the Department of Civil and Mining Engineering, University of Wollongong.



## NONLINEAR CONSOLIDATION

### REFERENCES

- ARENICZ, R. (1981). The Effect of the Initial Hydraulic Gradient on the Consolidation Process. *Archives of Hydrotechnics*, vol. 28, no. 2, pp. 251-263.
- BARDEN, L. (1965). Consolidation of Clay with Non-Linear Viscosity. *Geotechnique*, vol. 15, no. 4, pp. 345-362.
- BERRY, P.L. & POSKITT, T.J. (1972). The Consolidation of Peat. *Geotechnique*, vol. 22, no. 1, pp. 27-32.
- BERRY, P.L. & WILKINSON, W.B. (1969). The Radial Consolidation of Clay Soils. *Geotechnique*, vol. 19, no. 2, pp. 253-284.
- CHRISTENSEN, R.W. & WU, T.H. (1964). Analysis of Clay Deformation as a Rate Process. *ASCE J. of Soil Mech. and Found. Eng. Div.*, vol. 90, no. SM6, pp. 125-157.
- DAVIS, E.H. & RAYMOND, G.P. (1955). A Non-Linear Theory of Consolidation. *Geotechnique*, vol. 15, no. 1, pp. 161-173.
- ELNAGGAR, H.A., KRIZEK, R.J. & KARADI, G.M. (1972). Effect of Non-Darcian Behaviour on the Characteristics of Transient Flow. *J. of Hydrology*, vol. 13.
- ELNAGGAR, H.A., KRIZEK, R.J. & KARADI, G.M. (1973). Effect of Non-Darcian Flow on Time Rate of Consolidation. *J. of the Franklin Institute*, vol. 295, no. 5, pp. 323-337.
- GIBSON, R.F., ENGLAND, G.L. & HUSSEY, M.J.L. (1967). The Theory of One-Dimensional Consolidation of Saturated Clays. *Geotechnique*, vol. 17, no. 3, pp. 261-273.
- JANBU, N. (1965). Consolidation of Clay Layers based on Non-Linear Stress/Strain. *Proc. 6th Int. Conf. on Soil Mech. and Found. Eng.*, Montreal, vol. 2, pp. 83-87.
- McNABB, A. (1960). A Mathematical Treatment of One-Dimensional Soil Consolidation. *Quarterly of Applied Mathematics*, vol. 17, no. 4, pp. 337-347.
- OHTA, H. & HATA, S. (1973). Immediate and Consolidation Deformations of Clay. *Proc. 8th Int. Conf. on Soil Mech. and Found. Eng.*, Moscow, paper 2/30, pp. 193-196.
- PARLANGE, J.Y. (1973). Application of a New Analytical Method to a Model of Non-Darcian Consolidation in Clay Soils. *J. of Hydrology*, vol. 18.
- POOROOSHASB, H.B., LIELIEVRE, B. & SIVAPATHAM, T. (1973). Consolidation of Collapsible Clay Layers. *Proc. 8th Int. Conf. Soil Mech. and Found. Eng.*, Moscow, paper 4/28, pp. 167-171.
- POSKITT, T.J. (1967). A Note on the Consolidation of Clay with Non-Linear Viscosity. *Geotechnique*, vol. 17, no. 3, pp. 284-289.
- POSKITT, T.J. (1969). The Consolidation of Saturated Clay with Variable Permeability and Compressibility. *Geotechnique*, vol. 19, no. 2, pp. 234-252.
- POSKITT, T.J. (1970). Settlement Chart for Anisotropic Soils. *Geotechnique*, vol. 20, no. 3, pp. 325-330.
- POSKITT, T.J. (1971). The Numerical Solution of Non-Linear Consolidation Problems. *Int. J. for Numerical Methods in Engineering*, vol. 3, no. 1, pp. 5-11.
- POTTER, D. (1973). *Computational Physics*. J. Wiley, New York, pp. 77-81.
- RAYMOND, G.P. (1969). Consolidation of Deep Deposits of Homogeneous Clay. *Geotechnique*, vol. 19, no. 4, pp. 478-494.
- SCHMIDT, J.D. & WESTMANN, R.A. (1973). Consolidation of Porous Media with Non-Darcy Flow. *ASCE J. of the Eng. Mech. Div.*, no. EM6, pp. 1200-1215.
- SHAPIRO, N. (1970). A Note on Non-Linear Relationship Between Stress and Deformation. *Rheological Problems in Rock Mass (Problema Reologii Gornogo Poroda)*, Kijev.

ARENICZ & CHOWDHURY

- SHIRINKULOV, T. & DASIBIEKOV, A. (1966). A Note on Solution of One-Dimensional Problem of Consolidation of Three-Composite Soil Media with Non-Linear Rheological Properties. *News of the Academy of Sciences of Uzbekistan Soviet Socialist Republic (Izvestia Akademii Nauk Uzbeckoj Sovietskoj Socjalisticzeskoj Republiki)*, Mechanics, no. 5, pp. 27-32.
- SWARTZENDRUBER, D. (1962a). Modification of Darcy's Law for the Flow of Water in Soils. *Soil Science*, vol. 93, pp. 22-29.
- SWARTZENDRUBER, D. (1962b). Non-Darcy Behaviour in Liquid-Saturated Porous Media. *J. of Geoph. Res.*, vol. 67, no. 13, pp. 5205-5213.
- SWARTZENDRUBER, D. (1968). The Application of Darcy's Law. *Soil Sci. Soc. of America Proc.*, vol. 32, pp. 11-18.
- SZEFER, G. (1977). Non-Linear Problems of Consolidation Theory. *Polish-French Symposium of Applied Mechanics*, Cracov.

APPENDIX A – NOTATION

- $\partial$  – partial derivative
- $n$  – volume porosity of soil
- $F$  – fluid (superscript)
- $S$  – skeleton (superscript)
- $\rho$  – density
- $t$  – time
- $v$  – velocity vector
- $\lambda$  – surface porosity
- $T$  – Cauchy's partial stress tensor
- $\rho b$  – external body force
- $p$  – effective liquid pressure (pore water pressure)
- $B$  – deformation tensor
- $F$  – gradient deformation tensor
- $T$  – transposition symbol (superscript)
- $I$  – unit tensor
- $I_1^B, I_2^B, I_3^B$  – principal invariants of deformation tensor
- $\rho_R$  – initial density
- $n_R$  – initial (volume) soil porosity
- $K$  – permeability tensor
- $$\frac{ds}{dt}(\Omega) = \frac{\partial}{\partial t}(\Omega) + \text{div}(v^S \Omega)$$
- $$\frac{df}{dt}(\Omega) = \frac{\partial}{\partial t}(\Omega) + \text{div}(v^F \Omega)$$

### NONLINEAR CONSOLIDATION

div – divergence

$$\nabla(\Omega) = \Omega_{i, jj}$$

$$J = \left| \det \frac{x^i}{X^k} \right|$$

$x^i$  – Eulerean coordinate

$X^k$  – Lagrangean coordinate

$$\dot{\Omega} = \frac{d\Omega}{dt}$$

$\varepsilon$  – tensor of small deformations

$H$  – displacement gradient

$\Xi$  – relative change of fluid density =  $(\rho^F - \rho_R^F)/\rho_R^F$

$\beta$  – relative change of soil porosity =  $(n - n_R)/n_R$

$\theta$  – dilatation of fluid

$i_o$  – threshold gradient; value of hydraulic gradient below which no seepage takes place

$k$  – permeability coefficient

$A_1, N_1, Q_1, Q_2, R_1, a, b$  – physical parameters

$w$  – vertical displacement of soil skeleton

$z$  – vertical coordinate

$\sigma_{zz}$  – vertical stress of soil skeleton at depth  $z$

$h$  – thickness of layer

$g(t)$  – external load

$A, B, C, C_1, D_1, D_2, D_3, D_4, M_1, M_3, M_4$  – constants, as defined in Appendix D

$h^*$  – thickness of liquid flow zone

$\xi$  – dimensionless vertical coordinate =  $z/h$

$T$  – dimensionless time =  $t/Bh^2$

$\Psi$  – dimensionless effective liquid pressure =  $p/g_o$

$\omega$  – dimensionless displacement =  $w/h$

$\Psi_{zz}$  – dimensionless stress =  $\sigma_{zz}/g_o$

$q$  – dimensionless load function =  $g(T)/g_o$

$\chi$  – dimensionless thickness of liquid flow zone =  $h^*/h$

$\mu$  – dimensionless threshold gradient =  $hi_o/g_o$

APPENDIX B - ELEMENTS OF SZEFER'S GENERAL THEORY

The fundamental system of Szefer's consolidation theory contains twenty-two equations which are given below, in Szefer's original notation:

– continuity equation:

$$\frac{\partial(n\rho^F)}{\partial t} + \text{div}(n\rho^F v^F) = 0 \quad \dots\dots\dots (B1)$$

– dynamic equations:

$$\begin{aligned} & \text{div} (1 - \lambda) T^S + (1 - n) \rho^S b^S + n \nabla p - \nabla (\lambda p) \\ & - K^{-1} (v^S - v^F) = \frac{ds}{dt} \left\{ (1 - n) \rho^S v^S \right\} \quad \dots\dots\dots (B2) \end{aligned}$$

$$-n \nabla p + n \rho^F b^F + K^{-1} (v^S - v^F) = \frac{df}{dt} (n \rho^F v^F) \quad \dots\dots\dots (B3)$$

– geometric equations:

$$B = F F^T \quad \dots\dots\dots (B4)$$

– constitutive equations:

$$T^S = \alpha_0 I + \alpha_1 B + \alpha_2 B^2 \quad \dots\dots\dots (B5)$$

$$p = p (I_1^B, I_2^B, I_3^B, \rho^F) \quad \dots\dots\dots (B6)$$

$$n = n (I_1^B, I_2^B, I_3^B, \rho^F) \quad \dots\dots\dots (B7)$$

$$\lambda = (\lambda_1^B, \lambda_2^B, \lambda_3^B, \rho^F) \quad \dots\dots\dots (B8)$$

where:

$$K^{-1} = \Gamma_0 I + \Gamma_1 B + \Gamma_2 B^2 \quad \dots\dots\dots (B9)$$

$$\alpha_i = \alpha_i (I_1^B, I_2^B, I_3^B, \rho^F), \quad i = 0, 1, 2 \quad \dots\dots\dots (B10)$$

$$\Gamma_i = \Gamma_i (I_1^B, I_2^B, I_3^B, |v^S - v^F|, \rho^F), \quad i = 0, 1, 2 \quad \dots\dots\dots (B11)$$

$$\rho^S = \rho_R^S J_S^{-1} \quad \dots\dots\dots (B12)$$

Explanation of symbols is given in Appendix A.

A linearization procedure can be applied to the system of equations B1 to B8. The internal forces are negligible in the case of a static problem. Additionally, neglecting the body and internal forces in a liquid, and substituting:

$$\rho^S = \rho_R^S \quad \dots\dots\dots (B13)$$

$$\rho^F = \rho_R^F (1 + \Xi) \quad \dots\dots\dots (B14)$$

$$n = n_R (1 + \beta) \quad \dots\dots\dots (B15)$$

$$\lambda = \lambda_R = n_R \quad \dots\dots\dots (B16)$$

$$B = \varepsilon = \frac{1}{2} (H + H^T) \quad \dots\dots\dots (B17)$$

NONLINEAR CONSOLIDATION

$$K^{-1} = cI \quad \dots\dots\dots (B18)$$

$$c = \begin{cases} 0, & \text{for } p_{i,j} \leq j_0 \\ \frac{n}{n_R} k (p_{i,j} - i_0), & \text{for } p_{i,j} \geq i_0 \end{cases} \quad \dots\dots\dots (B19)$$

the system B1 to B8 can be transformed and reduced to the form (based on SZEFER, 1977):

$$\Xi + \beta + \theta = 0 \quad \dots\dots\dots (B20)$$

$$(1 - n_R) \operatorname{div} T^S - n_R \nabla p = 0 \quad \dots\dots\dots (B21)$$

$$\varepsilon = \frac{1}{2} (H + H^T) \quad \dots\dots\dots (B22)$$

$$v^F - v^S = \begin{cases} 0, & \text{for } p_{i,j} < i_0 \\ -n_R k (p_{i,j} - i_0) I, & \text{for } p_{i,j} > i_0 \end{cases} \quad \dots\dots\dots (B23)$$

$$T^S = 2N_1 \varepsilon - (A_1 I_1^\varepsilon + Q_1 \Xi) I \quad \dots\dots\dots (B24)$$

$$p = -Q_2 I_1^\varepsilon - R_1 \quad \dots\dots\dots (B25)$$

$$\beta = a I_1^\varepsilon - b \Xi \quad \dots\dots\dots (B26)$$

where  $\theta$  indicates the dilation of liquid. In the above equations, all terms of higher order have been neglected.

In the case of one-dimensional problems, the equation system B20 to B26 can be simplified and re-arranged even further, to the following convenient form:

$$\left( 2N_1 - A_1 + \frac{Q_1 Q_2}{R_1} \right) \frac{\partial^2 w}{\partial z^2} + \left( \frac{Q_1}{R_1} - \frac{n_R}{1-n_R} \right) \frac{\partial p}{\partial z} = 0 \dots (B27)$$

$$kH \frac{\partial^2 p}{\partial z^2} = \frac{b-1}{n_R R} \frac{\partial p}{\partial t} + \left( \frac{1+a}{n_R} - \frac{n_R-b}{n_R} \frac{Q_2}{R_1} \right) \frac{\partial^2 w}{\partial z \partial t} \dots\dots\dots (B28)$$

$$\sigma_{zz} = \left( 2N_1 - A_1 + \frac{Q_1 Q_2}{R_1} \right) \frac{\partial w}{\partial z} + \frac{Q_1}{R_1} p \quad \dots\dots\dots (B29)$$

$$\Xi = -\frac{1}{R_1} p - \frac{Q_2}{R_1} \frac{\partial w}{\partial z} \quad \dots\dots\dots (B30)$$

$$\beta = \frac{b}{R_1} p + \left( a + b \frac{Q_2}{R_1} \right) \frac{\partial w}{\partial z} \quad \dots\dots\dots (B31)$$

$$\text{where: } H = \begin{cases} 0, & \text{for } \frac{\partial p}{\partial z} \leq i_0 \\ 1, & \text{for } \frac{\partial p}{\partial z} > i_0 \end{cases} \dots\dots\dots (B32)$$

In the above equations, the commonly used notation for stress and displacement has been introduced.

APPENDIX C- SOLUTION OF SZEFER'S EQUATIONS FOR THE ONE-DIMENSIONAL CASE ASSUMING SATURATED UNDRAINED SOIL

Assuming that both the top and bottom edges of a uniformly loaded layer of soil are impermeable, and considering the one-dimensional case, the exact solution of the system of equations 1 to 5 is represented by the following formulae:

$$p = \frac{\left( 1 + a + \frac{b-1}{R_1} Q_2 \right) \frac{g(t)}{1-n_R}}{\frac{b-1}{R_1} \left( 2N_1 - A_1 + \frac{Q_1 Q_2}{R_1} \right) - \left( \frac{Q_1}{R_1} - \frac{n_R}{1-n_R} \right) \left( 1 + a + \frac{b-1}{R_1} Q_2 \right)} \quad (C1)$$

$$w = \frac{\frac{b-1}{R_1} (h-z) \frac{g(t)}{1-n_R}}{\frac{b-1}{R_1} \left( 2N_1 - A_1 + \frac{Q_1 Q_2}{R_1} \right) - \left( \frac{Q_1}{R_1} - \frac{n_R}{1-n_R} \right) \left( 1 + a + \frac{b-1}{R_1} Q_2 \right)} \quad (C2)$$

$$\sigma_{zz} = \frac{\left\{ \frac{1-b}{R_1} \left( 2N_1 - A_1 + \frac{Q_1 Q_2}{R_1} \right) + \frac{Q_1}{R_1} \left( 1 + a + \frac{b-1}{R_1} Q_2 \right) \right\} \frac{g(t)}{1-n_R}}{\frac{b-1}{R_1} \left( 2N_1 - A_1 + \frac{Q_1 Q_2}{R_1} \right) - \left( \frac{Q_1}{R_1} - \frac{n_R}{1-n_R} \right) \left( 1 + a + \frac{b-1}{R_1} Q_2 \right)} \quad (C3)$$

$$\bar{u} = \frac{-\frac{1}{R_1} (1+a) \frac{g(t)}{1-n_R}}{\frac{b-1}{R_1} \left( 2N_1 - A_1 + \frac{Q_1 Q_2}{R_1} \right) - \left( \frac{Q_1}{R_2} - \frac{n_R}{1-n_R} \right) \left( 1 + a + \frac{b-1}{R_1} Q_2 \right)} \quad (C4)$$

$$\beta = \frac{\frac{1}{R_1} (b+a) \frac{g(t)}{1-n_R}}{\frac{b-1}{R_1} \left( 2N_1 - A_1 + \frac{Q_1 Q_2}{R_1} \right) - \left( \frac{Q_1}{R_1} - \frac{n_R}{1-n_R} \right) \left( 1 + a + \frac{b-1}{R_1} Q_2 \right)} \quad (C5)$$

Explanation of symbols is given in Appendix A.



*NONLINEAR CONSOLIDATION*

APPENDIX D- TRANSFORMATION OF EQUATIONS INTO  
DIMENSIONLESS FORM

Integrating equation 1 with respect to  $z$ , and considering the boundary conditions (equations 7 to 11), gives:

$$\left(2N_1 - A_1 + \frac{Q_1 Q_2}{R_1}\right) \frac{\partial w}{\partial z} + \left(\frac{Q_1}{R_1} - \frac{n_R}{1-n_R}\right) p = -g(t) \dots\dots (D1)$$

which, together with equation 2, allows for the elimination of variable  $w$ , and yields:

$$\left\{ \frac{b-1}{R_1} - \frac{\left(\frac{Q_1}{R_1} - \frac{n_R}{1-n_R}\right) \left(1 + a + \frac{b-1}{R_1} Q_2\right)}{2N_1 - A_1 + \frac{Q_1 Q_2}{R_1}} \right\} \frac{\partial p}{\partial t} \frac{1 + a + \frac{b-1}{R_1} Q_2}{2N_1 - A_1 + \frac{Q_1 Q_2}{R_1}} \frac{\partial g}{\partial t}$$

$$= n_R k \frac{\partial^2 p}{\partial z^2} \dots\dots\dots (D2)$$

Denoting by:

$$B = \frac{1}{n_R k} \left\{ \frac{b-1}{R_1} - \frac{\left(\frac{Q_1}{R_1} - \frac{n_R}{1-n_R}\right) \left(1 + a + \frac{b-1}{R_1} Q_2\right)}{2N_1 - A_1 + \frac{Q_1 Q_2}{R_1}} \right\} \dots\dots (D3)$$

$$A = - \frac{1}{n_R k} \frac{1 + a + \frac{b-1}{R_1} Q_2}{2N_1 - A_1 + \frac{Q_1 Q_2}{R_1}} \dots\dots\dots (D4)$$

Equation D2 can be rewritten as:

$$H \frac{\partial^2 p}{\partial z^2} = B \frac{\partial p}{\partial t} + A \frac{\partial g}{\partial t} \dots\dots\dots (D5)$$

Introducing the dimensionless variables:

$$\zeta = \frac{z}{h} \dots\dots\dots (D6)$$

$$T = \frac{t}{Bh^2} \dots\dots\dots (D7)$$

$$\Psi = \frac{p}{g_0} \dots\dots\dots (D8)$$

$$\omega = \frac{w}{h} \dots\dots\dots (D9)$$

$$\Psi_{zz} = \frac{\sigma_{zz}}{g_0} \dots\dots\dots (D10)$$

$$q = \frac{g(T)}{g_0} \dots\dots\dots (D11)$$

where  $g_0 = \max \{ g(t) \}$  ..... (D12)

and putting:

$$C = \frac{A}{B(1-n_R)} \dots\dots\dots (D13)$$

$$C_1 = \frac{A}{B} \dots\dots\dots (D14)$$

$$D_1 = \frac{\left( R_1 \frac{n_R}{1-n_R} - Q_1 \right) g_0}{R_1 (2N_1 - A_1) + Q_1 Q_2} \dots\dots\dots (D15)$$

$$D_2 = \frac{n_R}{1-n_R} \dots\dots\dots (D16)$$

$$D_3 = \frac{-(g_0 + Q_2 D_1)}{R_1} \dots\dots\dots (D17)$$

$$D_4 = \left( a + b \frac{Q_2}{R_1} \right) D_1 + \frac{b g_0}{R_1} \dots\dots\dots (D18)$$

$$M_1 = \frac{-R_1 q_0}{R_1 (2N_1 - A_1) + Q_1 Q_2} \dots\dots\dots (D19)$$

$$M_3 = \frac{-Q_2 M_1}{R_1} \dots\dots\dots (D20)$$

$$M_4 = \left( a + b \frac{Q_2}{R_1} \right) M_1 \dots\dots\dots (D21)$$

$$H^* = \begin{cases} 0, & \text{for } \frac{\partial \Psi}{\partial \xi} < \mu = \frac{h}{g_0} i_0 \\ 1, & \text{for } \frac{\partial \Psi}{\partial \xi} \geq \mu = \frac{h}{g_0} i_0 \end{cases} \dots\dots\dots (D22)$$

*NONLINEAR CONSOLIDATION*

the dimensionless system equivalent to equations 1 to 5 can be found :

$$H^* \frac{\partial^2 \Psi}{\partial \xi^2} = \frac{\partial \Psi}{\partial T} + C_1 \frac{\partial g}{\partial T} \dots\dots\dots (D23)$$

$$\frac{\partial \omega}{\partial \xi} = D_1 \Psi + M_1 q \dots\dots\dots (D24)$$

$$\Psi_{zz} = D_2 \Psi - q \dots\dots\dots (D25)$$

$$\Xi = D_3 \Psi + M_3 q \dots\dots\dots (D26)$$

$$\beta = D_4 \Psi + M_4 q \dots\dots\dots (D27)$$

together with the boundary conditions :

$$\Psi(\xi = 0, T) = 0 \dots\dots\dots (D28)$$

$$\omega(\xi = 1, T) = 0 \dots\dots\dots (D29)$$

$$\Psi(\xi = 1, T) = -Cq, \text{ for } H^*(\xi = 1, T) = 0 \dots\dots\dots (D30)$$

$$\left. \frac{\partial \Psi}{\partial \xi} \right|_{\xi = 1, T} = \mu, \text{ for } H^*(\xi = 1, T) = 1 \dots\dots\dots (D31)$$

Explanation of symbols is given in Appendix A.

APPENDIX E— DETAILS OF NUMERICAL SOLUTION

Rewriting equation 12 as finite differences and using the Crank-Nicholson method for  $i^{\text{th}}$  time and for  $j^{\text{th}}$  discrete values of  $\xi$  (designated using  $m$  inside points,  $j = 1, 2 \dots m$ ), this system of algebraic equations can be obtained:

$$L_i - L_{i-1} = \frac{\Delta T}{2(\Delta \xi)^2} E(Y_i L_i + Y_{i-1} L_{i-1}) - C_1(q_i - q_{i-1}) \dots\dots\dots (E1)$$

where, for simplification of the notation, the following matrices have been introduced:

$$E = \begin{bmatrix} -2 & 1 & 0 & \dots & 0 & 0 & 0 \\ 1 & -2 & 1 & \dots & 0 & 0 & 0 \\ 0 & 1 & -2 & \dots & 0 & 0 & 0 \\ \vdots & \vdots & \vdots & \dots & \vdots & \vdots & \vdots \\ 0 & 0 & 0 & \dots & -2 & 1 & 0 \\ 0 & 0 & 0 & \dots & 1 & -2 & 1 \\ 0 & 0 & 0 & \dots & 0 & 1 & -2 \end{bmatrix} \dots\dots\dots (E2)$$

$$L = \begin{pmatrix} \Psi_{i,1} \\ \vdots \\ \Psi_{i,j} \\ \vdots \\ \Psi_{i,m} \end{pmatrix} \dots\dots\dots (E3)$$

$$Y = \begin{pmatrix} H_{i,1}^* \\ \vdots \\ H_{i,j}^* \\ \vdots \\ H_{i,m}^* \end{pmatrix} \dots\dots\dots (E4)$$

Considering the whole system (equations 12 to 16) together with the boundary conditions (equations 17 to 20), the numerical solving procedure has been formulated as the three following steps:

- (a) iterational (on account of function  $Y$ ) solution to the system of algebraic equations E1 using the Gauss method of elimination and taking into account the boundary conditions (equations 17 to 20), the homogeneous initial conditions, and the value of  $H_{i,j}^*$  from a previous time instant as a starting value for iteration. As a result, this step gives a value of dimensionless pore water pressure  $\Psi_{i,j}$  ;
- (b) the computation of dimensionless displacement of the skeleton from:

$$\omega_{i,j} = \omega_{i,j-1} + (D_1 \Psi_{i,j} + M_1 q_1)(\Delta \xi) \dots\dots\dots (E5)$$

and also the functions  $\Psi_{zz}$ ,  $\Xi$ ,  $\beta$  from Equations 14 to 16, respectively, using the above mentioned initial and boundary conditions;

- (c) the computation of dimensional functions :

$$p_{i,j} = g_o \Psi_{i,j} \dots\dots\dots (E6)$$

$$w_{i,j} = h \omega_{i,j} \dots\dots\dots (E7)$$

$$(\sigma_{zz})_{i,j} = g_o (\Psi_{zz})_{i,j} \dots\dots\dots (E8)$$

$$n_{i,j} = (1 + \beta_{i,j}) n_R \dots\dots\dots (E9)$$

$$\rho_{i,j} = (1 + \Xi_{i,j}) \rho_R^F \dots\dots\dots (E10)$$

On the basis of this, a flow chart and computer program for CDC CYBER-72 have been prepared.

Analysing both the roles and the dimensions of all physical parameters in the system of equations 1 to 5, the following data have been chosen arbitrarily for a layer of clay soil (corresponding dimensionless values have been given in brackets):

### NONLINEAR CONSOLIDATION

- (a) consolidating load - increases linearly during 100 days ( $0.585 \times 10^{-3}$ ) from zero to  $20 \text{ MN/m}^2$  (1.0), and then remains constant up to 100,000 days (0.585);
- (b) thickness of consolidated layer—20m (1.0);
- (c) values of the threshold gradient ( $\partial p/\partial z$ )—0 (Darcy's law), 0.17, 0.33,  $0.50 \text{ MN/m}^3$  (0, 0.17, 0.33, 0.50);
- (d) values of remaining physical parameters:  
 $Q_1 = 742 \text{ MN/m}^2$ ,  $Q_2 = -263 \text{ MN/m}^2$ ,  $N_1 = 220 \text{ MN/m}^2$ ,  
 $R_1 = -263 \text{ MN/m}^2$ ,  $A_1 = -146 \text{ MN/m}^2$ ,  $k = 10^{-4} \text{ m}^4/\text{MN day}$ ,  
 $a = 2.825$ ,  $b = 0.509$ ,  $n_R = 0.277$ ,  $\rho_R = 1.000 \text{ tonne/m}^3$   
( $C = -0.333$ ,  $C_1 = -0.258$ ,  $D_1 = 0.047$ ,  $D_2 = 0.293$ ,  
 $D_3 = 0.029$ ,  $D_4 = 0.118$ ,  $M_1 = -0.015$ ,  $M_3 = 0.015$ ,  
 $M_4 = -0.050$ )

All computations have been executed up to 100,000 days, after which the values of all functions remain practically unchanged. Hence, these values can be taken as the final ones, and they are indicated by the symbol  $\infty$  on the graphs. The results of computation for  $\partial p/\partial z = 0$  and 0.33 are presented graphically by the diagrams in the text.

Explanation of symbols is given in Appendix A.

## **INTEGRITY AND UPLIFT TESTING OF PILES IN A ROCK FILLED RECLAMATION**

**G.L. EVANS\*, P.P. WONG\* and H. SANDERS\***

### **SYNOPSIS**

A pilot study was undertaken by the Hong Kong Housing Department to ascertain the performance of 18 piles driven or cast through 9.5 m of crushed rock fill in a reclamation. These piles represented a range of available pile types, including steel sheet piles, H-piles, tubular piles, precast concrete piles, bored piles and a barrette. Testing included dynamic monitoring during driving, steady state vibration tests after driving, and uplift load tests on driven piles, as well as sonic logging in the cast-in-place piles. The results indicated that the integrity tests were generally reliable, but tended to be conservative. Values of skin friction and stiffness were derived from pull out tests and compared with the indirect integrity tests, with which they were in reasonable agreement.

### **INTRODUCTION**

To ascertain the constraints and possible construction problems associated with piling through crushed rock reclamation fill, a pilot study was carried out in 1984 by the Hong Kong Housing Department at Junk Bay, as reported by EVANS et al (1987). The study involved the driving of fourteen steel and concrete piles of various types and sections through 9.5 m of angular coarsely graded rock fill and 9 m of soft alluvium (silty sand) into completely decomposed volcanic rock. Rock level was at about 24 m depth, but the driven piles were stopped before reaching this level. Four cast-in-place piles were installed to rock level, to determine the rates of construction and possible concreting problems.

Integrity tests were carried out on all piles to assess their structural condition. Most driven piles were later extracted for visual inspection, and for verification of the results from the various types of integrity tests. This paper describes the various tests used, and evaluates their suitability.

#### *The Site*

The site chosen for the pilot study was at the seaward edge of a reclamation in Junk Bay, Hong Kong (Figure 1). The site was flat (elevation of about + 8.25 m above Principal Datum) and located near the head of Junk Bay. The site was formed during the latter part of 1983 and early 1984 as part of an

\* Housing Department, Hong Kong.



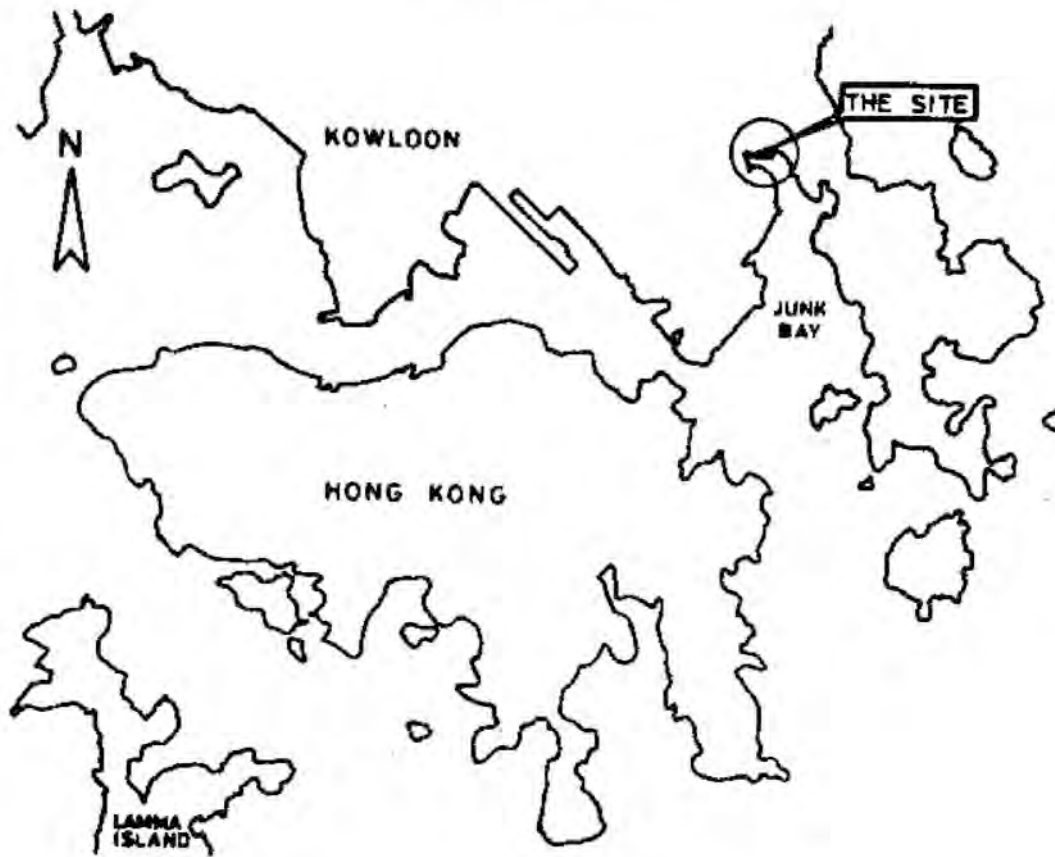


Fig. 1. Location of Site.

extensive site formation contract. Filling comprised crushed rock transported to the site by lorry or barge.

The inferred soil profile, the pile locations and the installed pile levels are shown in Figure 2. Beneath the 0.5 m thick surface soil layer was a 9.5 m thick layer of crushed rock fill, which was in turn underlain by a 9 m thick layer of alluvium. The alluvium was underlain by completely decomposed volcanic rock (CDV) which transitioned to moderately/slightly decomposed volcanic rock (MDV/SDV) at a depth of 24 m. The rock fill was slightly decomposed tuff, crushed primarily to cobble sized material (60 to 200 mm).

#### *The Piles*

The piles used in this test included four steel H-piles, three steel sheet piles, three prestressed high strength concrete piles, four steel tubular piles, three large diameter machine bored piles and a barrette (Figure 2). The three

INTEGRITY TESTING

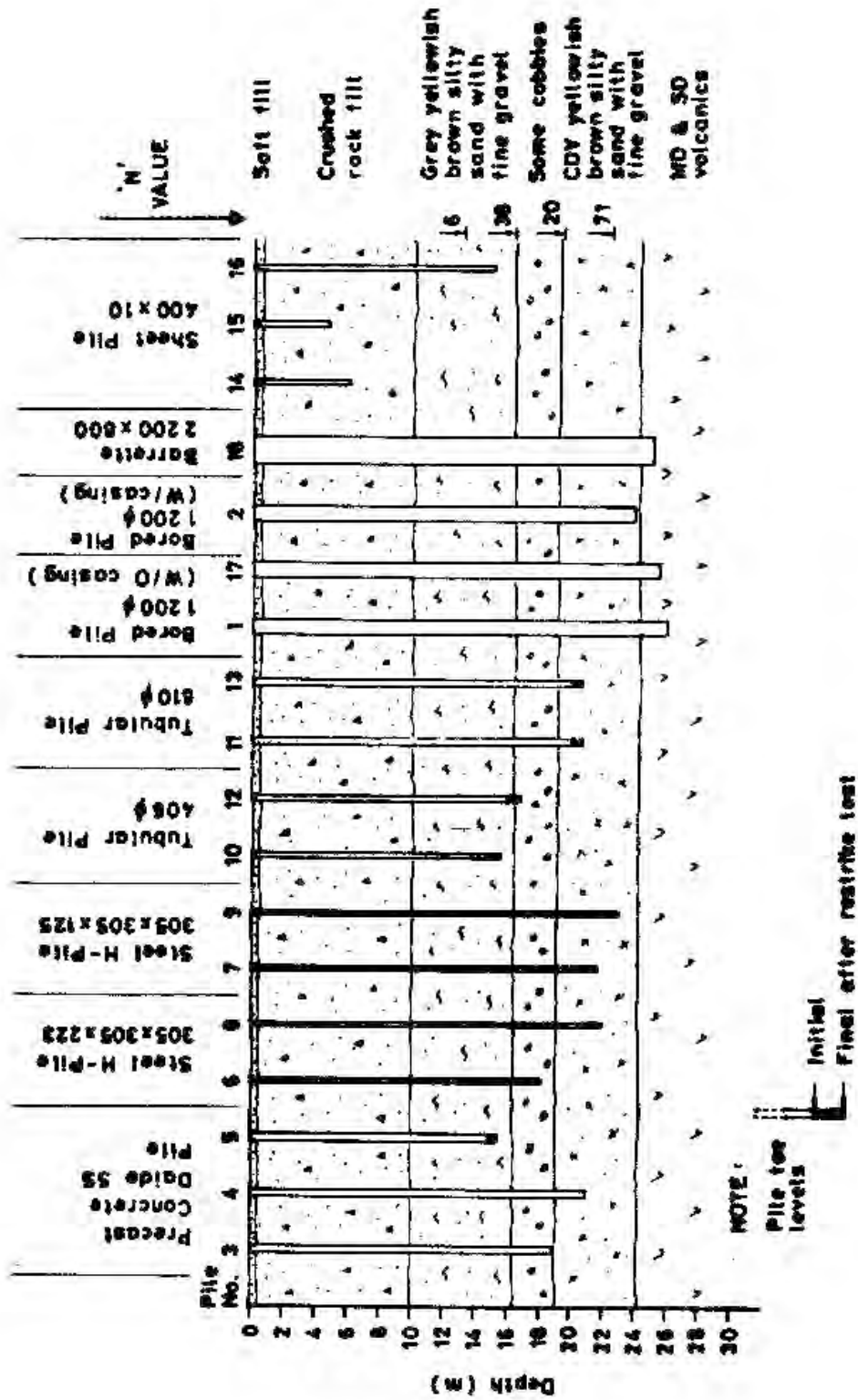


Fig. 2. Ground Profile and Piles.

prestressed concrete piles were 'Daido' piles, which are commonly available in Hong Kong. 'Daido' is the Japanese trade name used by the local manufacturer. The 'Daido SS' pile is a prestressed, tubular, 500 mm diameter pile with a wall thickness of 100 mm. The pile concrete is a high grade mix, steam cured and autoclaved at high temperature, with a crushing strength of at least 78 MPa.

#### TESTING METHODS

Integrity tests were performed during and after installation of the piles to assess the presence, location and severity of structural damage. The types of tests chosen were those that are in general use in Hong Kong, and the opportunity was taken where possible to assess each test method for reliability and accuracy. The tests conducted were :

- (a) dynamic monitoring and analysis of driven piles (by classical wave equation techniques) during the driving operation to quantify driving stresses and to check for damage in the piles ;
- (b) steady-state vibration testing of Daido piles after driving to assess their structural integrity ;
- (c) uplift loading tests on driven piles to quantify the skin friction resistance in the rock fill and underlying alluvium ;
- (d) sonic logging ;
- (e) mechanical coring of the bored piles and the barrette to assess the concrete quality.

The test methods are further described below.

##### *Dynamic Analysis*

The dynamic analysis test involves the measurement of strain and acceleration of the pile head during impact to determine the stresses of driving, the energy imparted to the pile, the driving efficiency, and to estimate the static load capacity, as described by SMITH (1960) and BERINGEN *et al* (1980). Two strain gauges and two accelerometers were attached to the pile about 1 m from the top. These devices were connected to a signal conditioning unit, an oscilloscope and a high precision tape recorder. For selected blows of the diesel hammer, detailed analysis of the strain and acceleration readings provided plots of force against time, to which finite difference analysis was applied to provide the output information. Figure 3 outlines the expressions used in this analysis.

INTEGRITY TESTING

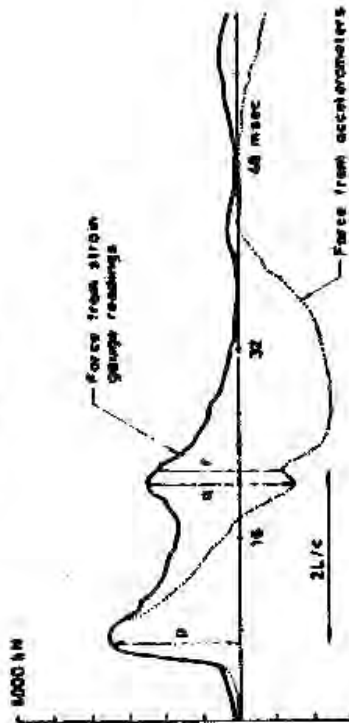
Determination of Static Resistance

$W_{dyn} - W_{dyn} = P_{dyn} \text{ (kN)}$   
 $V_{low} = 2 \times \left( \frac{F_{imp}}{EA} \right) - \left( \frac{P_{dyn}}{mE} \right) \times \frac{L}{c} \text{ (m/s)}$   
 $Smith : P_{st} = \frac{P_{dyn}}{1 + J_s \times V_{low}} \text{ (kN)}$   
 $Case : P_{st} = P_{dyn} - J_c = \frac{EA}{c} \times V_{low} \text{ (kN)}$

- Where :
- c : total dynamic resistance (kN)
  - W<sub>dyn</sub> : dynamic friction (kN)
  - P<sub>dyn</sub> : dynamic tip resistance (kN)
  - V<sub>low</sub> : velocity of pile tip (m/s)
  - F<sub>imp</sub> : max. pile force at impact (kN)
  - E : Young's modulus (kN/m<sup>2</sup>)
  - A : pile area at instrumentation level (m<sup>2</sup>)
  - c : wave speed (m/s)
  - m : pile mass (kN)
  - L : length of pile below gauges (m)
  - $\frac{EA}{c}$  : pile impedance; for uniform piles they are equal but as the area is the area at instrumentation level m is not determined from this area only when there are changes in pile dimensions

- J<sub>c</sub> : Case damping factor (dimensionless)
- J<sub>s</sub> : Smith damping factor (s/m)
- P<sub>st</sub> : Static tip resistance (kN)
- Stiff capacity = W<sub>dyn</sub> + P<sub>st</sub> (kN)

TYPICAL PLOT  
(FORCE VS TIME)



- L : pile length
- c : wave speed in pile
- Z axis : time in milliseconds
- Y axis : force in kN
- W<sub>dyn</sub> =  $\frac{2D - r}{2}$  (Total dynamic resistance)
- W<sub>dyn</sub> = q (Dynamic friction resistance)
- P<sub>dyn</sub> =  $\frac{2D - r}{2} - q$  (Dynamic point resistance)
- F = p (Maximum impact force)

Fig. 3. Interpretation of Dynamic Monitoring of Pile Driving.

Analysis of typical hammer blows were performed after each 5 m of penetration for each driven pile. A further test was done some days after driving (i.e. the restrike test), to analyse and assess the changes in driving resistance after a time lapse with reconsolidation around the piles.

#### *Vibration Testing*

The vibration method of integrity testing involves the application of an oscillating vertical force of varying frequency to the head of the pile. Measurements are made of the vibrating force and the pile velocity with time, to determine the pile's response. Only the Daido piles were subjected to vibration tests, as the primary purpose of this test is to detect faults in the concrete, and to estimate stiffness.

Plots were made of the changes in pile head velocity with changes in frequency, which is generally in the range 0 to 1000 Hz. At low frequencies (less than 100 Hz), it is assumed that the pile/soil mass is vibrated as a unit, and the measurements reflect the stiffness to vertical load application. At high frequencies, the pile is excited independently of the soil, and a measurement is obtained of the pile length (or the distance down to any crack or defect in the pile). A detailed explanation of the interpretation of this type of test is given in CIRIA Report No. PG4 (CIRIA, 1977), whilst TIJOU (1984) provides an account of some Hong Kong experiences with the test. The basic test method adopted for this study has been derived from the work of DAVIS & DUNN (1974).

The test results are usually presented in the form of a graph of the pile's mechanical admittance (defined as the ratio of pile head velocity,  $V$ , to vibration force,  $F$ ) as a function of frequency,  $f$ . The gradient of the initial portion of this curve reflects the pile stiffness, whilst the distance between successive resonant peaks allows calculation of the pile length. Concrete quality (or alternatively, the cross sectional area) can be obtained by reference to the geometric mean height of the resonant portions of the vibration curve.

Several values of pile stiffness can be derived from the admittance curves. A pile supported on a rigid base provides the maximum possible stiffness that the pile could have, and is designated  $E'_{\max}$ . On the other hand, a pile with no base support would have the minimum possible stiffness, usually designated  $E'_{\min}$ . This latter stiffness can be compared with stiffness results from uplift tests.

DAVIS & DUNN (1974) show that  $E'_{\max}$  can be calculated from the expression :

### INTEGRITY TESTING

$$E' \text{ max} = \frac{AcEc}{L} L d \left( \frac{P}{Q} \right)^{\frac{1}{2}} \text{ [kN/mm]} \dots\dots\dots (1)$$

- where
- Ac = cross-sectional area of pile
  - Ec = modulus of elasticity of concrete
  - L = length of pile
  - d = damping factor
  - P, Q = maximum and minimum values, respectively, of measured mechanical admittance (i.e. peak & trough at resonance)

Similarly,  $E' \text{ min}$  is given by :

$$E' \text{ min} = \frac{AcEc}{L} L d \left( \frac{Q}{P} \right)^{\frac{1}{2}} \text{ [kN/mm]} \dots\dots\dots (2)$$

An important limitation of the vibration test pointed out by HOLDEN (1984) is that the quality of the test results usually deteriorates for pile length to diameter (L/D) ratios exceeding 20. Only for end-bearing piles through soft deposits will the results be reasonable for L/D ratios of up to 30. It is claimed by TIJOU (1984), however, that in Hong Kong successful tests have been carried out at favourable sites for L/D ratios up to 50. The Daido piles tested in this pilot study had L/D ratios of 32 and 48, which are outside the normally acceptable limits.

The equipment attached to the piles in this study comprised :

- (a) an electrodynamic vibrator;
- (b) a force transducer, incorporated in the vibrator assembly;
- (c) a particle velocity transducer (geophone).

A harmonic oscillator, which is connected by cable to the vibrator, is usually located with the recording equipment. The latter included a self-calibrating spectrum analyser to carry out analysis of the velocity transducer output, and an analogue XY plotter.

#### *Uplift Loading Tests*

The resistance to an uplift load was measured, as this would be an aid in future predictions of negative skin friction effects at similar sites. The test method required, firstly, the application of an upward force at the top of the pile to cause a constant rate of uplift, and as a second stage of the test, each pile was subjected to a maintained load. A jacking system capable of applying



up to 4000 kN was used, along with four dial gauges reading to 0.01 mm. Precise levelling techniques were also used to verify the dial gauge readings, by reference to a benchmark remote from the test area.

For the first part of the tests, the piles were subjected to a varying uplift load in order to cause a steady deflection of the pile of 1 mm per 5 minutes. Loads and deflections were measured every minute. Following this test, the second stage was performed by applying about eight increments of load, each of which was about one eighth of the maximum load previously measured. Each increment was maintained for sufficient time that the pile head movement had decreased to 0.05 mm in 10 minutes.

#### *Sonic Logging Tests*

The sonic logging method, as described by CIRIA (1977) and TIJOU (1984), involves the measurement of travel times of sonic pulses from a transmitter probe (lowered within a cast-in tube in the pile) passing through the pile material to a receiver probe located in a similar tube nearby. The location of poor concrete quality, such as areas of segregation, mud or soil inclusions, or low concrete strength, can be detected by variations in the signal traces of the arriving waves.

The two piezo-electric probes were lowered down different vertical tubes, which were filled with water to provide a medium to transmit the pulses into the pile. The two probes were then both steadily raised at the same rate to keep them within the same horizontal plane, whilst output results were displayed on an oscilloscope and then photographed. Pulses were generated at about 10 Hz, and the probes were raised at about 100 mm/sec. The three bored piles and the barrette were each subjected to sonic logging in this manner, in order to assess the quality of their construction.

#### *Concrete Coring*

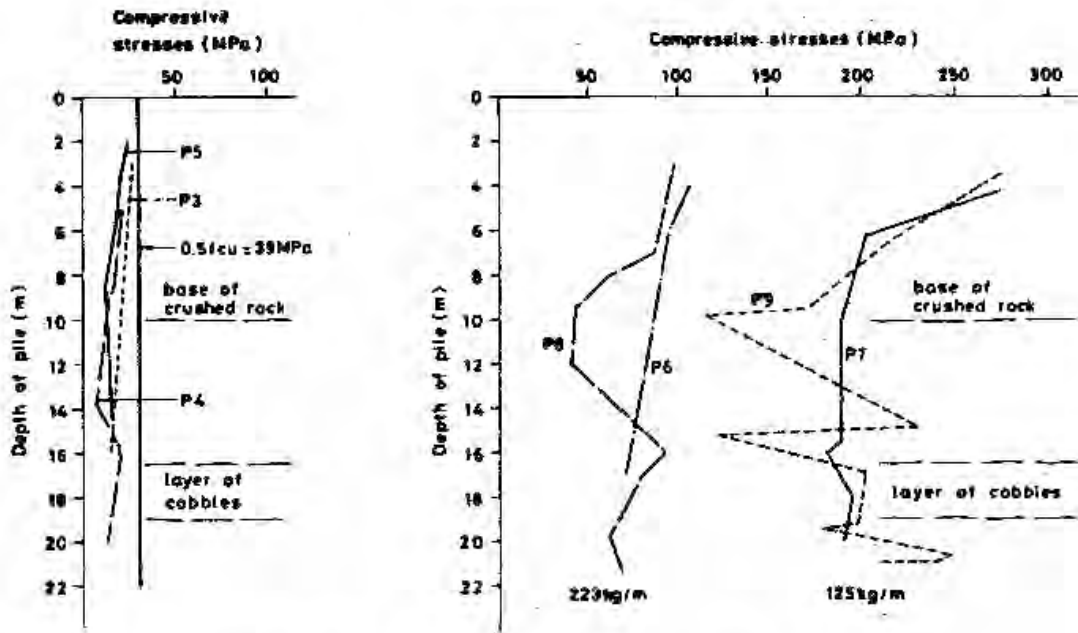
Concrete core samples from the cast-in-place bored piles and the barrette were obtained to provide a physical check on the condition of the concrete and to check the integrity tests performed. Drilling was generally conducted in the centre of the pile, and cores 110 mm in diameter were obtained.

### DYNAMIC TESTING OF DRIVEN PILES

#### *Impact Stresses*

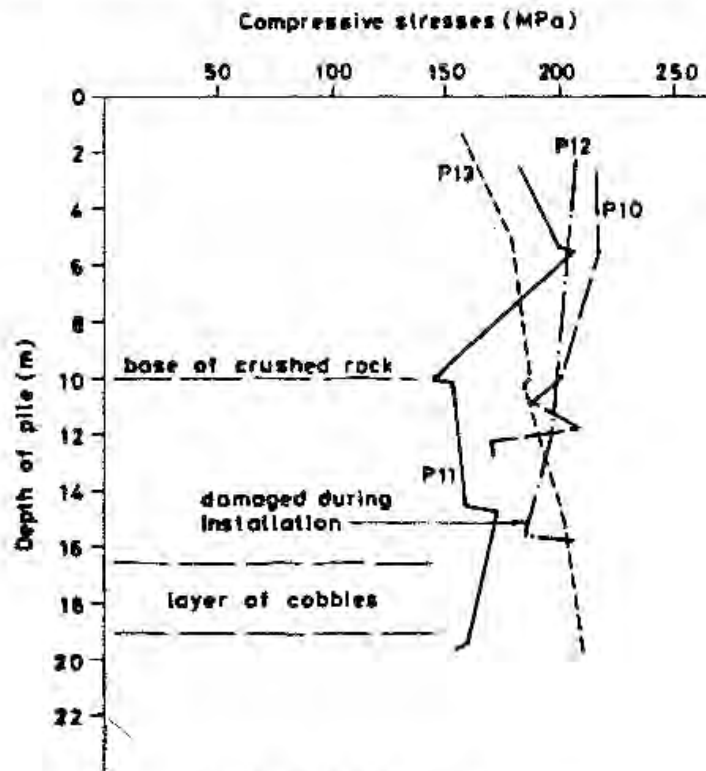
Plots of force versus time were obtained from the accelerometers and strain gauges fixed to the pile head. The peak compressive stress at the top

INTEGRITY TESTING



(a) Concrete Daido Piles

(b) Steel H-Piles



(c) Steel Tubular Piles

Fig. 4. Compressive Stresses at Impact.

of the pile occurred typically within 4 to 6 milliseconds after commencement of impact by the hammer. Figure 4 shows the measured peak compressive stresses for all driven piles throughout their installation.

As shown in Figure 4a, the impact stresses in the Daido Piles reduced steadily with depth, from initial values of about 30 MPa within the first few metres of penetration. In each case, it appears that throughout driving the compressive stresses were within the maximum allowable value for the concrete (50% of the concrete compressive strength of 78 MPa).

The impact stresses for the four H-piles show a gradual reducing trend with depth (Figure 4b). It seems that the lighter of the two sections (the 305 × 305 × 125 kg/m section) may have had inadequate cushioning in the early stages of driving, as impact stresses for both piles of this type apparently approached 80% of the yield stress of the pile material (assumed to be 350 MPa) and reached 89% of the allowable stress (0.9 × yield stress).

The peak impact stresses for all of the steel tubular piles are shown in Figure 4c. A more haphazard distribution of stresses was evident, with no consistent trend of changing stresses during penetration. Generally, stresses were in the range from 150 to 220 MPa, as compared to the material's yield stress of 350 MPa.

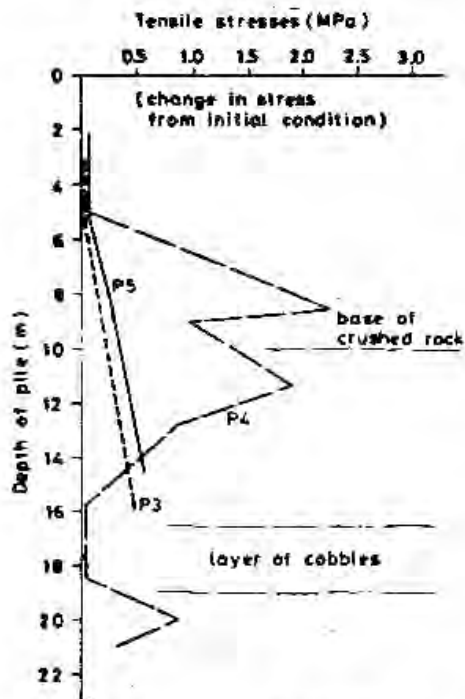
### *Tensile Stresses*

Tensile stresses are produced in a pile when there is low resistance at the tip and the initial compressive wave is reflected as a tensile wave. It is probable, therefore, that tensile stresses in all piles in this study would likely be zero, or very small, in the crushed rock fill, but they would steadily increase as the pile toe approached the bottom of the fill layer where the strata is softer. Tension would also remain high when driving through the softer alluvium below the fill.

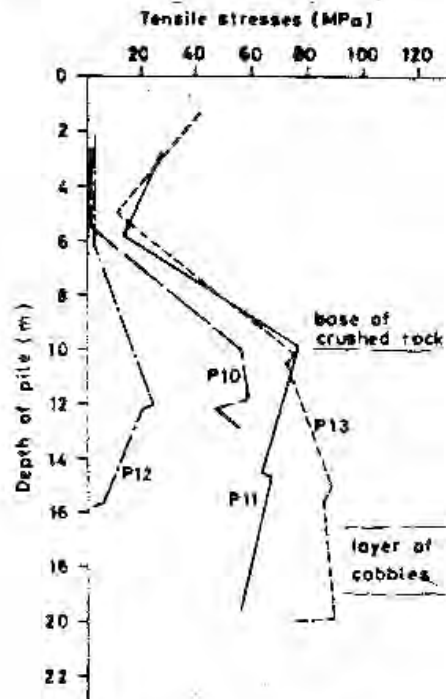
Figure 5 shows the distribution of tensile stresses for all piles. Although there is some scatter, tension is higher near the fill/alluvium interface and in the alluvium, as expected.

For the Daido piles, any assessment of tensile stresses must take into account the amount of compressive prestress existing in the pile. The 500 mm diameter Daido piles used in this study were manufactured with a prestress of 5.26 MPa, which was provided by 10 longitudinal reinforcement bars, each with a diameter of 11 mm.

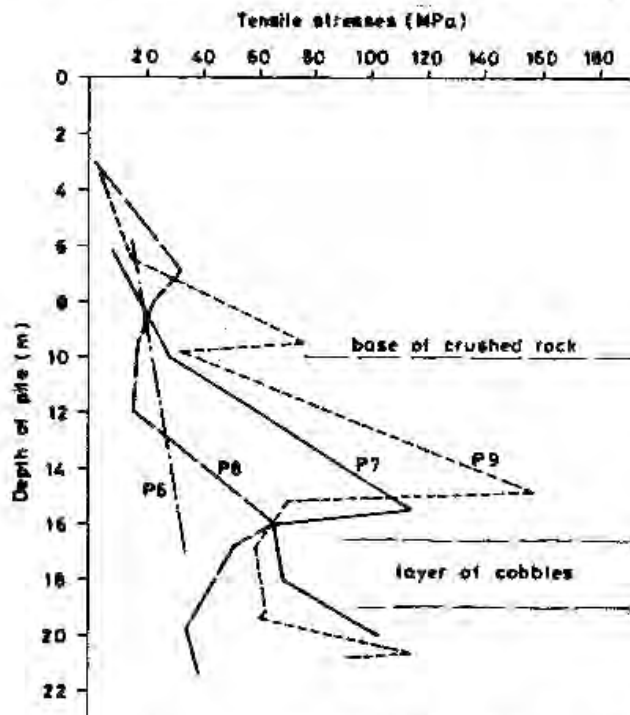
INTEGRITY TESTING



(a) Concrete Daido Piles Driven with Diesel Hammer



(c) Steel Tubular Piles Driven with Drop Weight



(b) Steel H-Piles Driven with Diesel Hammer  
Fig. 5. Tensile Stresses During Driving.

The measurements of stress with the dynamic monitoring equipment show the change in stress across the pile section, not the absolute stress in the pile. The results of tension measurements in Daido piles in Figure 5a reflect this change in stress. The peak value of 2.2 MPa (pile no. 4) would therefore correspond to a net compressive stress remaining in the pile of  $5.26 - 2.2 = 3.1$  MPa. Both of the other two Daido piles also remained in a state of compression throughout the driving.

All steel piles, on the other hand, experienced considerable tensile stresses towards the bottom of the rockfill layer and in the alluvium. Figure 5b shows that the lighter of the two H-pile sections (i.e. pile nos. 7 and 9 with  $305 \times 305 \times 125$  kg/m sections) experienced the greatest tension, up to 180 MPa. The 610 mm diameter tubular piles experienced tensile stresses of up to 90 MPa (Figure 5c).

#### VIBRATION TESTING OF DAIDO PILES

##### *Pile Integrity*

Two Daido piles (pile nos. 4 and 5) were subjected to vibration testing. The remaining Daido pile (no. 3) was inaccessible at the time, due to the excessive height of free standing pile left above ground after driving. No defects were revealed by these tests. Minor irregularities were apparently detected at a number of points in each of the two piles tested (Table 2), indicated by peaks of resonance at several values of frequency on the admittance curves. These were shown to be insignificant by a television inspection down the 300 mm central hole in the piles, as no faults were revealed by this inspection.

##### *Vertical Stiffness*

The dynamic vertical stiffness was obtained from the data from pile no. 4, as given in Table 1. This pile was later subjected to a pull out test to determine static frictional resistance.

**Table 1. Stiffness Values for Daido Pile No. 4**

Measured initial stiffness	$E'$	383 kN/mm
Stiffness assuming zero base support	$E'_{\min}$	218 kN/mm
Stiffness assuming perfectly rigid base support	$E'_{\max}$	302 kN/mm

## INTEGRITY TESTING

It is unexpected that the value of  $E'$ , the initial stiffness, should exceed  $E'_{\max}$  for a pile on a rigid stratum. This anomalous result probably reflects the lack of precision of the test in this case, where the  $L/D$  ratio is as high as 48.

The stiffness with no base support (i.e.  $E'_{\min}$ ) can be compared with the stiffness measured in a pullout test. Considering the uncertainties of the vibration test, it is likely that the vibration method would give a predicted pull-out test stiffness in the range of 200 to 250 kN/mm.

Table 2. Summary of Vibration Test Results

Pile No.	Pile Type	Initial Pile Head Stiffness, $E'$ (kN/mm)	Free Pile Mechanical Admittance, $N$ (sec/kg)	Depth to Reflecting Feature (m)
4	Daido	383	8.2	3.4–4.3 19.0–24.5
5	Daido	761	7.4	4.9–6.3 9.7–12.5 12.7–16.4

## PULL OUT TESTS

### *High Strength Prestressed Concrete Piles*

With the three Daido piles, it soon became apparent that the pile's tensile capacity was inadequate for the tensile loads applied in pull out tests. Daido pile no. 4 was subjected to a maximum pullout load of 1215 kN which caused severe horizontal cracking around the perimeter of the pile at the top, but this force could not extract the pile.

Figure 6 shows the load displacement curve for pile no. 4. The nonlinear behaviour is attributed to the progressive yielding of the soil's frictional bond at early displacements, and later to the onset of cracking in the pile stem.

Although the initial tangent stiffness as shown in Figure 5 is 730 kN/mm (which compares with pile no. 5 at 761 kN/mm), it appears that the progressive yielding of the soil during extraction created a stiffness of about 185 kN/mm for the second leg of the curve. This stiffness value compares with the value of 218 kN/mm found from the dynamic test (Table 1). The third section of the yield curve appears to relate to the onset of cracking in the concrete, where the stiffness was reduced to 105 kN/mm.



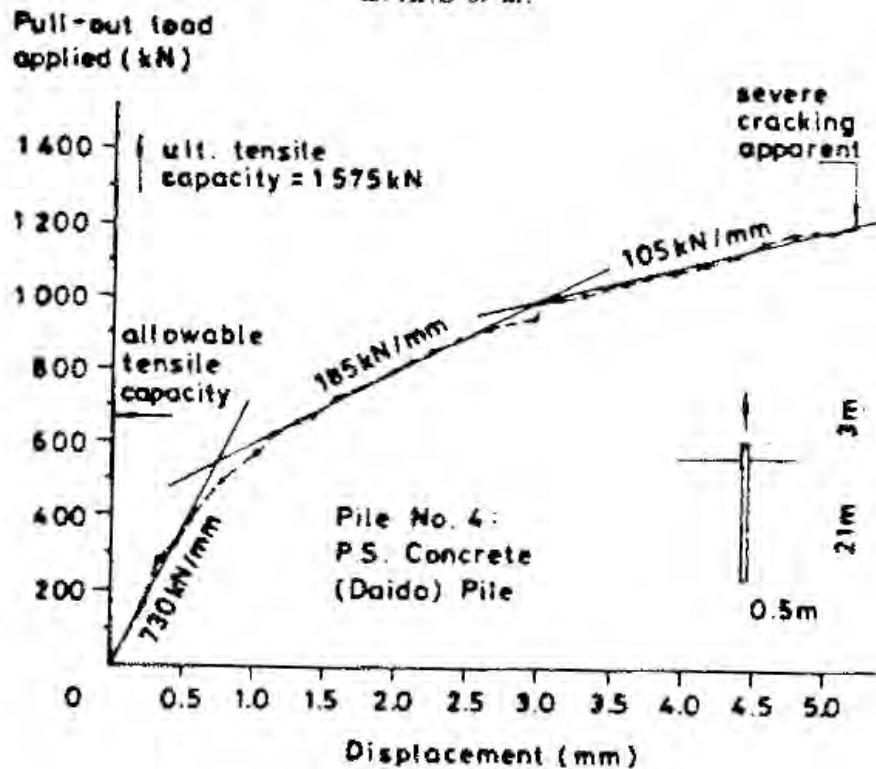


Fig. 6. Results of Pull Out Test, Pile No. 4.

*Steel H-Piles*

H-piles nos. 8 and 9 were successfully tested in uplift and a failure load was obtained. The testing of H-piles nos. 6 and 7 was not successful. On both occasions, the contractor had difficulty in meeting the specified rate of uplift of 1 mm per 5 minutes. The jacking equipment was successfully modified for subsequent tests on piles nos. 8 and 9. In the case of pile no. 7, a maintained load test was carried out which complied with the specification.

Ultimate loads for the two successful constant uplift rate tests and the maintained load (ML) test for H-pile no. 7 are shown in Table 3.

Table 3. Uplift Test Results from Steel H-Piles

Pile No.	Pile Section	Depth to Toe (m)	Ultimate Load (kN)	Ave. Skin Friction (kPa)
7	305 × 305 × 125 kg/m	21.8	860 (ML test)	32
8	305 × 305 × 223 kg/m	22.0	860	30
9	305 × 305 × 125 kg/m	23.0	980	35

### INTEGRITY TESTING

The average skin friction determined is obviously the combined resistance in the rock fill and the strata below this. It is probable that the skin friction in the rock fill is quite low compared with the deeper, more cohesive materials. An assessment of the different values of skin friction was made from uplift data from the tubular piles, because these piles were driven to a greater range of depths.

#### *Tubular Piles*

Uplift load tests on each of the four steel tubular piles were completed satisfactorily. Ultimate loads from the tests are summarised in Table 4.

**Table 4. Uplift Load Test Results from Steel Tubular Piles.**

Pile No.	Pile Section	Depth to Toe (m)	Ultimate Load (kN)	Ave. Skin Friction (kPa)
10	406 $\phi$ 123 kg/m	15.6	741	37
12	406 $\phi$ 123 kg/m	16.8	811	38
11	610 $\phi$ 277 kg/m	20.6	2142	54
13	610 $\phi$ 277 kg/m	20.6	1560	40

**Average ultimate skin friction (kPa)**

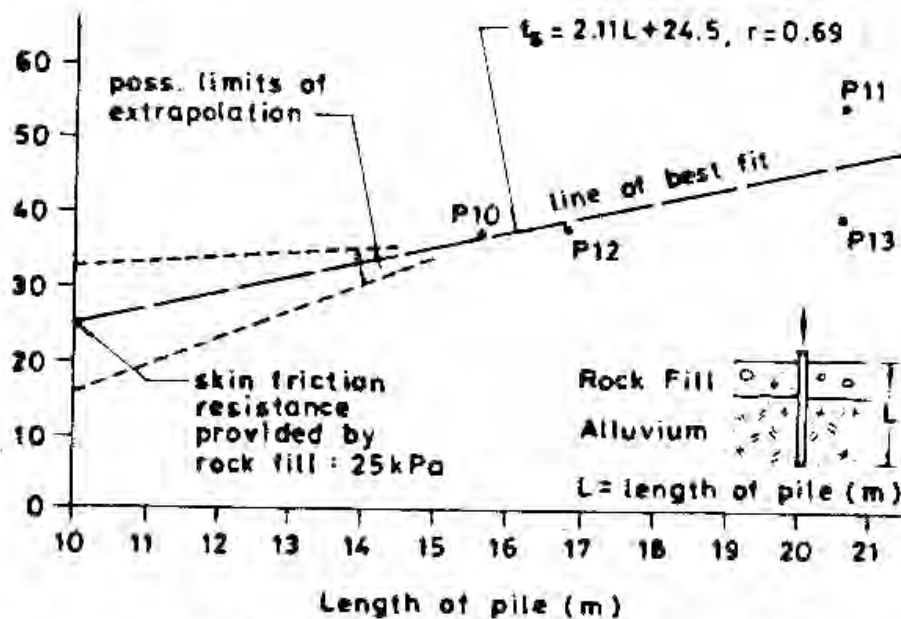


**Fig. 7. Skin Friction Resistances for Steel Tubular Piles.**

In Figure 7, the average (total) skin friction values obtained from the four tests on tubular piles are plotted against the length, *L*, of the piles, and an assessment of the skin friction within the rock fill layer is given by extrapolating the line of best fit back to *L* = 10 m. This provides the net friction value for a length of pile in the rock fill layer only. In this case, the extrapolation indicates an average rock fill skin friction of about 25 kPa, although the experimental scatter of the limited data available suggests a possible range of 16 to 32 kPa. Based on a rock fill friction of 25 kPa, the skin friction mobilised in the alluvium can be shown to be an average of 62 kPa, with a range of 53 to 81 kPa.

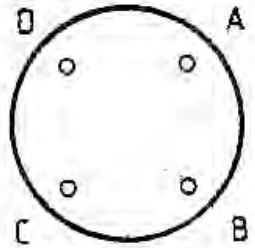
TESTING OF CAST-IN-PLACE PILES

*Bored Piles*

Three 1200 mm diameter bored piles, nos. 1, 2 and 17, were installed to assess the problems of excavation and concrete placement through the crushed rock reclamation fill. Pile nos. 1 and 17 were installed with a temporary liner (i.e. the liner was extracted during concreting), whilst the liner for pile no. 2 was left in place.

Standard driven steel liner and clam shell excavation were used for the installation. Concrete was placed under water with a tremie, but before concrete pouring, four 50 mm diameter tubes were placed to provide access for the sonic logging test probes.

Table 5. Summary Results of Sonic Logging in Bored Piles



Traverse	Pile No. 1	Pile No. 2	Pile No. 17
A - B	No defects	No defects for 21.5 m	Minor faults at 8 m to 20 m
B - C	No defects	Minor faults at 7 m	No defects for 20 m
A - C	No defects	Minor faults at 13 m	Not done
A - D	No defects	Minor faults at 12.5 m	Low density at 17 m
C - D	Minor faults at top of pile	No defects	No defects for 22 m
B - D	No defects	Minor faults at 13 m	No defects for 22 m

## INTEGRITY TESTING

*Sonic Logging.* The sonic logging performed in all three bored piles generally revealed no irregularities, or only minor ones, in the density of the concrete. Table 5 summarises the results. In pile no. 17 (unlined), a low density zone was detected at 17 m below the top of the pile in one of four chords that were tested across the pile section.

*Concrete Coring.* Coring was undertaken only in pile no. 17, as there was sufficient confidence from the sonic logging in the condition of pile nos. 1 and 2. The concrete cores showed no evidence of segregation or voids. In all respects, the density was uniform and was judged to be satisfactory. The suspected area of low density at 17 m indicated by the sonic logging was not revealed by the coring.

### *Barrette Piles*

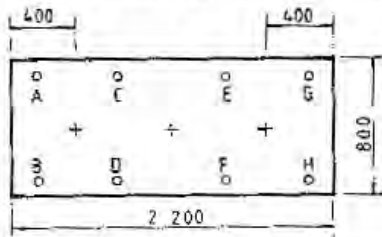
The 2200 × 800 mm barrette pile was installed under bentonite without excessive difficulty, but there was a loss of about 10 m<sup>3</sup> of bentonite slurry (about 25% of the volume) during excavation in the rock fill layer. Occasional use of a rock chisel was necessary, but in general the rectangular cable-operated grab was sufficient to advance the hole through the fill. All excavation was carried out with the surface of the bentonite slurry at or near ground surface. After placing a grid of tubes for the sonic logging, the barrette pile was concreted with a tremie under the bentonite.

*Sonic Logging.* Sonic logging of the barrette was carried out by two independent testing agencies, after results from the initial firm showed a considerable number of possible defects in the concrete. The locations and results of both exercises can be compared in Table 6.

It appears from the data in Table 6 that the interpretation of the sonic profiles through the concrete is a subjective process that relies on experience and knowledge from previous defect correlation studies. This exercise in the barrette has highlighted the possible range of interpretation for sonic logging in a typical construction quality control environment.

*Concrete Coring.* Three coring holes were undertaken in the barrette to obtain core samples of the concrete. Only the bore in the centre of the pile continued in a truly vertical alignment throughout the pile. The remaining bores (located 400 mm from each end) deflected slightly from vertical, providing 17.7 m and 21.8 m of concrete core, respectively, before penetrating the side of the pile.

Table 6. Summary Results of Sonic Logging in Barrette Pile



Barrette (Pile No. 8)  
unlined, 25.1 m long.  
O sonic logging hole  
+ coring

Traverse	Testing Agency No. 1	Testing Agency No. 2
C - F	No defects	(No test)
C - D	(No test)	No defects
B - H	Minor fault at 18.5 & 21 m. Segregation at 13 - 16 m	(No test)
C - E	(No test)	No defects
A - B	Segregation at 13 - 16 m	No defects
A - D	(No test)	No defects
A - C	Segregation at 13 - 16 m	No defects
D - H	(No test)	No defects
C - H	No defects	No defects
F - H	(No test)	No defects
H - F	No defects	(No test)
C - H	(No test)	No defects
C - G	Minor fault at 11 m	(No test)
E - G	(No test)	No defects
A - G	Segregation at 13 - 16 m	(No test)
D - G	(No test)	No defects
B - C	Segregation at 13 - 16 m	No defects
D - E	No defects	No defects
E - F	No defects	(No test)
B - D	(No test)	Minor fault at 12 - 15 m

No defects were detected in any of the 64.6 m of total core recovered. None of the problem areas suggested by the sonic logging (Table 6) were detected or intersected, despite the boreholes being located near the zones of possible poor quality concrete.

## DISCUSSION

### *Value of Integrity Testing*

The various methods of integrity testing used in this study gave a comprehensive and generally accurate assessment of the conditions of the piles. When anomalies were later investigated by physical inspection or coring,



### INTEGRITY TESTING

the integrity test results were usually pessimistic (i.e. erring on the conservative side) in predicting the structural condition.

Dynamic monitoring of the progress of pile driving yields much data about stresses, load capacity and condition of a pile. The necessary instrumentation was fitted in this study with minimal delay and was found to be sufficiently robust for the hard driving. Where either compressive or tensile stress could be of primary concern in concrete piles, dynamic monitoring can be used on selected piles to ensure that over stressing is avoided under hard or variable driving conditions.

Dynamic monitoring carried out during the driving of steel tubular pile no. 12, which was later found to be distorted and damaged for about 600 mm at the tip, showed no evidence of a structural problem when compare with similar monitoring of the other tubular piles. Without more severe buckling of the pile, and subsequent development of a "soft" toe for example, dynamic monitoring would usually continue to show that adequate load bearing capacity was available in the pile. For pile no. 12, this is thought to be a reasonable assessment of its condition.

Although vibration testing of Daido (and other) concrete piles has become a standard practice, this study has shown that internal underwater television inspection inside the tubular piles provides a reliable alternative to the vibration test when L/D ratios are high. Television inspection was found to be rapid and easily interpreted, and unlike vibration testing, it is not limited to those piles of convenient height above ground nor does it rely on the expertise of the operator for interpretation. Depending on cost effectiveness, television inspection of Daido piles could be adopted as a quality control method.

The sonic logging tests offered slightly pessimistic assessments of the structural condition of the bored piles and barrette. It could therefore be concluded that in this exercise, reliable and satisfactory results were obtained from the use of this test method. It was clearly shown, however, that sonic logging depends significantly on qualitative interpretations by the operator. It would therefore seem necessary to calibrate the test method to a specific concrete mix and construction method before relying on the procedure to give a more accurate assessment of a bored pile.

#### *Predicted and Observed Pile Behavior*

The vibration testing of two of the three prestressed concrete piles indicated a vertical load stiffness of 200 to 250 kN/mm. In the later uplift testing, the initial stiffness was much higher at 720 kN/mm, although after some yield



the uplift testing showed a stiffness of 185 kN/mm, which is comparable with the vibration test result.

The uplift testing of the four steel tubular piles provided data for a back-calculation of the average skin friction mobilised within the rock fill layer. Despite some scatter of the results, the best estimate of the rock fill skin friction for the steel piles was between 16 and 32 kPa.

It is normally assumed for pile driving into a coarse granular material that the load resistance of the pile in the dynamic case is approximately equal to that in the static case. For this reason, the estimated static side resistance from dynamic monitoring has been compared to the side resistance from uplift tests (Table 7).

**Table 7. Comparison of Predicted and Observed Average Skin Friction Values from Dynamic Monitoring and Static Uplift Tests of Tubular Piles**

Pile No.	Dia. (mm)	Depth to Toe (m)	Estimated Ultimate Side Resistance from Dynamic Tests (Restrike Case)		Observed Ultimate Side Resistance from Uplift Tests	
			Load (kN)	Ave. Skin Friction (kPa)	Load (kN)	Ave. Skin Friction (kPa)
10	406	15.6	790	40	741	37
11	610	16.8	320	10	811	38
12	406	20.6	190	7	2142	54
13	610	20.6	602	15	1560	40

In Table 7 it can be seen that the side resistances predicted by the dynamic monitoring in general significantly underestimate the actual values measured in uplift tests. This discrepancy is probably brought about because of an increase in the ultimate bearing capacity of piles that develops with time after driving. This is unlikely to occur in coarse rock fill, and may have therefore been confined to the underlying alluvium and completely weathered rock. A more appropriate comparison in this case would be between the side friction mobilised whilst the piles were being driven only through the rock fill. It is shown in Figure 7 that a best estimate of the skin friction in the rockfill is 25 kPa, with a range up to 32 kPa.

#### CONCLUSIONS

1. The various forms of integrity testing used in this investigation were found to be generally reliable in assessing the structural condition of piles, but a pessimistic result was usually obtained.

### INTEGRITY TESTING

2. With steady state vibration testing in this study, the results were not always accurate, possibly because the test is better for relatively short piles with length to diameter ratios no greater than 20 to 30.
3. Underwater television inspection of annular concrete piles was shown to be a good alternative method of quality control for routine use.
4. Sonic logging (or sonic coring) was found to depend very much on the expertise of the operator. It was shown that unless previous calibration had been performed for a specific concrete mix and construction method, sonic logging may give an overly pessimistic assessment of concrete quality.
5. Uplift testing of selected driven steel tubular piles suggested that the skin friction mobilised in the rock fill was of the order of 25 kPa, but could be up to 32 kPa.
6. For the steel tubular piles, side resistance load capacities and skin friction values obtained from dynamic monitoring of driving by wave equation techniques were in general of the same order or lower than the actual skin friction values obtained from static uplift load testing. This conclusion is based on a very limited number of tests, however and further research on this aspect of skin friction is needed.

### ACKNOWLEDGEMENTS

The following government department, contractors and testing agencies were involved in the trial piling exercise described in this paper, and their assistance and co-operation is gratefully acknowledged:

- (a) Junk Bay Development Office of the Territory Development Department-site formation;
- (b) S.Y. Engineering Co. Ltd.-main piling contractor for pile installation and uplift load tests;
- (c) Bachy Soletanche Group - bored piling subcontractor;
- (d) Materials Consultants (Asia) Ltd.-vibration testing and sonic logging;
- (e) Testconsult CEBTP Far East Ltd - sonic logging;
- (f) Cedec Geotechnical Services (Hong Kong) Ltd - dynamic pile testing.

Special thanks are due to a large number of Housing Department staff for help with these tests, and particularly to Mr W.L. Pump who wrote the initial report on these tests. Permission to publish this paper, granted by the Director of Housing, is gratefully acknowledged.

REFERENCES

- BERINGEN, F.L., VAN HOOYDONK, W.R. & SCHAAP, L.H.J. (1980). Dynamic Pile Testing; An Aid in Analysing Driving Behaviour. *Proceedings of the Seminar on Application of Stress Wave Theory*, Stockholm, pp. 1-21.
- CIRIA (1977). *Integrity Testing of Piles: A Review*. Report No. PG4, Construction Industry Research and Information Association, London, 36 p.
- DAVIS, A.G. & DUNN, C.S. (1974). From Theory to Field Experience with the Non-destructive Vibration Testing of Piles. *Proceedings of the Institution of Civil Engineers, Part 2*, London, Vol. 57, pp. 571-593.
- EVANS, G.L., SANDERS, H. & WONG, P.P. (1987). The Performance of Driven Piles in a Crushed Rock Filled Reclamation. *Hong Kong Engineer*, in press.
- FEDERATION OF PILING SPECIFIERS (1975). Specification for Cast - in - Place Piles Formed under Bentonite Suspension. *Ground Engineering*, March, p. 50.
- HOLDEN, J.C. (1984). The Construction of Bored Piles in Weathered Sedimentary Rock. *Proceedings of the 4th Australia/New Zealand Conference on Geomechanics*, Perth, vol. 2, pp. 378-384.
- SMITH, E.A.L. (1960). Pile Driving Analysis by the Wave Equation. *ASCE Journal of the Soil Mechanics and Foundations Division*, vol. 86, no. SM4.
- TIJOU, J.C. (1984). Integrity and Dynamic Testing of Deep Foundations-Recent Experiences in Hong Kong (1981-1983). *Hong Kong Engineer*, vol. 12, no. 9, September, pp. 15-22.

## **IMPROVEMENT OF DISPERSIVE SOILS BY MIXING WITH BANGKOK CLAY OR BENTONITE**

D.T. BERGADO<sup>1</sup> and K.Y. KANG<sup>2</sup>

### SYNOPSIS

Several dams in northeast Thailand made of dispersive soils have failed by surface and piping erosion. These dispersive soils are inorganic sandy silty clays or clayey silts of low plasticity which have a higher content of dissolved sodium in the pore water. The addition of bentonite had no effect on the dispersivity. On the other hand, addition of from 20% to 30% Bangkok clay rendered the soil nondispersive. The liquid and plastic limits increased linearly with increasing percentage of Bangkok clay, while the maximum dry density decreased and the optimum moisture content increased. The effective angle of shearing resistance ( $\phi'$ ) slightly decreased with increases in the percentage of Bangkok clay, while the effective cohesion ( $c'$ ) slightly increased. The crumb test gave a preliminary indication of the dispersivity of the soil; however, pinhole and chemical tests are necessary to ascertain the dispersivity.

### INTRODUCTION

Dispersive soils are clayey silty soils which are highly erodible and have a higher content of dissolved sodium in the pore water than ordinary soils. They are eroded by a process in which the individual colloidal clay particles go into suspension in practically still water.

In Thailand, several earth structures have encountered problems due to internal erosion of dispersive soils. The recent trend of research has shown that chemical stabilization is used frequently to improve these soils. In this study, dispersive soils from three separate locations in Thailand, namely Phitsanulok canal site, Lam Sam Lai dam site, and Ampun dam site, were studied. Both the original dispersive soils and the soil mixed with soft Bangkok clay or bentonite were tested for dispersive identification tests, index tests, and tests for physical and engineering properties. The purposes of this study were to evaluate the dispersivity and the physical properties of the original dispersive soil, the dispersive soil-Bangkok clay mixture, and the dispersive soil-bentonite mixture. Most of the experimental results presented in this paper were derived from the work of KANG (1985).

<sup>1</sup> Assistant Professor of Geotechnical Engineering, Asian Institute of Technology, Bangkok, Thailand.

<sup>2</sup> Soil Engineer, Technical Research Institute, Daewoo Engineering Co. Ltd., Seoul, South Korea.

DESCRIPTION AND IDENTIFICATION OF DISPERSIVE SOILS

Dispersive soils contain a clay fraction which has a high potential to be in a dispersed state when the soil mass interacts with water. The dispersion occurs when the repulsive force (electrical surface forces) between individual clay particles exceeds the attractive forces (van der Waals attraction), and when the clay mass is in contact with water, individual clay particles are progressively detached from the surface and go into suspension (SHERARD et al, 1972). Dispersive soils have sodium as the main factor contributing to their dispersivity. HOLMGREEN & FLANAGAN (1977) described why sodium causes soil dispersivity. The effectiveness of sodium as a dispersing agent is related to its ionic charge of plus one. For the same negative charge on a clay particle, an ion swarm of univalent sodium contains twice as many ions as does a corresponding swarm of divalent ions such as calcium or magnesium ions. Osmotic potentials are thus greater in sodium systems because osmotic potential is proportional to the number of ions in the double layer. Furthermore, because of its single valence, the coulombic attraction of a sodium ion to the charged particle surface is less than that for polyvalent ions. Sodium ion swarms therefore range further from the particle surface, forming a thicker double layer. In addition, LAMBE & WHITMAN (1969) reported that as the negative charge on a clay particle is balanced by the cations in the double layer, two advancing particles begin to repel each other when their double layers first come into contact. The repulsive force between adjacent particles for any given spacing is therefore directly related to the sizes of the double layers. Thus, a net repulsive force is more probable for a sodium ion system. DECKER & DUNNIGAN (1977) indicated that dispersive soils in nature commonly had alkaline pore water with pH greater than 8.5.

The dispersion ratio (double hydrometer) test is an indicator test developed by the Soil Conservation Service (VOLK, 1937) to evaluate the susceptibility of soils to erosion. A grain size curve determined by the ordinary hydrometer test is compared with one that is determined by the hydrometer test without chemical dispersant. The dispersion ratio is defined as the ratio of the percent finer than 0.005 mm diameter measured without to that measured with chemical dispersant. The criteria for soil classification is given in Table 1, as set by the Soil Conservation Service (SHERARD et al, 1972). This test should be used only as a general guide to the identification of the erodibility of clayey soils.



## DISPERSIVE SOILS

Table 1. Criteria for Dispersion Ratio Test.

Degree of Dispersion (%)	Classification
Less than 35	Nondispersive
35 to 50	Moderately Dispersive
50 to 75	High Dispersive Potential
Greater than 75	Extremely Dispersive

EMERSON (1967) described a rapid field test for the evaluation of the dispersive nature of clays called the crumb test. The test consists of dropping a small, moist (natural moisture) clod of soil into a clear beaker of distilled water or 0.001 normal sodium hydroxide (NaOH) solution, or both. If the soil is dispersive, a colloidal cloud develops around the periphery of the clod. The tendency for the clay particles to go into colloidal suspension is observed after 5 to 10 minutes of immersion. SHERARD et al (1976b) developed a dispersivity rating system as follows :

- Grade 1 - no reaction: crumb may spread on the bottom of the beaker without a sign of cloudy water caused by colloids in suspension.
- Grade 2 - slight reaction: the water gets slightly cloudy at the surface of crumb.
- Grade 3 - moderate reaction: an easily recognizable cloud of colloid in suspension, usually spreading out in thin streaks on the bottom of the beaker without totally covering the bottom area.
- Grade 4 - strong reaction: colloidal cloud covers approximately the whole bottom of the beaker in a very thin skin. In extreme cases, all water becomes cloudy.

The pinhole test was developed for identification of dispersive soils by SHERARD et al (1976a) and modified by COUMOULOS (1977) and SCHAFER (1978). As seen in Figure 1, distilled water is caused to flow through a 1 inch (25 mm) long specimen with water content near the plastic limit. The water is caused to flow under a hydraulic head of 2 to 40 inches (50 to 1020 mm) through a 1 mm diameter hole. The classification of the soil is based on the appearance of the water, the rate of flow and final size of hole in the specimen. Criteria for evaluating pinhole test results are shown in Table 2.



BERGADO & KANG

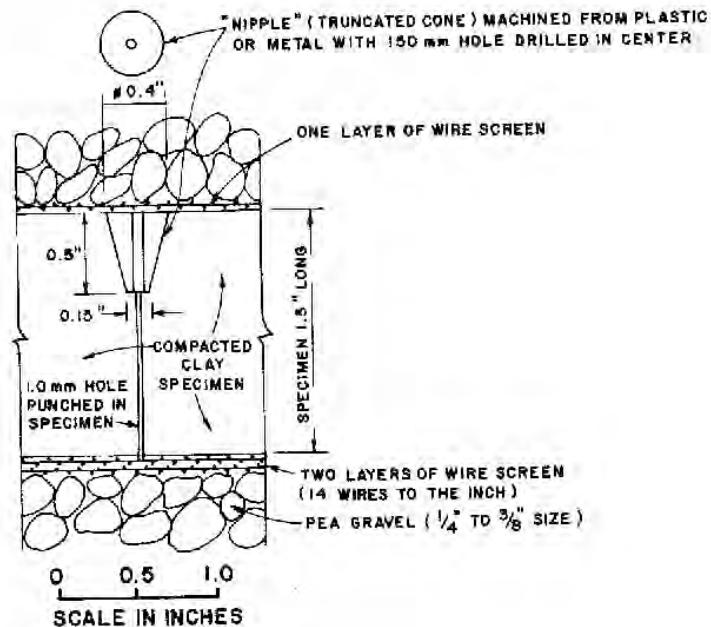
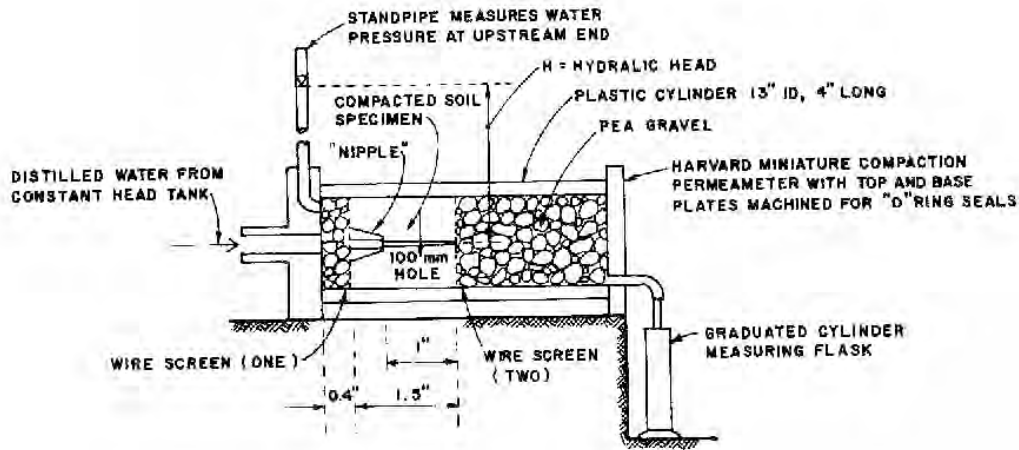


Fig. 1. Pinhole Test Apparatus and Section through Pinhole Test Specimen (After SHERARD et al, 1976 a).

The soil chemical test procedure is covered in Agriculture Handbook No. 60, edited by RICHARDS (1954). He reported an empirical relation between the Exchangeable Sodium Percentage (ESP) and Sodium Adsorption Ratio (SAR). The relative abundance of monovalent and divalent ions are manifested as the ratio defined as follows:

*DISPERSIVE SOILS*

**Table 2. Criteria for Pinhole Test.**

Classification	Description
D1 and D2	Dispersive soils: fail (5 × original diameter) rapidly under 2 inches head
ND4 and ND3	Intermediate soils : erode Slowly under 2 inches or 7 inches head
ND2 and ND1	Nondispersive soil : no colloidal erosion under 15 inches or 40 inches head

$$SAR = \frac{Na^+}{\sqrt{0.5(Ca^{++} + Mg^{++})}} \dots\dots\dots (1)$$

in which Na<sup>+</sup>, Ca<sup>++</sup>, and Mg<sup>++</sup> refer to the concentrations of the designated soluble cations in the porewater expressed as milliequivalents (meq) per litre. RICHARDS (1954) has related the ESP to SAR by the following regression equation:

$$ESP = \frac{-0.0126 + 0.01475 SAR}{1 + (-0.0126 + 0.01475 SAR)} \times 100 \dots\dots\dots (2)$$

The soil is classified as dispersive when it falls into the nonsaline-alkali soil group shown in Table 3.

**Table 3. Soil Classification According to Chemical Composition of the Pore Fluid.**

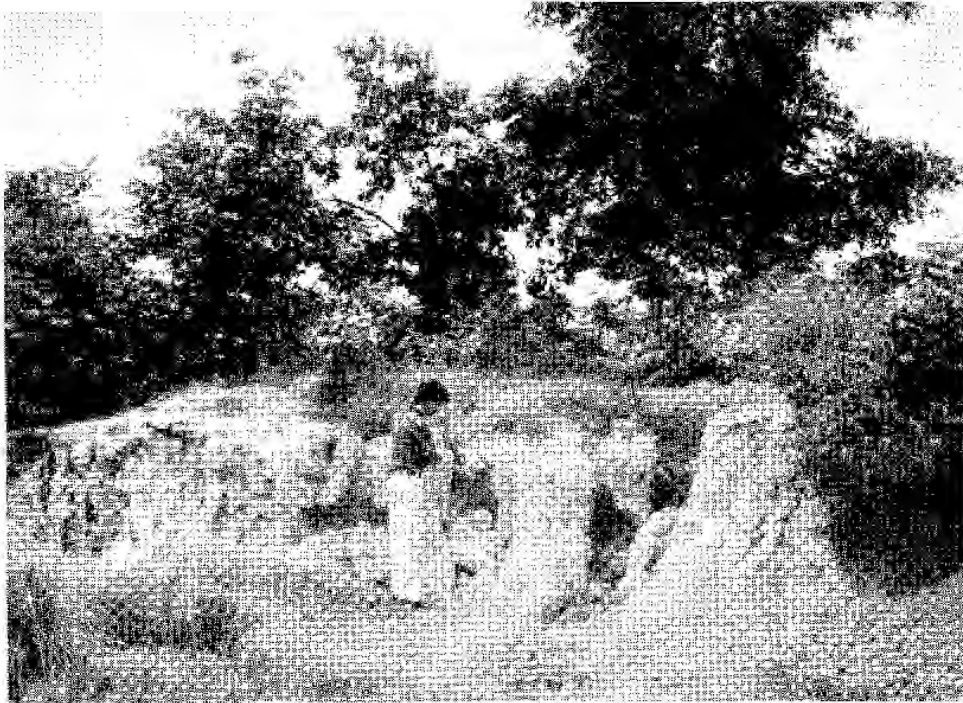
Soil Group	ESP	EC	pH	Dispersivity
Saline	< 15	> 4	< 8.5	Dispersive
Saline-Alkali	> 15	> 4	< 8.5	Nondispersive
Nonsaline-Alkali	> 15	> 4	> 8.5	Dispersive

Note : EC = electrical conductivity (mmhos/cm)

**ENGINEERING PROBLEMS OF DISPERSIVE SOILS**

Engineering problems may occur when dispersive soils are used as construction materials and/or foundation materials. Problems due to dispersive soils occur frequently on earth dams, earth embankments, irrigation canal banks, building foundations, etc. The damages could be any combination of surface erosion, piping, slaking or gully erosion, as mentioned by past investigators (SHERARD et al, 1972; EMERSON, 1964; NAKANO, 1967;

(a)



(b)

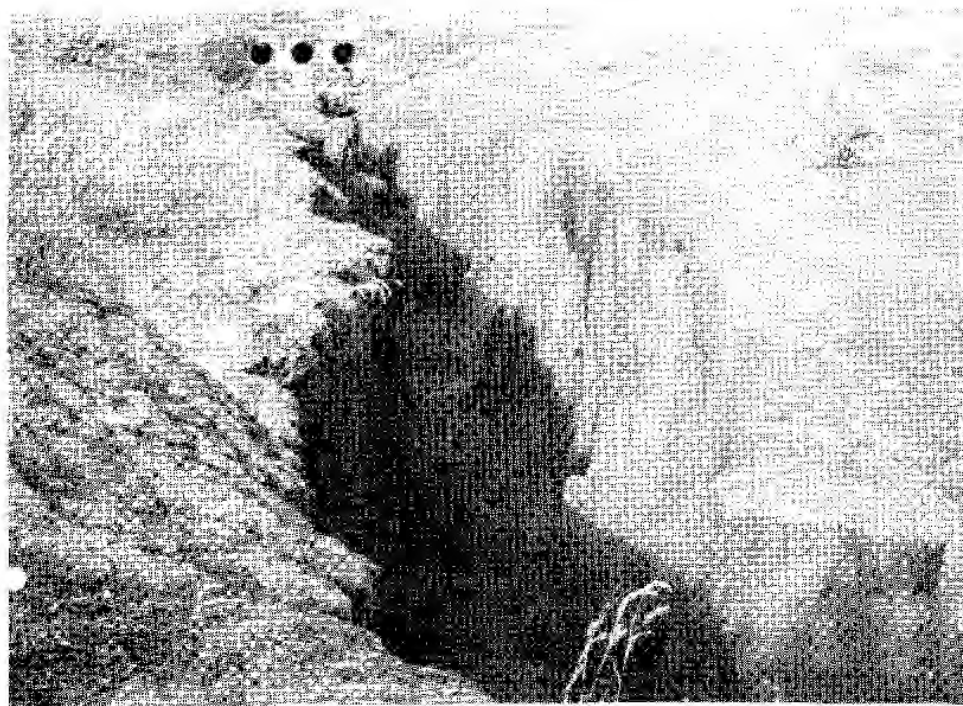
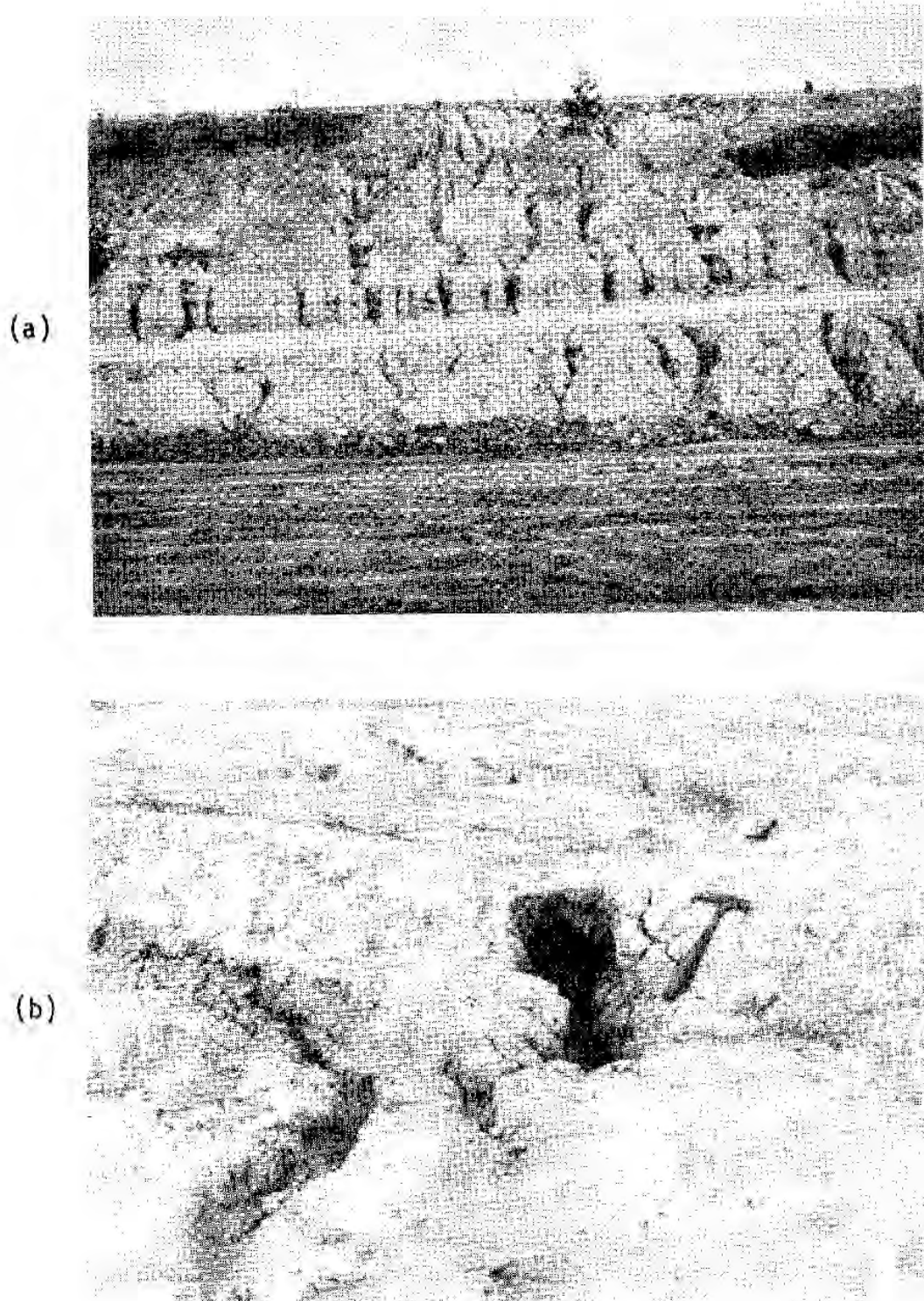


Fig. 2. Surface Erosion in Dispersive Soils.

*DISPERSIVE SOILS*



**Fig. 3. Tunnelling and Piping Erosion in Dispersive Soils.**



INGLES & AITCHISON, 1969; COLE & LEWIS, 1960; COLE et al, 1977; FERNANDO, 1979; SHIEH, 1981; KIM, 1982; GARCIA, 1983; TAI, 1983; CHEN, 1984; and KANG, 1985). Examples of damage by surface erosion are illustrated in Figure 2.

Since 1970, a number of earth dams in northeast Thailand have failed due to serious piping erosion, tunnel erosion and surface erosion, mainly attributed to the presence of dispersive soils (Figure 3). The piping and tunnelling occurred during the first reservoir filling. The surface erosion is caused by rainfall runoff. COLE et al (1977) summarized the damaged dams in Thailand, as given in Table 4, including the chemical and physical properties of the construction materials. The locations of these dams are shown in Figure 4.

SHERARD et al (1972) described the typical dispersive soil piping failure of homogenous earth dams that start with a very small initial leak in a narrow crack, eroding in a few hours into a tunnel of substantial diameter. The initial narrow crack could be caused by drying and shrinkage of plastic material, differential settlement, earthquake, hydraulic fracturing, geological weakness in the foundation or merely poor compaction. AITCHISON (1960) suggested that the mechanism for piping failures in earth dams could involve the dispersion of the clay fill material at the exit point of the percolating water, leading to the progressive loss of fine clay particles in suspension. Piping failures due to the action of percolating rainwater have generally been described as surface erosion.

PARKER & JENNE (1967) reported in detail the potential damage to highway embankments caused by piping. It was pointed out that piping damage originates from desiccation cracks. Where the hydraulic gradient is sufficient, fine-grained sediments are transported in suspension along the crack to appear at an incipient pipe outlet in the embankment. This type of pipe may also occur as a result of localized subsidence due to the saturation of surficial sediments, resulting in sinks or stress cracks.

Damage due to dispersive soils also occurs in excavation cutslopes. Piping failure during rainfall begins when rainwater enters desiccation cracks in the upper parts of the slope, percolates vertically downward and then flows horizontally, washing out dispersive clay in suspension. Irrigation canal banks made of dispersive soils are also damaged due to the interaction with the retained water. Such a situation occurred in the Lam Pao Irrigation Canal Project in Thailand, as reported by TAI (1983).

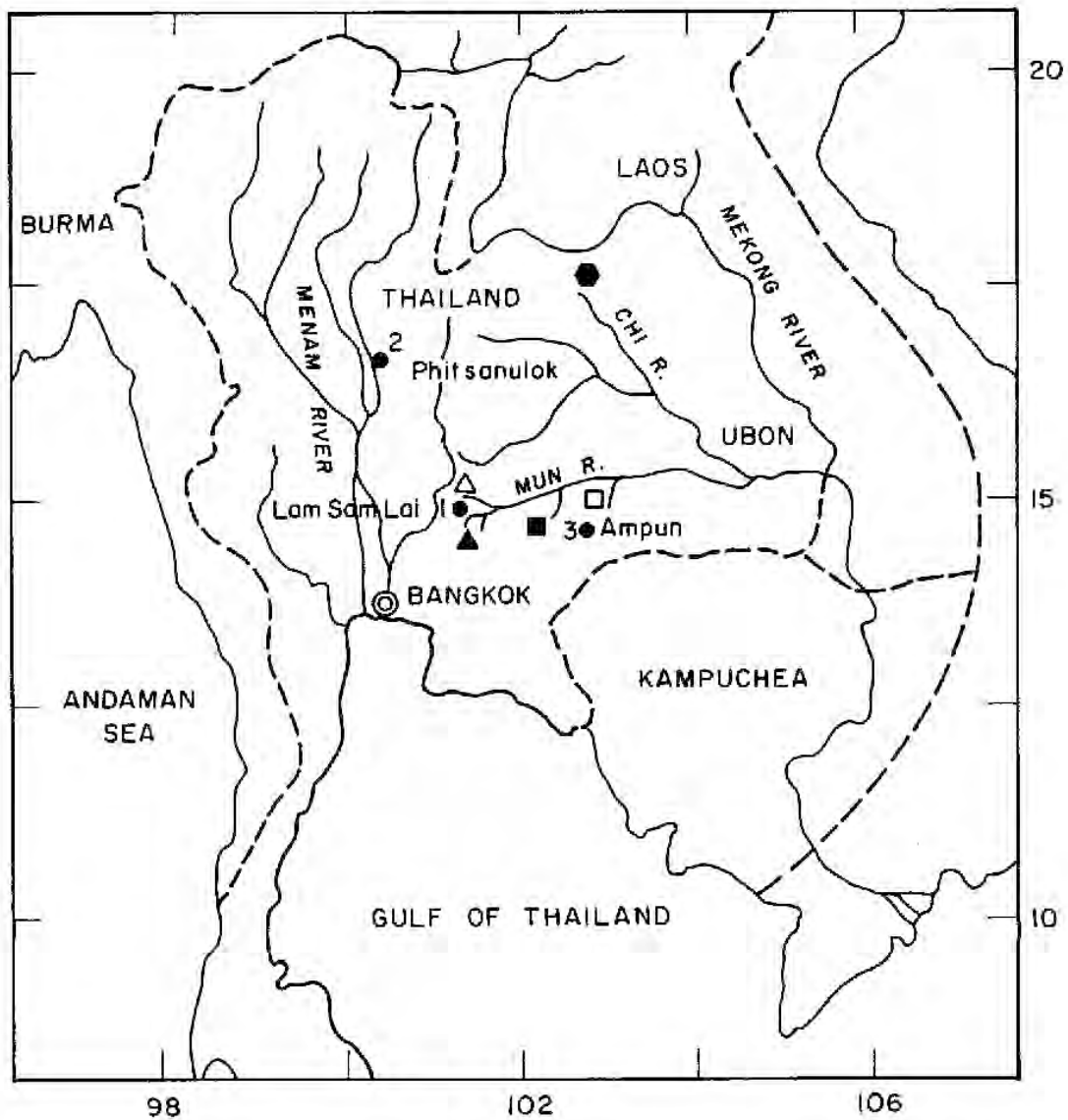
Table 4. Soil Properties Related to Dam Failure in Thailand.

Dam and Year of Completion	Number of Specimens Tested	Sodium (%) Dispersion			Pore Water Salt Concentration (meq/l)			Clay Size Minerals*	Compaction, Moisture	Water-tightness	Tunnel Erosion**	Comments
		Mean	Range	Mean	Range	Mean	Range					
		Range	Mean	Range	Mean	Range						
Lam Chiang Krai, 1972	29	84	74-95	49	5-68	40	4-93	Q I M	no tests	3 leaks, then failed	minor	pipng consistent with dispersive soil, having salts above 15 meq/l
Huay Sawai, 1972	39	71	14-96	36	0-67	6	1-17	Q K M	no tests	3 leaks, repaired	severe	2 leaks due to settlement cracks above spillway conduit
Lam Sam Lai, 1970	13	68	9-93	38	9-62	8	2-14	M(?) K	dry	failed	very severe	failure almost certainly due to dispersion pipng
Ampun, 1972	16	66	19-95	29	1-64	5	1-11	Q K L	variable poor	failed at closure section	moderate	sodium high, but soil may not be dispersive
Huay Saneng, uncompleted	24	60	25-93	10	0-63	3	0-13	K 70-90% M or M+V 10 to 30%	fair	water not stored yet	none	sodium high, but soil may not be dispersive
Nam Un, 1973	3	32	25-37	0	0	1	1-1	no test	good	excellent	none	not dispersive
Lam Phra Plerng, 1967	4	30	23-37	12	12-13	8	4-11	no test	good	some leakage through foundations	none	not dispersive

\* M = montmorillonite, K = Kaolinite, Q = Quartz, I = illite, V = vermiculite.

\*\* Very severe = large deep tunnels in many places; severe = deep tunnels in some places; moderate = shallow tunnels in some places; minor = occasional small tunnels.





**LEGEND**

- |                       |                   |                     |
|-----------------------|-------------------|---------------------|
| △ Lam Chieng Krai Dam | □ Huay Saneng Dam | 1. Lam Sam Lai Dam  |
| ▲ Lam Phra Plerng Dam | ● Nam Un Dam      | 2. Phitsanulok Site |
| ■ Huay Sawai Dam      |                   | 3. Ampun Dam        |

Fig. 4. Location Map.

The dispersive soils encountered mostly in northeast Thailand have been studied previously (COLE et al, 1977; FERNANDO, 1979; SHIEH, 1981; KIM, 1982; TAI, 1983; GARCIA, 1983; CHEN, 1984; and KANG, 1985).

### DISPERSIVE SOILS

These soils have been classified predominantly as CL in the Unified Classification System, indicating silty clay of low to medium plasticity, with some silty sand, sandy silt and clayey silt. The results of past investigations are summarized in Tables 5 and 6. Dispersive soils have sodium as the predominant chemical in the pore water, and COLE et al (1977) found an average sodium percentage of 66 to 80%. The pH value of these dispersive soils ranged from 5.4 to 9.0 (KIM, 1982). In comparison, AIT clay from near Bangkok is classified as silty clay of high plasticity (CH) and has a low pH

**Table 5. Classifications of Dispersive Soils Previously Studied in Thailand.**

Source	Location	Unified Classification	Description of Soil
FERNANDO (1979)	Lam Sam Lai Dam	SC-CL	Reddish brown silty clay with low to medium plasticity
	Lam Chieng Krai Dam	SM-CL	Yellow and brownish yellow silty clay and sandy clay
	Huay Sawai Dam	CL	low plasticity clay
SHIEH (1981)	Nakhon Rachasima	ML-CL	sandy silty clay
KIM (1982)	Ban Sawai	CL	reddish brown to light purple silty clay
	Sukhothai	ML-CL	yellowish sandy silt to clayey silt
TAI (1983)	Lam Pao Dam	SM-SC	pinkish white nonplastic silty clayey sand
CHEN (1984)	Khon Kaen University	CL	yellowish red silty clay

**Table 6. Atterberg Limits of Dispersive Soils Previously Studied in Thailand.**

Source	Location	Liquid Limit (%)	Plastic Limit (%)
FERNANDO (1979)	Lam Sam Lai Dam	14.7-35.0	10.8-18.9
SHIEH (1981)	Nakhon Rachasima	37.3 ± 0.5	12.5 ± 0.8
KIM (1982)	Ban Sawai area	39.5	19.6
	Sukothai area	24.8	13.4
TAI (1983)	Lam Pao Dam	-	N.P.
CHEN (1984)	Khon Kaen University	24.3	13.8
GARCIA (1984)	Khon Kaen area	14.7-21.9	14.6-15.5

of 3.9 and almost equal proportions of sodium (26%) compared to calcium and magnesium cations. The main clay-size minerals of these dispersive soils are quartz and kaolinite (CHANDRA & GARCIA, 1984; COLE et al, 1977). SHIEH (1981) found that the percentages of clay minerals at Lam Sam Lai dam were 50 to 60% kaolinite and 20 to 25% for both montmorillonite and illite. AIT clay contains kaolinite and illite in almost equal amounts (33 to 38%), with less montmorillonite, chlorite and quartz (CHANDRA & GARCIA, 1984).

#### METHODS OF STABILIZATION

Lime has been effectively used to stabilize dispersive soils. The addition of hydrated lime tends to increase the total concentration of calcium cations and reduce the high sodium content, controlling the dispersivity. The general order of replaceability of the cations is given by the lyotropic series as  $\text{Na}^+ < \text{K}^+ < \text{Ca}^{++} < \text{Mg}^{++} < \text{Al}^{+++}$ . Any cation will tend to replace the cation to the left of it, and the monovalent cations are usually replaceable by multivalent cations. Pozzolanic reactions between the lime and clay particles producing calcium silicate hydrates may also increase the soil strength, and the resulting cementation reduces soil erosion. The percentage of lime needed to render the soil nondispersive ranges from 1 to 2% by weight (FERNANDO, 1979; KIM, 1982; TAI, 1983; CHEN 1984; and COLE et al, 1977). Similar results were obtained by HALIBURTON et al (1975), SHERARD et al (1972), and LOGANI & HECTOR (1979). Although the hydrated lime is effective, there is a disadvantage in that the stabilized soil becomes brittle and susceptible to cracking.

Ordinary table salt (sodium chloride) has also been used to stabilize dispersive soils. VAN OLPHEN (1963) stated that as the concentration of ions increased when sodium chloride was added; a charge reversal on the clay is likely to result because of anion absorption on the particle edges. Then, further sodium chloride addition causes the concentration of sodium cations to increase in the clay surface as the absorbed anions are replaced, and a flocculated structure results. The principal disadvantage is that, being soluble, salt may be leached out from the soil by subsequent rainfall. CHANDRA & CHEN (1985) showed that 1% sodium chloride gave maximum strength in the soil they investigated.

The addition of 5% flyash to dispersive soils has been found to yield optimum strength by CHANDRA & CHEN (1985). Flyash is a waste product from the burning of powdered coal in thermal power plants. The effectiveness

## DISPERSIVE SOILS

of flyash depends on its pozzolanic activity, which is due to its high calcium content. The addition of 1% gypsum has also been found by CHEN (1985) to be most effective in stabilizing dispersive soils. SHERARD et al (1976a) has indicated that the additional calcium cations generated by the addition of gypsum decreased the percentage of sodium, controlling dispersivity. Addition of 0.5% aluminum sulfate has also been utilized by CHEN (1985) as a stabilizing agent. Apparently, the addition of aluminum ions has decreased the percentage of sodium ions, controlling dispersivity. Cement has been used as additive for controlling soil dispersivity (TAI, 1983). The addition of cement would saturate the pore water with calcium hydroxide; thus, the effect of lime released from cement hydration has an effect similar to the addition of lime.

## SAMPLING OF DISPERSIVE SOILS

The soil samples in this study were collected from Phitsanulok irrigation canal embankment, Ampun dam site, and Lam Sam Lai dam site in Thailand. These locations were suggested by the officials of the Royal Thai Irrigation Department, particularly Dr Suphon Chirapuntu. The site locations are shown on Figure 4.

### *Site Descriptions*

The Phitsanulok irrigation canal embankment is 176 km long with a maximum height of 5 m and an average width of 15 m. The embankment material is a pale brown to yellow brown sandy silt.

The Ampun dam is a homogeneous earthfill embankment with a maximum height of 10 m, a crest length of 2.8 km and a crest width of 6 m. The embankment material is mostly classified as a clayey to silty sand. The natural soil below the base of the dam consists of brown sandy silt (ML) to silty clay of low plasticity (CL). The detailed section of the dam after repair is shown in Figure 5. According to COLE et al (1977), a washout occurred during the first filling of the reservoir in 1972, at the location where the final closure was made. It was believed that tunnel erosion was facilitated by the presence of undercompacted dispersive soils near the face of the embankment.

The Lam Sam Lai dam is located at Prakong Village, Pak-Thongchai District, Nakhon Ratchasima Province. The dam has a maximum height of 14 m, a crest length of 2.5 km and a crest width of 7 m. The details of the dam cross-section are given in Figure 6. The dam material consists of sand, silt and clay, particularly yellowish-brown silty to sandy clay. The dam failed by

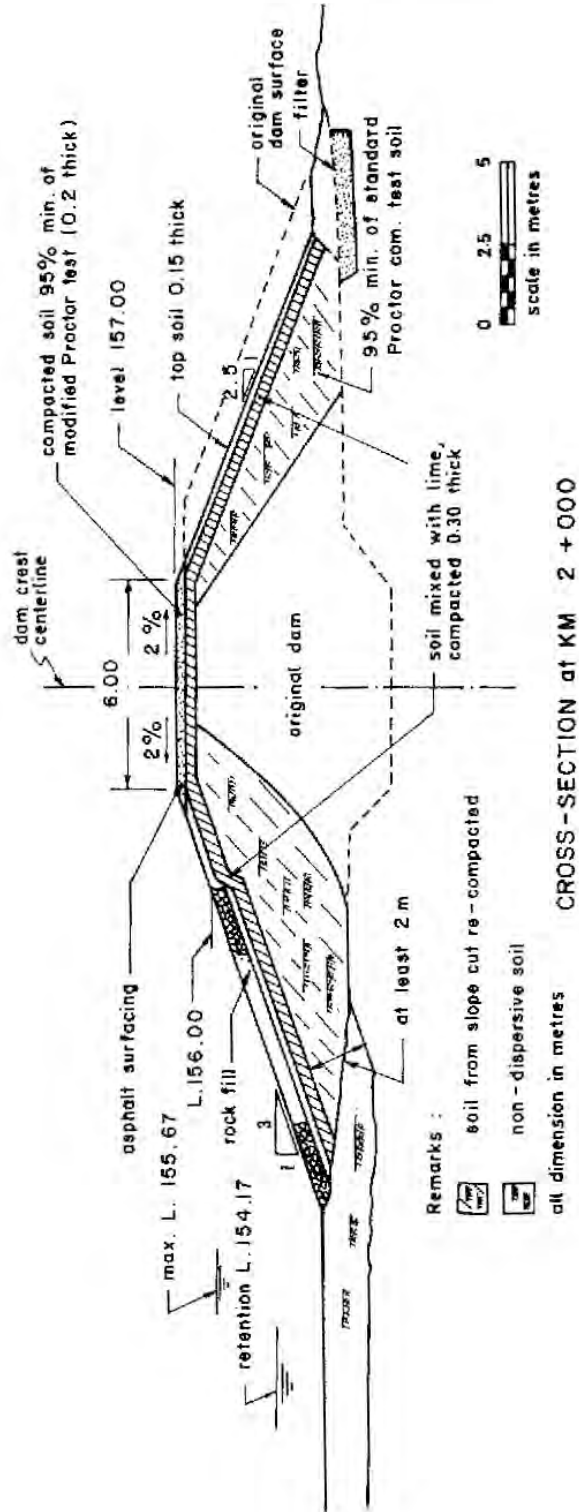


Fig. 5. Cross Section of Improved Ampun Dam.

## DISPERSIVE SOILS

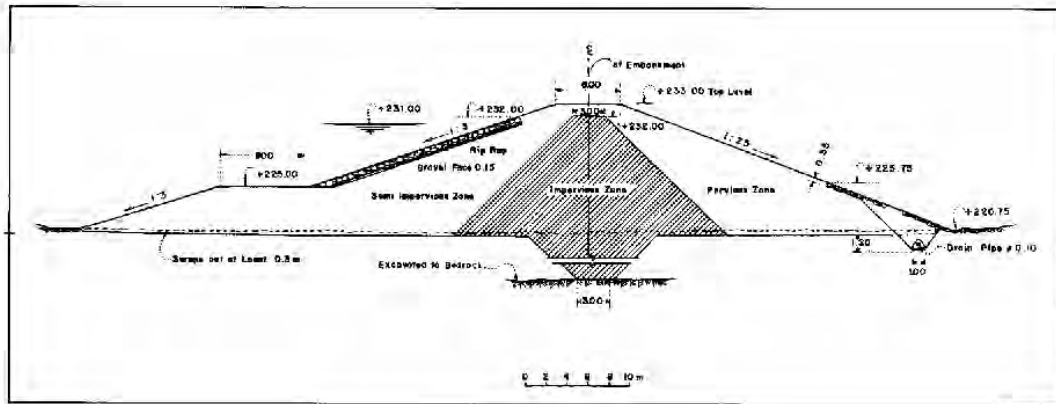


Fig. 6. Cross-section of the Lam Sam Lai Dam.

pipng during the first reservoir filling, when the embankment suffered severe tunnel erosion.

### *Sampling*

Prior to collecting soil samples, crumb tests were performed to ensure that the soil was dispersive according to the guidelines proposed by SHERARD et al (1976b), see Table 1. For laboratory tests, a 50 to 70 kg disturbed soil sample was taken from each of the three sites. The soil samples were taken at the locations where severe erosion had developed and where the worst dispersivity was indicated in the crumb tests, with the help of officials from the Royal Irrigation Department of Thailand. About 0.80 m of the surface soil was first removed at each site, before samples were taken. In Phitsanulok, samples were taken from KM 40 + 300, Ban Ta Tong, Phitsanulok Province. In Lam Sam Lai dam, the samples were taken from the dam embankment. The sample of dispersive soil from Ampun dam was taken at KM 2 + 200, in the dam embankment.

A sample of Bangkok clay, used for mixing purposes, was collected from a depth of 1.5 to 2.5 m using a helical auger. This sample was obtained from a location behind the ET Building inside the AIT Campus near Bangkok.

### *Preparation of Test Specimens*

The dispersive soil samples were first air dried and pulverized by a rubber hammer. Then, the samples were sieved through a No. 10 US Standard Sieve, oven dried, and stored in plastic bags. The Bangkok clay sample was first



**BERGADO & KANG**

oven dried, then pulverized by placing it in a rotating drum full of ball bearings. Finally, it too was sieved through a No. 10 US Standard Sieve and stored in plastic bags.

Before each test, a desired proportion of dispersive soil and Bangkok clay or dispersive soil and bentonite was first mixed in the dry condition. A predetermined amount of distilled water was then gradually added. The specimen was next stored in a humid room for 24 hours to allow for moisture equilibration. Specimens for pinhole tests were compacted using a Harvard miniature compaction apparatus.

**LABORATORY TEST PROGRAM AND RESULTS**

The testing program is outlined in Table 7. In the following sections, both test procedures and results are presented and discussed.

**Table 7. Field and Laboratory Testing Program.**

Type of Test	Mixing Material	Specimen Designation	Number of Specimens	Test Description and Objectives
Specific Gravity	Nil	P-0,A-0, L-0 clay	4	To determine physical properties
Grain Size Analysis	Nil	P-0, A-0, L-0 clay	4	Includes hydrometer test; for determining physical properties
Atterberg Limits	Bangkok clay	P-0, 10, 20, 30, 40, 50 A-0, 10, 20, 30, 40, 50 L-0, 10, 20, 30, 40, 50	18	Use distilled water ; for determining physical properties (LL, PL, PI)
	Bentonite	P-10, 20, 40 A-10, 20, 40 L-10, 20, 40	9	
Compaction	Bangkok clay	H-P0, P20, P30 S-P0, P20, P30 H-A0, A20, A30 S-A0, A20, A30 S-C0, C20, C40		Use standard and Harvard miniature compaction methods; determine $\gamma_{dmax}$ and $w_{opt}$ ; determine permeability
Pinhole	Bangkok clay	P-0, 10, 20, 30, 40 A-0, 10, 20, 30, 40 L-0, 10, 20, 30, 40	15	Use Harvard miniature compaction method ; determine dispersivity classification
	Bentonite	P-10, 20, 30 A-10, 20, 30 L-10, 20, 30	9	
Chemical	Bangkok clay	P-0, 40 A-0, 40 L-0, 40, C-0	7	To determine chemical properties
	Bentonite	P-40 A-40 L-40 Bentonite	4	

## DISPERSIVE SOILS

### Physical Properties

Index properties such as natural moisture content, Atterberg limits, specific gravity and grain size (with hydrometer analyses) were determined for both original and mixed soil samples. The grain size distributions of dispersive soils from each site, and of Bangkok clay, are shown in Figure 7. According to the Unified Classification System, the original soils from Ampun dam and

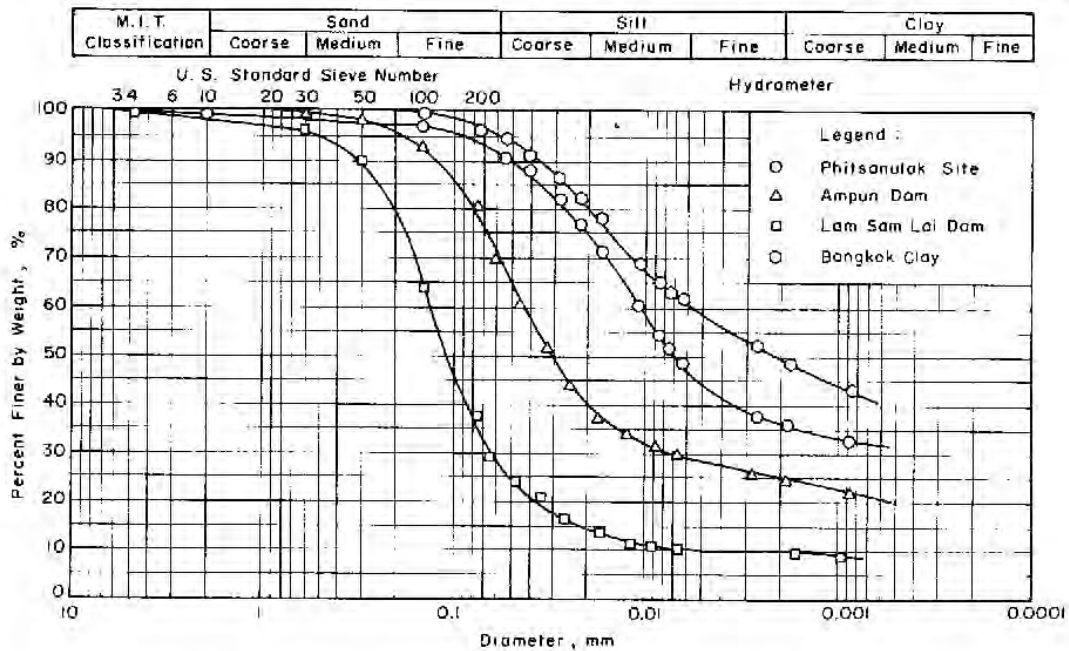


Fig. 7. Grain Size Distribution of Original Soils.

Phitsanulok are both classified as inorganic clays of low to medium plasticity (CL), and the soil from Lam Sam Lai dam is classified as well-graded silty fine sand to sandy silt (SM). The plasticity characteristics of the original soils are given in Table 8. Adding Bangkok clay and bentonite increased the Atterberg limits linearly, as shown in Figure 8. Figure 9 shows the mixtures of dispersive soil and Bangkok clay lie in the CL region of the plasticity chart, while the corresponding mixtures with bentonite lie in the CH region.

The relationship between dry density and optimum moisture content obtained from standard Proctor compaction tests and Harvard miniature compaction tests for soil samples from Phitsanulok and Ampun dam are shown in Figures 10 and 11, respectively. The maximum dry density decreased while the optimum moisture content increased with increasing proportions of Bangkok clay, as expected. The reduction in maximum dry density caused

Table 8. Results of Atterberg Limits Tests.

Site	Proportion of Mixing (%)	LL (%)	PL (%)	PI (%)	Proportion of Mixing (%)	LL (%)	PL (%)	PI (%)		
Phitsanulok	Bangkok	10	41.8	18.5	23.3	Bentonite	0	40.5	18.0	22.5
	Clay	20	42.5	19.0	22.5	10	61.2	17.7	43.5	
		30	45.5	19.7	25.8	20	92.1	19.1	73.0	
		40	47.0	20.5	26.5	30	123.3	20.8	102.4	
		50	48.0	21.0	27.0					
Ampun Dam	Bangkok	10	25.5	12.2	13.3	Bentonite	0	23.2	13.0	10.2
	Clay	20	28.4	10.7	17.4	10	46.4	19.1	27.3	
		30	33.0	12.0	21.0	20	74.5	12.8	61.7	
		40	39.7	14.0	25.7	30	103.5	13.0	90.5	
		50	42.9	15.0	27.9					
Lam Sum Lai	Bangkok	10	21.1	N.P.	-	Bentonite	0	19.6	N.P.	-
	Clay	20	23.4	15.6	7.8	10	45.8	11.7	34.1	
		30	27.5	11.5	16.0	20	74.4	13.2	61.2	
		40	34.0	12.5	21.5	30	106.8	14.0	92.8	
		50	37.0	14.0	23.0					

DISPERSIVE SOILS

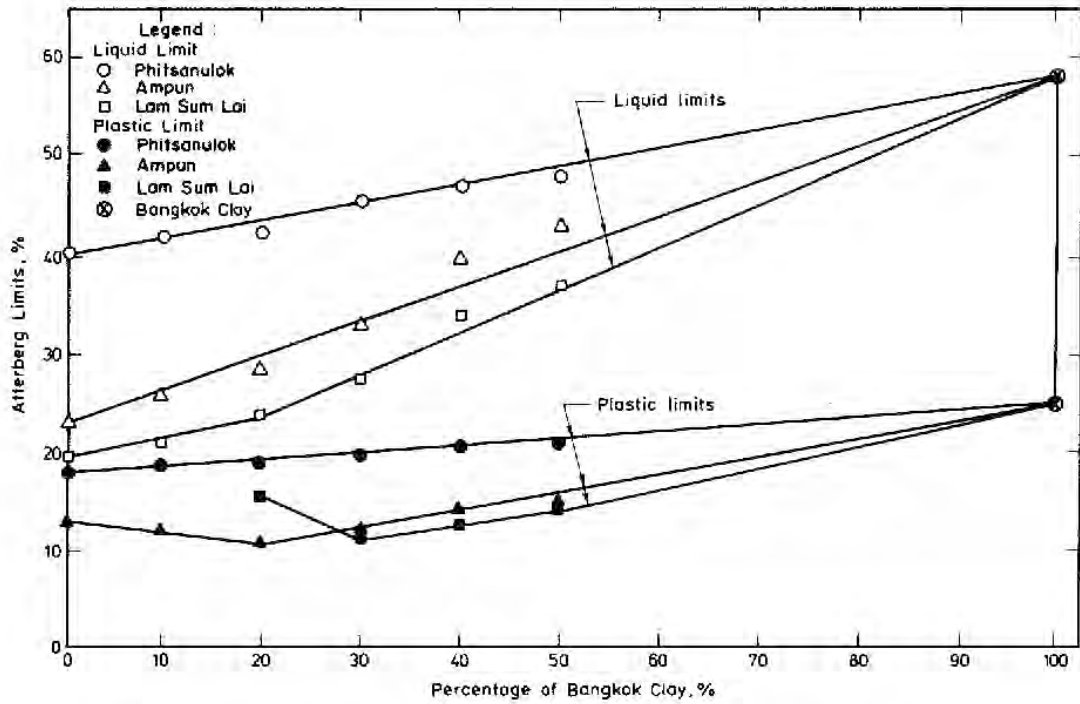


Fig. 8. Change in Atterberg Limits with Increasing Bangkok Clay Content.

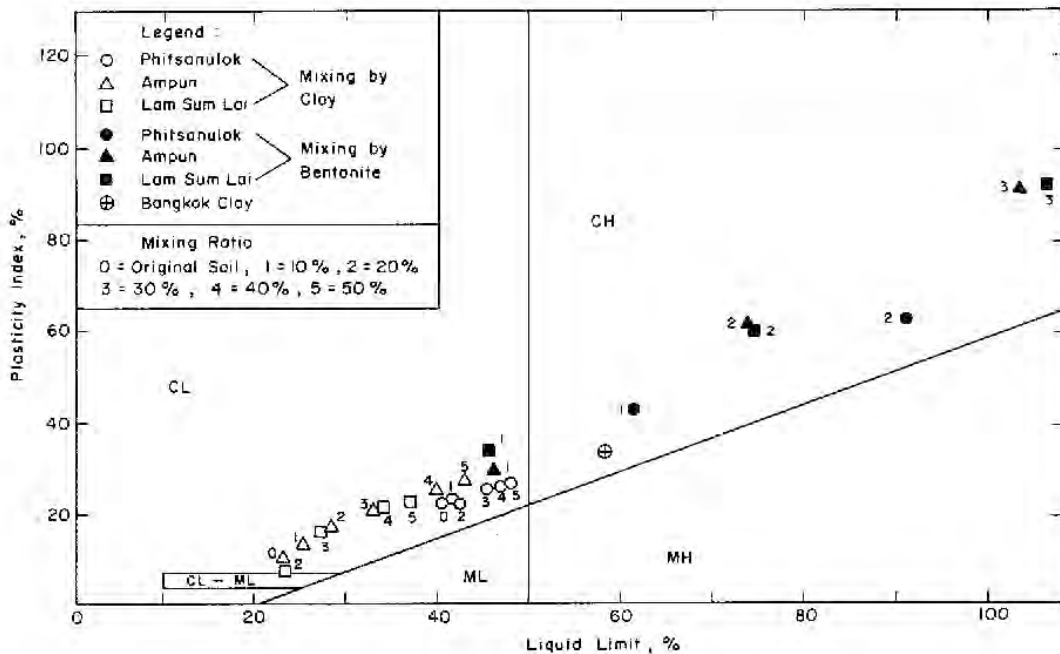


Fig. 9. Plasticity Chart of Dispersive Soils with Additives.

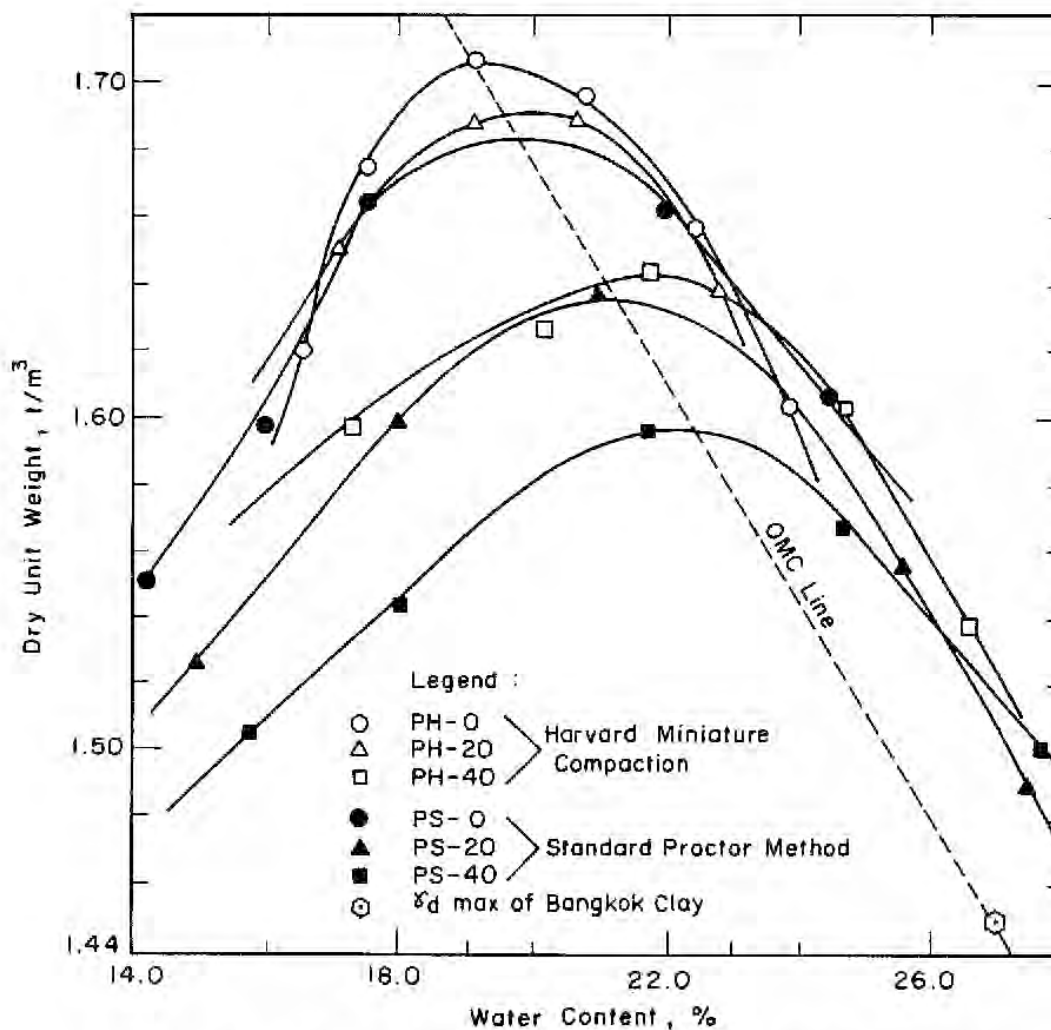


Fig. 10. Optimum Water Content and Dry Unit Weight of Phitsanulok Soil.

by the addition of Bangkok clay was much more for the Ampun dam soil than for the Phitsanulok soil. This may be due to the more sandy nature of the Ampun dam soil.

#### Tests for Dispersivity

*Crumb Test.* The crumb test is considered the quickest and simplest field test for identifying dispersive soils. But for some reasons not yet clear, this test has failed to identify some kaolinite clays that were found to be dispersive by other tests (FORSYTHE, 1977). Sometimes, because of its qualitative nature, it is difficult to differentiate between different grades or classifications.

DISPERSIVE SOILS

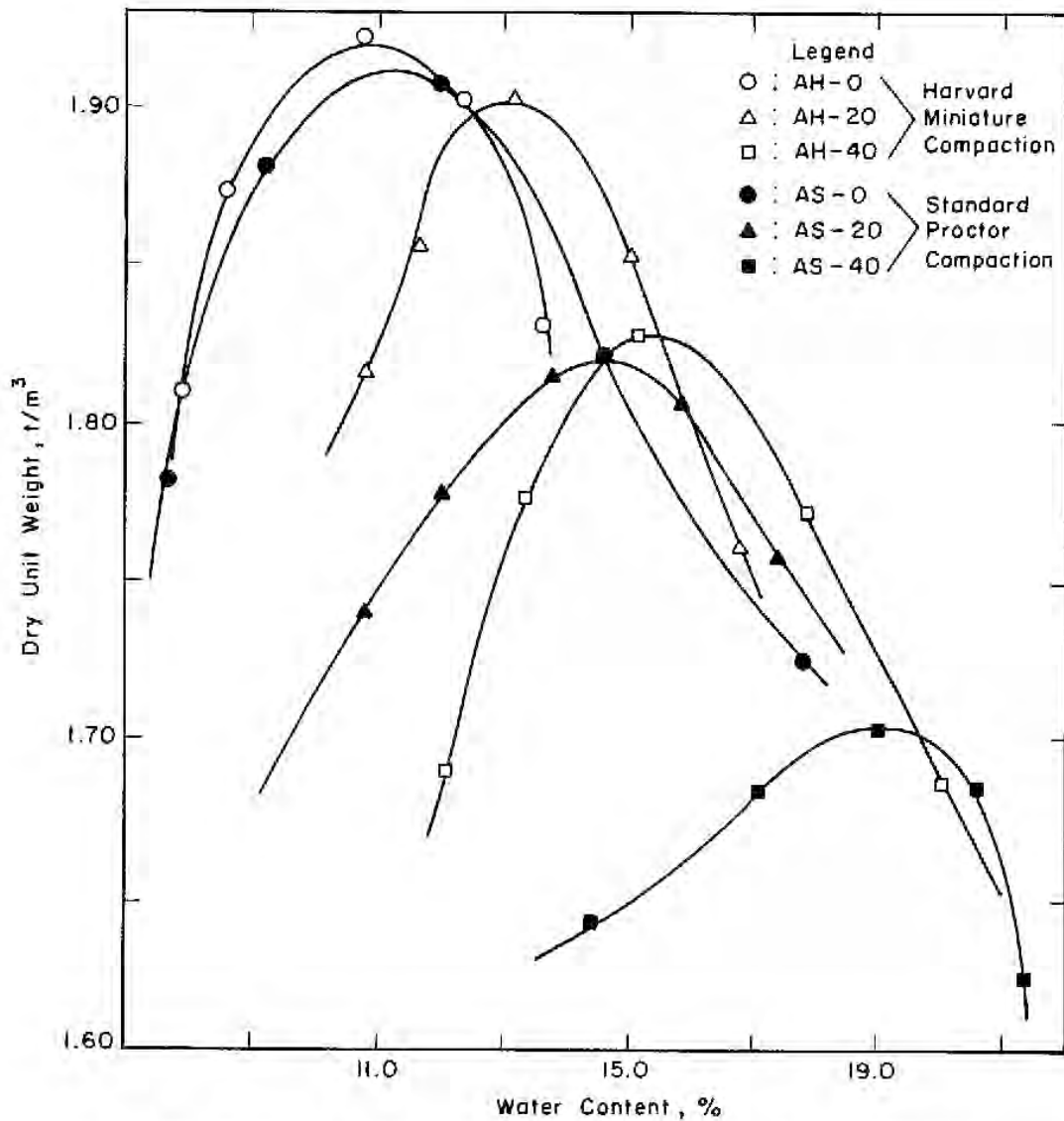


Fig. 11. Optimum Water Content and Dry Unit Weight of Ampun Dam Soil.

The original soil samples from the three sites were identified as dispersive by means of crumb tests in the field. Most of the samples from Phitsanulok and Lam Sam Lai dam were classified as grade 3 to grade 4, which means moderate to strong reaction with water, but the Ampun dam Samples showed only a slight reaction (grade 2).

*Pinhole Test.* Admixtures of both Bangkok clay and bentonite were used for this test. The standard procedure suggested by SHERARD et al (1976a) was followed; results are tabulated in Table 9. For dispersive soils classified as D1 or D2, the flow rates increased rapidly from 0.50 ml/sec to 3.5 ml/sec



Table 9. Results of Pinhole Tests on Remoulded Specimens.

Site	Additives (%)	w <sub>i</sub> (%)	γ <sub>d</sub> (t/m <sup>3</sup> )	Flow Rate (ml/sec)			Diameter of outlet (mm)	Color (side)	Particle Falling	Passing Time (head) (min)	Classification	
				5 cm	16 cm	38 cm						
Phitsanulok	nil	16.4	1.692	9.7	-	-	4.5	SM	few	5.0 (2")	D1	
	Clay	10	17.3	1.682	3.5	-	-	4.0	SM	few	8.5 (2")	D2
		20	19.0	1.672	0.8	-	-	1.5	SM	few	10.0 (2")	ND4
		30	19.7	1.666	0.4	4.0	-	3.0	BV	none	5.0 (7")	ND3
		40	20.5	1.629	-	1.5	2.0	6.1	BV	none	5.0 (40")	ND2
	Bentonite	10	17.7	1.776	7.3	-	-	4.5	D-SM	few	4.7 (2")	D1
		20	19.1	1.634	7.1	-	-	5.0	D-SM	few	5.0 (2")	D1
		30	20.8	1.582	7.7	-	-	5.0	D-SM	none	4.4 (2")	D1
	Ampun Dam	nil	10.0	1.892	4.0	-	-	4.5	SM	few	2.0 (2")	D1
		Clay	10	11.4	1.884	0.6	6.0	-	3.0	BV-CC	f.-n.	5.0 (7")
20			12.7	1.871	0.5	2.0	2.7	5.8	BV-CC	none	5.0 (40")	ND2
30			13.8	1.840	-	1.0	1.4	3.5	CC	none	4.0 (40")	ND1
40			14.9	1.784	-	-	1.2	2.9	CC	none	5.0 (40")	ND1
Bentonite		10	11.5	1.793	8.5	-	-	5.5	SM	few	3.5 (2")	D1
		20	-	1.741	7.9	-	-	5.0	SM	few	4.0 (2")	D1
		30	13.0	1.691	9.3	-	-	5.0	SM	few	4.0 (2")	D1
Lam Sam Lai Dam		nil	10.4	1.808	8.8	-	-	5.0	SM	few	3.5 (2")	D1
		Clay	10	10.4	1.759	8.7	-	-	5.0	SM	few	5.0 (2")
	20		15.6	1.734	3.9	-	-	4.0	BV	few	8.7 (2")	D2
	30		12.1	1.704	0.8	6.2	-	4.0	BV	f.-n.	3.5 (7")	ND4
	40		14.6	1.683	0.6	6.3	-	4.0	BV	none	4.2 (7")	ND4
	Bentonite	10	11.7	1.722	8.4	-	-	5.0	SM	few	3.7 (2")	D1
		20	12.8	1.706	7.3	-	-	5.0	SM	few	4.4 (2")	D1
		30	14.0	1.632	9.8	-	-	5.0	SM	few	3.4 (2")	D1

DISPERSIVE SOILS

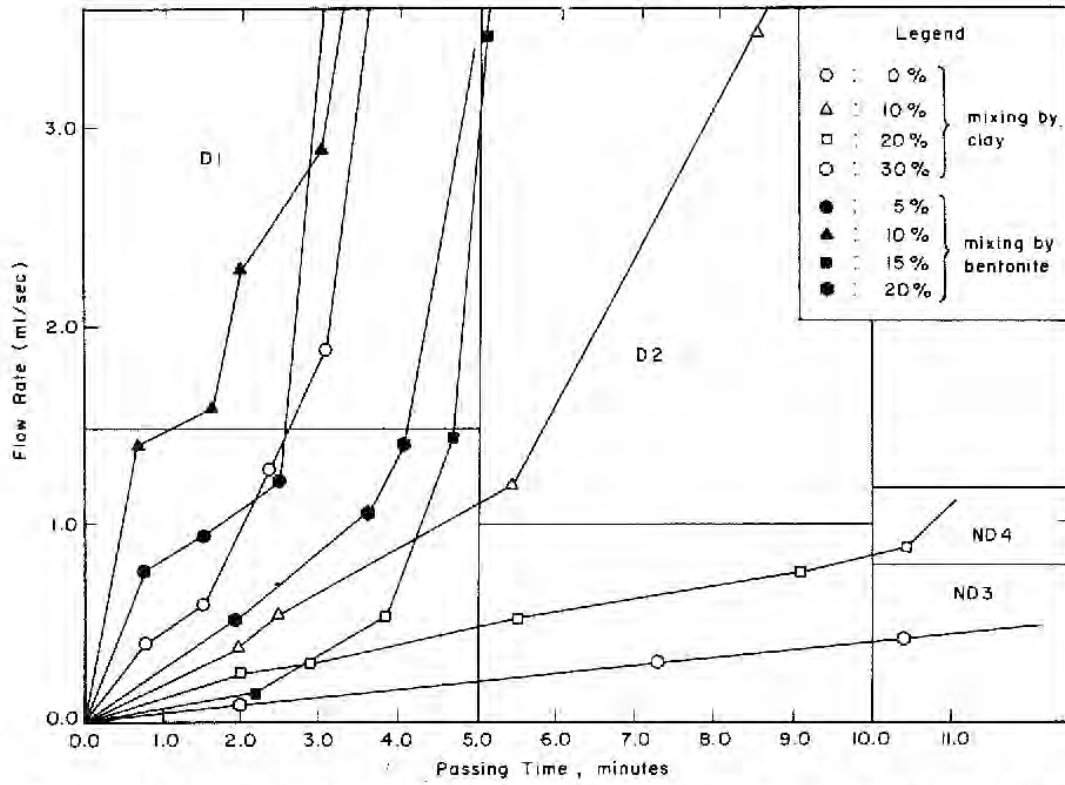


Fig. 12. Flow Rate and Passing Time of Phitsanulok Soil in Pinhole Test, 50 mm Head.

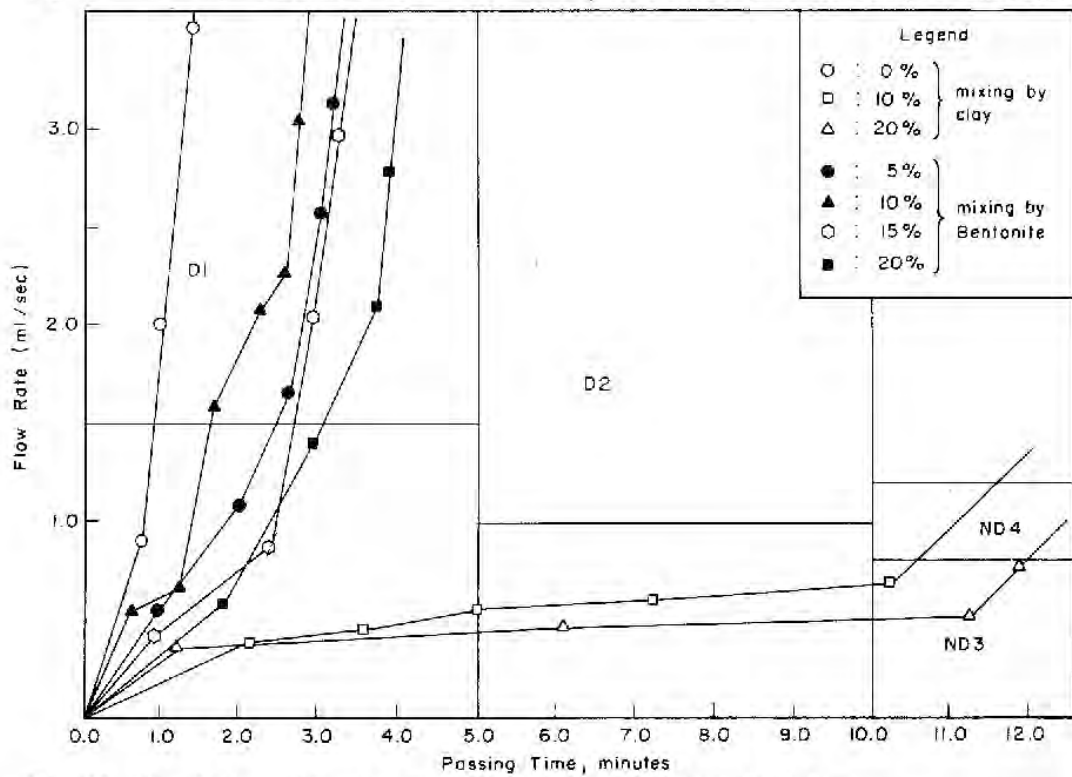


Fig. 13. Flow Rate and Passing Time of Ampun Dam Soil in Pinhole Test, 50 mm Head.

in the first 5 min period and tended to be steady in the next 5 minute period. The hole after the test was enlarged to 4 or 5 times its original size. The shape of the hole was quite uniform. As shown in Figures 12 and 13, the samples from Phitsanulok and Ampun dam become nondispersive with the addition of 20% Bangkok clay. The samples from Lam Sam Lai dam needed a 30% admixture to stabilize, as shown in Figure 14. It can be seen in Figures 12 to 14 that the use of bentonite as an admixture was not effective in stabilizing these dispersive soils.

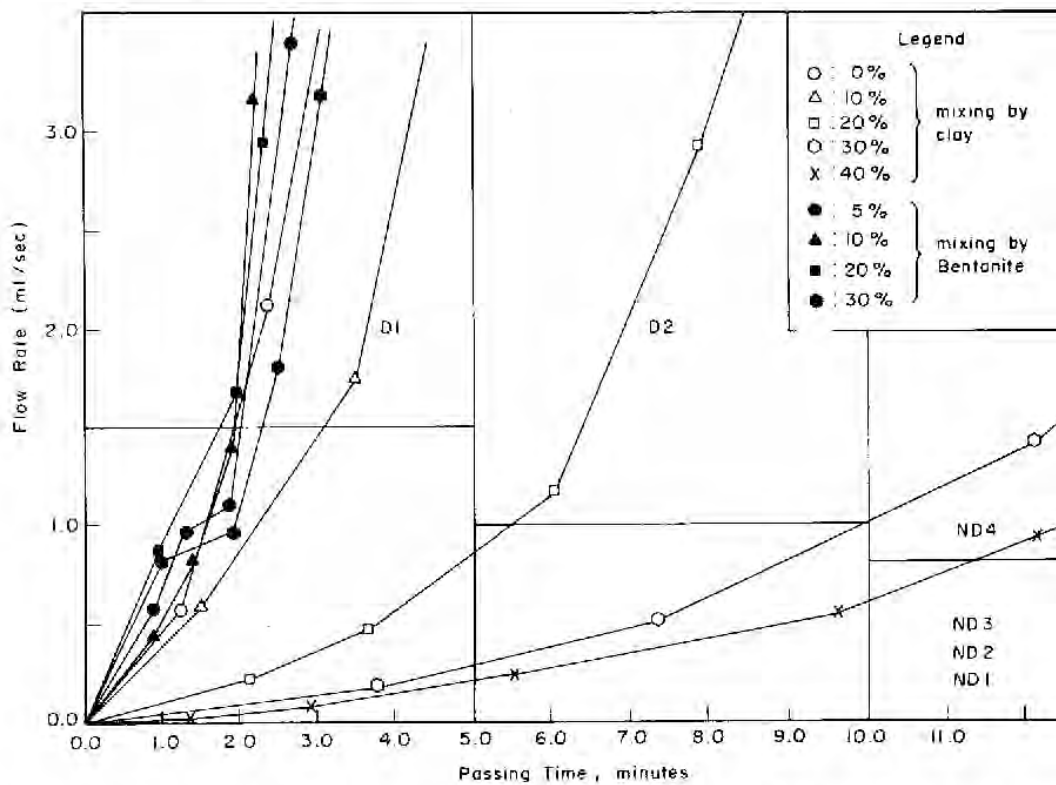


Fig. 14. Flow Rate and Passing Time of Lam Sam Lai Dam Soil in Pinhole Test, 50 mm Head.

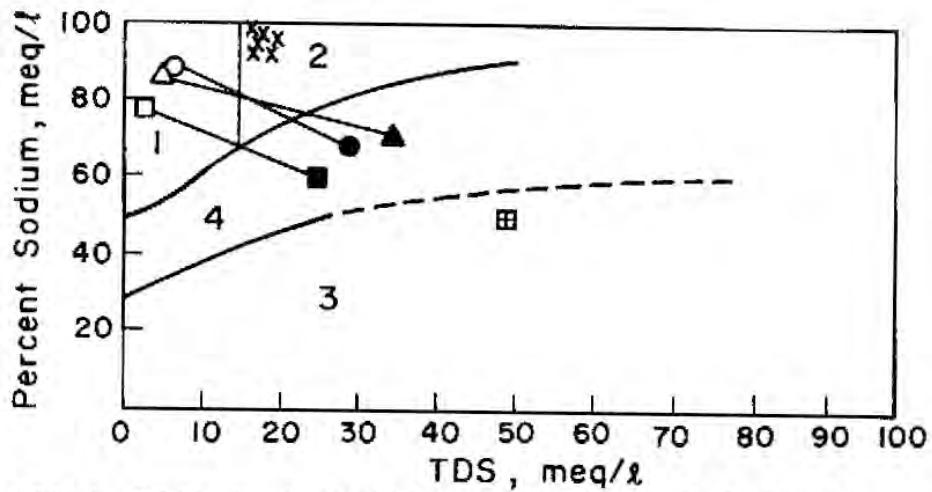
*Chemical Tests.* The results of chemical tests on saturation extracts of the soils are given in Table 10 and are plotted in Figures 15 and 16. The SAR and ESP were determined from equations 1 and 2, respectively. According to the relationship between sodium and total dissolved salts in the saturation extract (Figure 15), the original dispersive soils from each site fall in zone 1, which may have potential for breaching and tunnel erosion. When 40% Bangkok clay was added, the relationship changed to zone 4, which belongs to the transition state. The Bangkok clay itself falls into zone 3, which is

DISPERSIVE SOILS

Table 10. Results of Chemical Tests on Saturated Extracts.

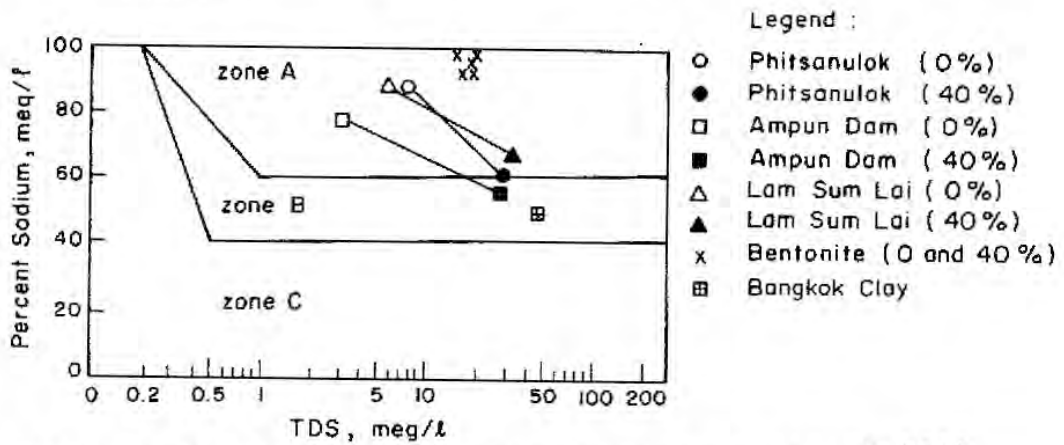
Site	Additives (%)	Saturation M.C. (%)	Saturated Paste			Saturated Extract							Classification	
			pH	EC	pH	EC	Na (meq/l)	K (meq/l)	Ca + Mg (meq/l)	SAR (%)	ESP (%)	TDS (meq/l)		Na (%)
Ampun dam	Bangkok	0	3.99	0.12	7.5	0.29	2.5	0.0	0.65	4.39	4.96	3.20	78.3	1
	Clay	40	4.08	1.43	5.4	2.87	16.0	0.92	11.8	6.59	7.80	28.7	55.8	4
	Bentonite	40	8.11	1.68	8.2	2.19	18.5	0.03	0.38	36.9	34.7	16.5	97.6	2
Lam Sam Lai Dam	Bangkok	0	6.28	0.34	7.7	0.58	5.5	0.06	0.70	9.30	11.1	6.26	87.8	1
	Clay	40	4.11	1.75	6.9	3.76	23.5	0.12	11.7	9.72	11.6	35.3	66.5	4
	Bentonite	40	8.11	1.68	8.3	1.63	16.0	0.06	1.89	16.5	18.7	18.0	89.1	2
Phitsanulok	Bangkok	0	6.15	0.37	7.6	0.73	7.5	0.04	0.92	11.1	13.1	8.46	88.7	1
	Clay	40	4.61	2.13	5.6	3.01	16.3	0.31	12.1	9.00	10.7	30.7	63.4	4
	Bentonite	40	7.91	1.68	7.9	1.61	16.1	0.03	0.38	36.9	34.7	16.5	97.5	2
Bangkok	Clay		82.73	3.90	4.4	4.89	26.0	0.80	24.0	7.51	8.94	50.8	51.2	3
Bentonite			377.46	8.66	7.4	2.5	21.0	0.08	0.54	40.4	35.0	21.6	97.1	2

Note : EC = electrical conductivity (mmhos/cm)



Note : Zone 1 : Breaching and Tunnel Erosion  
 Zone 2 : Breaching only  
 Zone 3 : Erosion Resistant Clay  
 Zone 4 : Transition

Fig. 15. Relationship between Percent Sodium and Total Dissolved Salts in Saturation Extracts.



Note : Zone A : Dispersive  
 Zone B : Intermediate  
 Zone C : Nondispersive

Percent Sodium (meq/l) =  $\frac{Na(100)}{Ca+Mg+Na+K}$   
 TDS = Ca+Mg+Na+K  
 = Total Dissolved Salts

Fig. 16. Relationship between Percent Sodium and Total Dissolved Salts in Saturation Extracts.

erosion resistant. In Figure 16, the original dispersive soils fall in zone A, which means dispersive soil. But the results tend to move to zone B (the intermediate zone) after mixing with 40% Bangkok clay. Bangkok clay

## DISPERSIVE SOILS

itself falls in zone B. In addition, using bentonite as an additive was not effective, as even bentonite itself was found to be dispersive.

The pH values were determined by means of a pH meter. The pH of the original dispersive soils was 7.5 to 7.7. Bangkok clay and bentonite, which were used as admixtures, had values of 4.4 and 7.8, respectively. The pH of the dispersive soils was very high when bentonite was used as an additive. At high pH, the proton concentration is low and the net surface charge on clay minerals is negative, resulting in a greater concentration of ions in the diffuse swarm and consequently greater repulsive interaction between particles. Bentonite additive was not effective, perhaps because of its high pH and high sodium percentage (Table 10).

### *Strength Tests*

Strength tests were carried out on freshly compacted samples at optimum moisture conditions. Unconsolidated undrained (UU) and isotropically consolidated undrained (CIU) triaxial tests were carried out at consolidation pressures similar to the field stresses with respect to slope stability. The results of the strength tests are summarized in Tables 11 and 12.

*UU Triaxial Tests.* The results of UU triaxial tests are given in Table 11. The stress-strain curves derived from a series of tests on samples from Ampun Dam are plotted in Figure 17. Increasing the Bangkok clay admixture lowered the shear strength. Considering the original dispersive soil from Ampun Dam, the resulting deviator stresses were quite large. With the addition of clay, the corresponding deviator stresses were quite low at the same confining pressures and depended on the clay admixture percentage. Similar results were obtained by TING et al (1982), in which the clay percentage in residual soils was varied.

*CIU Triaxial Tests.* The shear strength parameters  $a$  and  $\alpha$  as defined in Figure 18 in terms of effective stresses were obtained from the p-q plots. Table 12 tabulates the values of these parameters. To define the strength envelopes, two failure criteria were used, namely: maximum ratio of stresses,  $(\sigma'_1/\sigma'_3)_{\max}$ , and 12% strain. Both failure criteria indicated that the effective angle of shearing resistance ( $\phi'$ ) slightly decreased and the effective cohesion ( $c'$ ) slightly increased with the increase in Bangkok clay, especially in the case of the more sandy samples from Ampun Dam. Similar results were obtained by TING et al (1982), working with composite residual soils. However, for the case of the more fine grained soil obtained from Phitsanulok, the addition



BERGADO & KANG

Table 11. Results of Unconsolidated Undrained Triaxial Tests.

Site	Proportion Mixing by Clay (%)	Initial Condition			Sample No.	As Moulded				At Failure	
		$\gamma_d$ (t/m <sup>3</sup> )	w (%)	$S_r$ (%)		$\sigma_c$ (t/m <sup>2</sup> )	$\gamma_d$ (t/m <sup>3</sup> )	w (%)	$S_r$ (%)	$\sigma_1 - \sigma_3$ max (t/m <sup>3</sup> )	Axial Strain (%)
Ampun Dam	0	1.742	10.8	7.85	A-0-1	0	1.949	11.09	81.7	31.83	9.3
					A-0-2	20	1.939	10.83	78.3	80.69	10.1
					A-0-3	40	1.965	10.90	82.9	130.93	11.4
					A-0-4	60	1.949	11.09	81.7	182.16	13.3
					A-0-5	120	1.945	10.93	79.9	284.4	17.2
	20	1.906	13.6	91.3	A-20-1	0	1.904	13.25	90.9	26.45	16.1
					A-20-2	20	1.908	13.31	89.7	33.72	19.3
					A-20-3	40	1.909	13.14	88.7	42.06	20.0
					A-20-4	60	1.912	13.21	89.6	50.03	20.0
					A-20-5	120	1.900	13.27	91.4	80.85	20.0
	40	1.799	15.6	85.8	A-40-1	0	1.802	15.65	86.5	29.53	20.0
					A-40-2	20	1.796	16.01	87.6	36.49	20.0
					A-40-3	40	1.799	15.72	86.4	14.25	20.0
					A-40-4	60	1.795	15.43	84.3	55.41	20.0
					A-40-5	120	1.793	15.68	85.6	85.34	20.0
Phitsanulok	0	1.698	19.2	87.3	P-0-1	0	1.702	19.41	88.8	36.07	14.6
					P-0-2	20	1.689	19.84	88.9	46.25	17.3
					P-0-3	40	1.710	19.71	91.3	51.09	20.0
					P-0-4	60	1.706	19.36	89.1	56.54	20.0
					P-0-5	120	1.693	19.26	88.6	92.63	18.9
	20	1.688	20.0	89.5	P-20-2	20	1.686	20.34	90.8	44.15	18.4
					P-20-3	40	1.688	20.27	90.7	46.23	20.0
					P-20-4	60	1.684	20.31	90.3	56.12	20.0
					P-20-5	120	1.680	19.27	89.2	87.94	20.0
					P-40-1	0	1.632	22.12	90.8	30.54	16.3
	40	1.642	22.0	91.7	P-40-2	20	1.643	21.96	91.6	35.01	20.0
					P-40-3	40	1.637	22.41	92.7	38.07	20.0
					P-40-4	60	1.639	21.54	89.3	43.13	20.0
					P-40-5	120	1.639	22.07	89.8	78.11	20.0

Table 12. Summary of Shear Strength Parameters.

Site	Proportion Bangkok Clay (%)	Test No.	Total Stress Parameters		Effective Stress Parameters	
			c (t/m <sup>2</sup> )	$\phi$ (deg)	c' (t/m <sup>2</sup> )	$\phi'$ (deg)
Pitsanulok	0	P-0*	5.6	10.2	0.9	31.8
	20	P-20*	3.0	18.4	1.3	25.1
	40	P-40*	2.6	14.3	0.9	31.4
Ampun Dam	0	A-0*	12.1	29.2	0.0	38.7
	20	A-20*	3.3	21.3	0.6	32.4
	40	A-40*	3.6	16.9	2.1	23.2
Pitsanulok	0	P-0**	8.0	12.3	2.0	25.1
	20	P-20**	5.5	16.7	1.3	25.1
	40	P-40**	4.5	16.1	1.8	23.2
Ampun Dam	0	A-0**	14.9	32.9	0.0	38.7
	20	A-20**	4.8	20.1	0.6	32.4
	40	A-40**	8.3	12.3	3.5	17.8

Note: \*Failure criteria is 12% strain

\*\*Failure criteria is maximum obliquity ratio,  $(\sigma'_1/\sigma'_3)_{max}$

DISPERSIVE SOILS

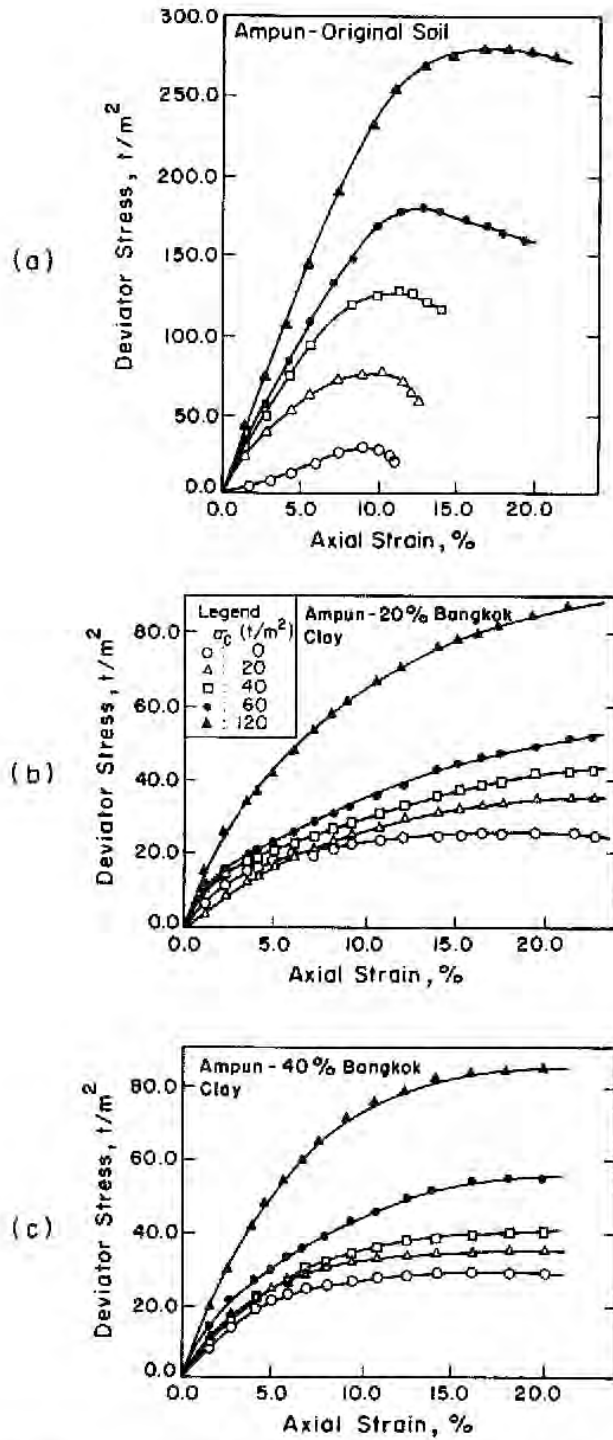


Fig. 17. Stress-Strain Curves from UU Triaxial Tests on Ampun Dam Soils.

BERGADO & KANG

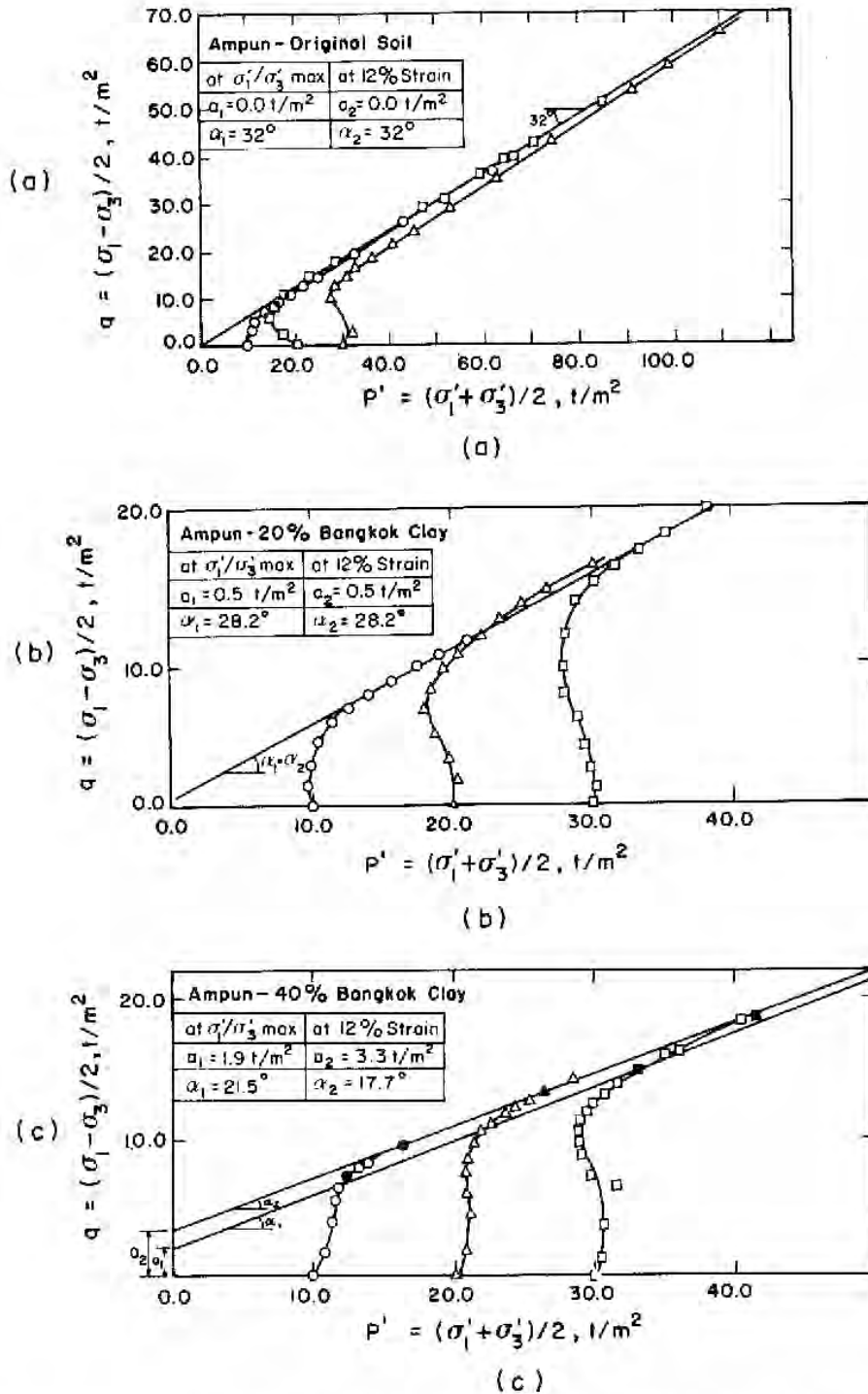


Fig. 18. Effective Stress Paths and Strength Envelopes from CU Triaxial Tests on Ampun Dam Soils.

### DISPERSIVE SOILS

of increasing percentages of Bangkok clay did not influence the strength parameters. This may be due to the already high clay content of the original soil.

### CONCLUSIONS

Based on the results of the experimental investigations carried out on three dispersive soils mixed with Bangkok clay or bentonite, the following conclusions can be drawn:

- 1) Bentonite is not suitable as an admixture to improve dispersive soils, perhaps due to its high pH and high percentage of sodium in the saturation extract. Bentonite itself has been found to be dispersive.
- 2) Both dispersive soils from Phitsanulok and Ampun dam, with Unified Soil Classifications of CL, changed to nondispersive soil when mixed with 20% Bangkok clay. On the other hand, the dispersive soils from Lam Sam Lai dam, with a USC designation of SM, required a larger amount (30%) of Bangkok clay to render it nondispersive.
- 3) Most of the dispersive soils in northeast Thailand are inorganic silty clays, clayey silts, and sand-silt mixtures of low to medium plasticity. Their liquid and plastic limits increased when mixed with increasing amounts of Bangkok clay. Their maximum dry densities decreased and corresponding optimum moisture contents increased almost linearly with increasing Bangkok clay percentages, as expected, in both standard Proctor and Harvard miniature compaction tests.
- 4) The dispersive soils in northeast Thailand have been responsible for dam failures due to piping, tunnelling, and surface erosion. The soils consist predominantly of kaolinite clay minerals and clay-size to silt-size quartz with high pH and high content of dissolved sodium, relative to the quantities of other cations such as calcium and magnesium, in its saturation extract.
- 6) The effective cohesion ( $c'$ ) slightly increased and the effective angle of shearing resistance ( $\phi'$ ) slightly decreased with increases in the percentage of Bangkok clay in the dispersive soil-Bangkok clay mixtures.

### ACKNOWLEDGMENTS

The authors are gratefully indebted to Prof. A.S. Balasubramaniam and Prof. Prinya Nutalaya for valuable advice during the research study. The

authors are also very grateful to Dr. Suphon Chirapuntu, Senior Soil Engineer at the Royal Thai Irrigation Department, for providing valuable information and assistance during the collection of soil samples. Finally, a heartfelt gratitude is extended to Mrs. Uraiwan Singchinsuk and Miss Nualchan Sangthongstit for their valuable help in the preparation of the manuscripts.

#### REFERENCES

- AITCHISON, G.D. (1960). Discussions on "Piping Failures of Earth Dams Built of Plastic Materials in Arid Climates," Cole & Lewis (1960). *Proc. 3rd Australia-New Zealand Conf. on Soil Mech. and Found. Eng.*, p. 230.
- CHANDRA, S. & CHEN, G.L. (1985). Improvement of Dispersive Soil By Using Different Additives. *Indian Geotechnical J.*, vol. 14, no. 3, pp. 202-216.
- CHANDRA, S. & GARCIA, E.B. (1984). Chemical and Mineralogical Study of Collapsible and Dispersive Soil. *Proc. Intl. Geotechnical Conf.*, Calcutta, India.
- CHEN, G.L.J. (1984). *Improvement of Dispersive Soil by Using Different Additives at Low and High pH Values*. M.Eng. Thesis, AIT, Bangkok, Thailand.
- COLE, D.C.H. & LEWIS, J.G. (1960). Piping Failure of Earth Dams Built of Plastic Materials in Arid Climates. *Proc. 3rd Australia-New Zealand Conf. on Soil Mech. and Found. Eng.*, pp. 93-99.
- COLE, B.A., RATANASEN, C., MAIKLAD, P., LIGGINS, T.B. & CHIRAPUNTU, S. (1977). Dispersive Clay in Irrigation Dams in Thailand. *Dispersive Clays, Related Piping and Erosion in Geotechnical Projects, ASTM STP-623*, American Society for Testing and Materials, pp. 25-41.
- COUMOULOS, D.G. (1977). Experience with Studies of Clay Erodibility in Greece. *Dispersive Clays, Related Piping and Erosion in Geotechnical Projects, ASTM STP-623*, pp. 42-57.
- DECKER, R.S. & DUNNIGAN, L.P. (1977). Development and Use of the Soil Conservation Service Dispersive Test. *Dispersive Clays, Related Piping and Erosion in Geotechnical Projects, ASTM STP-623*, pp. 94-109.
- EMERSON, W.W. (1964). The Slaking of Soil Crumbs as Influenced by Clay Mineral Composition. *Australian J. of Soil Research*, vol. 2, pp. 221-227.
- EMERSON, W.W. (1967). A Classification of Soil Aggregate Based on Their Coherence in Water. *Australian J. of Soil Research*, vol. 5, pp. 47-57.
- FERNANDO, M.J. (1979). *Distribution and Properties of Dispersive Soils in the Vicinity of the Lam Sam Lai Dam Site and Their Effects on Embankment Dam Construction*. M.Eng. Thesis, AIT, Bangkok, Thailand.
- FORSYTHE, P. (1977). Experience in the Identification and Treatment of Dispersive Soils in Mississippi Dams. *ASTM STP-623*, pp. 135-155.
- GARCIA, E.B. (1983). *Chemical and Mineralogical Studies of Collapsible and Dispersive Soils in North and Northeastern Thailand*. M. Eng. Thesis, AIT, Bangkok, Thailand.
- HALIBURTON, T.A., PETRY, T.M. & HAYDEN, M.S. (1975). Identification and Treatment of Dispersive Clay Soils. *United States Bureau of Reclamation Special Report*, PB-248 840.
- HOLMGREEN, G.G.S & FLANAGAN, C.P. (1977). Factors Affecting Spontaneous Dispersion of Soil Materials as Evidenced by the Crumb Test. *ASTM STP-623*, pp. 218-239.

### DISPERSIVE SOILS

- INGLES, O.G. & AITCHISON, G.D. (1969). Soil-Water Disequilibrium as a Cause of Subsidence in Natural Soils and Earth Embankments. *CSIRO Div. of Soil Mech. Research Paper No. 131*, pp. 342-352.
- KANG, K.Y. (1985). *Stabilization of Dispersive Soils By Mixing with Bangkok Clay and Bentonite*. M. Eng. Thesis, AIT, Bangkok, Thailand.
- KIM, G.W. (1982). *Dispersive Soils in Northeastern Thailand*. M. Eng. Thesis, AIT, Bangkok, Thailand.
- LAMBE, T.W. & WHITMAN, R.V. (1969). *Soil Mechanics*. John Wiley & Sons.
- LOGANI, K.L. & HECTOR, M. (1979). Techniques Developed During Foundation Treatment of the Ulum Dam Constructed of Dispersive Soils. *Proc. 13th Intl. Cong. on Large Dams*, vol. 1, pp. 729-748.
- NAKANO, R. (1967). On Weathering and Changes of Tertiary Mudstone Related to Landslide. *Soils and Foundations*, vol. 7, pp. 1-14.
- PARKER, G.G. & JENNE, E.A. (1967). Structural Failure of Western Highways Caused by Piping. *Highway Research Record No. 203*, pp. 57-76.
- RICHARDS, L.A. (1954). Diagnosis and Improvement of Saline and Alkali Soils. *Agriculture Handbook No. 60*, Dept. of Agriculture, USA.
- SCHAFFER, G.J. (1978). Pinhole Test for Dispersive Soils-Suggested Changes. *J. Geotech. Eng. Div. ASCE*, vol. 104, no. GT6, pp. 761-765.
- SHERARD, J.L., DECKER, R.S. & RAKER, N.L. (1972). Piping in Earth Dams of Dispersive Clays. *Proc. Conf. on Performance of Earth and Earth-Supported Structures*, ASCE, vol. 1, pp. 589-626.
- SHERARD, J.L., DUNNIGAN, L.P., DECKER, R.S. & STEELE, E.F. (1976a). Pinhole Test for Identifying Dispersive Soils. *J. Geotechnical Eng. Div. ASCE*, vol. 102, no. GT1, pp. 69-87.
- SHERARD, J.L., DUNNIGAN, L.P. & DECKER, R.S. (1976b). Identification and Nature of Dispersive Soils. *J. Geotechnical Eng. Div. ASCE*, vol. 102, no. GT4, pp. 287-302.
- SHIEH, J.L. (1981). *Engineering Properties of Dispersive Soils*. M. Eng. Thesis, AIT, Bangkok, Thailand.
- TAI, T.Y. (1983). *Improvement of Dispersive Soils by Using Soil Stabilization*. M. Eng. Thesis, AIT, Bangkok, Thailand.
- TING, W.H., MUN, K.P. & TOH, C.T. (1982). Characteristics of Composite Residual Granite Soil. *Proc. Seventh Southeast Asian Geotechnical Conf.*, Hong Kong, vol. 1, pp. 879-887.
- VAN OLPHEN, H. (1963). *An Introduction To Clay Colloid Chemistry*. John Wiley & Sons.
- VOLK, G.M. (1937). Method of Determination of Degree of Dispersion of Clay Fraction Soils. *Proc. Soil Science Soc. of America*, vol. 11, pp. 561-565.



## **STRENGTH OF SANDSTONES IN SATURATED AND PARTIALLY SATURATED CONDITIONS**

**K.S. RAO\***, **G. VENKATAPPA RAO\*\*** AND **T. RAMAMURTHY\*\***

### **SYNOPSIS**

The variation of strength with moisture content of four Indian sandstones in different test modes, including uniaxial compression, Brazilian, axial and diametral point load tests, has been investigated. The variation of pore water pressure with moisture is computed from Kelvin's equation using the pore size distributions obtained by analysis of water vapour adsorption isotherms. Changes in inter-particle electrical forces, usually known as surface energy, are also considered. The variation in strength with moisture content is examined by an effective stress concept which takes into account electrical forces as well as pore pressures. An attempt is then made to develop a unified mechanism which can explain the strength decrease due to saturation.

### **INTRODUCTION**

For harnessing the as yet untapped natural resources in India, extensive river valley development programmes are in progress. With spiralling civil engineering activities, the choice of favourable sites is becoming increasingly limited, posing unforeseen challenges to geotechnical engineers. The need for proper estimates of rock strength is felt in the design and construction of these projects, as influenced by insitu stresses and environmental conditions. Among the many factors which influence rock strength, moisture is one of the most important. It is well known that most underground rocks contain moisture, varying from less than 1% for some evaporites to over 35% for porous sandstones. In the majority of mines, especially in coal mines and underground excavations, rocks are nearly saturated. The presence of water invariably reduces rock strength and thereby weakens the underground workings. Though many theories exist to explain the strength reduction with increasing moisture content in rocks, there is no unified theory which explains such behaviour satisfactorily. In this paper, an attempt has been made to elucidate the strength and deformation characteristics of sandstones in the saturated and partially saturated states.

### **LITERATURE REVIEW**

#### *Effect of Moisture on Strength*

Due to their porous nature, rocks may contain moisture in their natural

\*Lecturer, \*\*Professors, Department of Civil Engineering, Indian Institute of Technology, New Delhi, India.

state. Numerous studies have shown that rock is generally weaker when tested 'wet'. Several researchers have compared uniaxial compressive strengths ( $\sigma_c$ ) of several rock types under oven dry, air dry and wet conditions (PRICE, 1960; COLBACK & WIID, 1965; BROCH & FRANKLIN, 1972; VAN EECKHOUT, 1976; RAO, 1984). From all these studies, it is evident that for all rock types, strength is the highest in oven dry conditions, followed closely by the air dry condition, but it is significantly lower in the wet condition. Strength reductions even up to 40 or 50% have been reported. It is also observed that the strength loss is the highest for sedimentary rocks and the least for metamorphic and igneous rocks.

The behaviour of rocks in tension under different humidities has been studied by FEDA (1966), WIID (1970), BROCH & FRANKLIN (1972), and VAN EECKHOUT (1976). A study of these results clearly indicates that the Brazilian strength ( $\sigma_{tb}$ ) decreases with increasing moisture content. Studies of point load tests conducted by BROCH (1979) have also shown decreasing strength with increasing moisture content for several rock types. Similarly, COLBACK & WIID (1965), RAMAMURTHY & GOEL (1973), VAN EECKHOUT (1976) and CHAMBERLAIN *et al* (1976) showed that peak strengths under triaxial conditions were least for saturated specimens. CHAMBERLAIN *et al* (1976) and WIID (1970) observed a decrease in elastic modulus,  $E$ , with increases in moisture content.

Apart from water, the presence of other fluids also effects rock strength, as observed by BOOZER *et al* (1962) and COLBACK & WIID (1965). It was found that strength is inversely proportional to the surface tension of the liquid with which the rock is saturated. VUTUKURI (1974) reported the effect of different liquids on tensile strength of limestones, and has shown that as the dielectric constant and surface tension of the liquid increased, the strength decreased.

#### *Strength Reduction Mechanisms*

Several mechanisms and theories have been put forward by different researchers to explain the influence of moisture on the strength of rocks (VAN EECKHOUT, 1976), but there appears to be no generally accepted explanation. The essential theories which are believed to be responsible for strength reduction due to moisture are:

- (i) Fracture energy reduction (using Griffith's criterion), arising out of the reduction in surface energy due to water adsorption by the rock;

*SANDSTONE STRENGTH*

- (ii) Capillary tension (pore water pressure deficiency) in unsaturated rocks, which is a function of the vapour pressure;
- (iii) Pore pressure increase due to confining pressure, with an increase in pore pressure resulting in a decrease in strength, as is the case with soils;
- (iv) Reduction in coefficient of friction with increase in moisture, leading to strength reduction; and
- (v) Chemical and corrosive deterioration if expanding lattice type clay minerals are present.

Mechanisms (ii) and (iii) above can be considered as a single mechanism, that is, as pore pressure change. All of the above mechanisms may not be responsible for the reduction of strength in all cases, as some are more likely than others in certain rock types and under certain loading conditions.

*Effective Stress Concept*

The concept of effective stress formulated by TERZAGHI (1936) has made possible the application of rational principles to many soil engineering problems that previously could only be treated in an empirical manner. LAMBE (1960) made the effective stress concept more general, in order to explain the behaviour of cohesive and noncohesive soils and partially saturated materials, by considering the molecular properties and inter-particle forces. Further, this concept has been generalised by SRIDHARAN (1968), who considered the influence of attractive and repulsive forces as well as pore water and pore air pressures, in the following form:

$$\bar{\sigma}_c = \bar{\bar{\sigma}} a_m = \sigma - \bar{u}_w - \bar{u}_a - R + A \quad \dots\dots\dots (1)$$

where  $\bar{\sigma}_c$  = effective contact stress,

$\bar{\bar{\sigma}}$  = mineral to mineral contact stress,

$a_m$  = mineral-to-mineral unit contact area,

$\sigma$  = externally applied pressure on unit area,

$\bar{u}_w$  = effective pore water pressure,

$\bar{u}_a$  = effective pore air pressure,

R and A = effective inter-particle repulsive and attractive pressures, respectively.

It is hypothesized that the effective contact stress, as defined above, is the stress controlling the engineering behaviour of soils. This concept has been found to be useful in understanding the strength, volume change and shrinkage

behaviour of soils (SRIDHARAN & RAO, 1971, 1973, 1979). With this in view, RAO *et al* (1981) and VENKATAPPA RAO *et al* (1983) have preliminarily examined whether a similar equation can explain the strength behaviour of rocks. In the present study, a detailed examination has been made in order to understand this phenomenon in greater detail.

The usefulness of the effective stress concept in understanding the strength reduction due to moisture in rocks is presented in the following sections.

#### *Pore Water and Pore Air Pressure*

The influence of pore pressures, particularly that of the pore water pressures, on the strength of rocks has been well demonstrated by HEARD (1960), HANDIN *et al* (1963), JAEGER (1966) and VUTUKURI (1974). In saturated rocks, an increase in pore water pressures results in a decrease in strength. On the other hand, the pore water pressures will be negative when the rock is unsaturated, which results in an increase in strength. Mechanism (ii) and (iii) cited in the earlier section consider these influences of pore pressure on the rock strength. The effective stress equation (equation 1) takes these pore pressures into account.

#### *Inter-Particle Forces*

The intrinsic strength of rock can be visualised as arising from two components. The primary component is that due to mineralogy and/or cementing materials, which may be taken as constant for given conditions. The other component, which is variable, is that due to surface forces (surface energy) which are dependent on the environment, for example, pore fluid, degree of saturation, temperature, etc. BRACE & WALSH (1962) defined surface energy of a solid as the work required to produce a certain amount of new surface. According to PUGH (1967), surface energy is the work done in separating crack surfaces against attractive interatomic forces. Thus, it is clear that what is customarily known as 'surface energy' ( $\gamma$ ) and is considered to vary with moisture content and pore fluid type, is commonly designated as interatomic attractive and repulsive forces (A-R), which were shown to be a function of moisture and pore fluid type in earlier sections.

An increase in moisture content or degree of saturation will result in an overall decrease of net attractive forces, due to an increase in surface energy. In other words, the surface energy (considered in terms of Griffith's criterion) will reduce the fracture energy and hence the rock strength. In the effective stress equation (equation 1), one can easily reconsider the net attrac-



## SANDSTONE STRENGTH

tive force term (A-R) as partly arising from mineralogical forces (which are constant for a given rock) and partly due to surface energy forces (which vary with moisture content). Thus, with an increase in moisture content, while the mineralogical forces remain nearly constant, the surface forces decrease, resulting in a lowering of the effective contact stress, and causing a decrease in strength.

In a similar manner, a decrease in friction may be said to occur from an increase in moisture content because of reductions in the value of (A-R) or surface energy. This will ultimately lead to a lowering of the strength due to increased moisture.

The effective stress concept directly takes into consideration the changes in strength due to changes in pore pressures, both positive and negative, as already indicated. A reduction in the strength of saturated rocks under confinement has also been observed by several researchers, as already reported. This is easily explained through the effective stress concept. Thus, it may be concluded that the effective stress concept has immense potential in understanding the strength due to environmental changes, and in unifying the existing mechanisms.

## EXPERIMENTAL STUDY

An investigation has been undertaken of the strength and deformation behaviour of four Indian sandstones from different geological formations in the partially and fully saturated states. An attempt has been made to explain the behaviour of these rocks by the effective stress concept, through a study of the variation of negative pore water pressure and surface energy changes.

### *Rocks Tested*

The four sandstones used in this investigation were obtained from geological formations ranging from the older Vindhya (600 m y) to the recent Sivalik Systems (25 m y), as detailed in Table 1. The detailed geological and petrological properties of the rocks are detailed below.

*Kota Sandstone.* This sandstone is from Kota, Rajasthan, belonging to the Bhandar series of upper Vindhya (Table 1). This rock type is a common foundation for several river valley projects, e.g. Ranapratap Sagar and Jawahar Sagar in Rajasthan. The colour is variegated shades of red, buff and grey, mottled or speckled because of the variable dissemination of the colouring matter or its removal by deoxidation. Kota sandstone is anisotropic,

**Table 1. Geological Classification of Rocks Studied.**

Rock Type and Location	Geological System	Series	Geological Age (m y)
Kota Sandstone, Rajasthan	Upper Vindhya	Bhander	600
Singrauli Sandstone, Singrauli, Madhya Pradesh	Lower Gondwanas	Raniganj, Purewa (bottom)	150
Jhingurda Sandstone, Singrauli, Madhya Pradesh	Lower Gondwanas	Raniganj, Purewa (top)	150
Jamrani Sandstone, Jamrani, Uttar Pradesh	Lower Sivaliks	Chinji	25

showing perfect thin bedding planes. A scanning electron micrograph is shown in Figure 1. Thin section studies show that the rock mainly consists of moderately sorted, well cemented fine to medium sand grains. Quantitative estimation from thin section studies and the X-ray diffraction pattern show that the rock contains 95% quartz and 5% ferruginous cementing material (Table 2).

*Singrauli Sandstone.* This sandstone is obtained from the Singrauli coal fields, Madhya Pradesh, comprising an area of about 2,200 sq km of lower Gondwanas. The Singrauli sandstone tested belongs to the Purewa bottom series of the Raniganj group of the Gondwana system (Table 1). It is black or blackish grey in colour, isotropic in appearance, and is composed mainly of moderately to poorly sorted, well cemented medium to coarse grains, as seen in the scanning electron micrograph shown in Figure 1. The quantitative estimation of different minerals is given in Table 2.

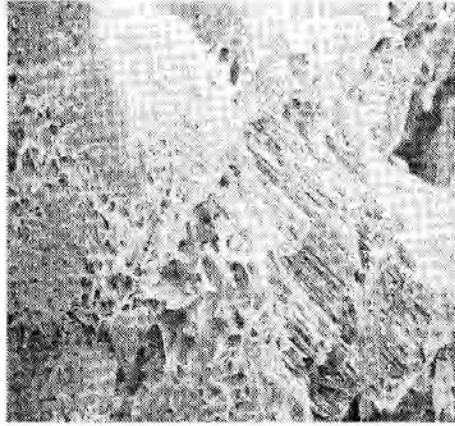
**Table 2. Mineralogical Analysis of Sandstones Tested.**

Rock	Detrital Grains (%)			Cementing Material (%)	
	Quartz	Feldspar	Mica	Argillaceous (Kaolinite)	Others
Kota Sandstone	95	-	-	-	5
Singrauli Sandstone	56	16	10	10	Ferruginous Carbonaceous (trace)
Jhingurda Sandstone	40	-	10	50	-
Jamrani Sandstone	40	44	9	-	7 Siliceous and Carbonaceous (trace)

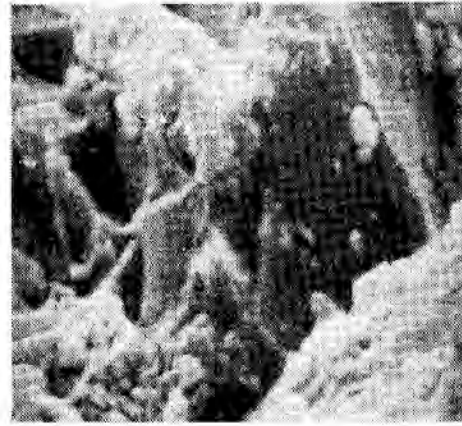
*Jhingurda Sandstone.* This sandstone is obtained from the Jhingurda coal mines of Singrauli, Madhya Pradesh. It is white coloured and isotropic



*SANDSTONE STRENGTH*



(a) × 622



(b) × 2220



(c) × 2142



(d) × 1043

**Fig. 1. Scanning Electron Micrographs; (a) Kota, (b) Jamrani, (c) Singrauli, and (d) Jhingurda Sandstones.**

in appearance, belonging to the Purewa top series of the Raniganj group of the Gondwana system (Table 1). It is coarse grained and fragile in terms of strength. The scanning electron micrograph presented in Figure 1 and thin sections show that the particles are well sorted, ranging from fine to coarse. The predominant presence of well developed hexagonal flaky kaolinite clay minerals is also revealed. Further, quantitative estimates from these studies show that it contains 40% quartz, 50% kaolinite and 10% muscovite mica.

*Jamrani Sandstone.* This sandstone is from the Jamrani Hydel Project, Uttar Pradesh, where a 145 m high dam across the Gola river is under construction. This isotropic sandstone belongs to the lower Siwaliks of the eastern Himalayas (Table 1). Its colour is grey to greenish grey. The scanning electron micrograph presented in Figure 1 and thin sections show that the sandstone consists of fine to coarse particles and is of varied sorting. The micas, especially muscovite and biotite, occur as well defined flakes and shreds in contact with the adjacent and more rigid quartz grains.

#### *Specimen Preparation*

For laboratory investigations, cylindrical cores 38 mm in diameter were obtained from rock blocks by use of diamond impregnated core drills. The base of the conventional laboratory drilling machine was fitted with a special frame to obtain specimens at different orientations ( $\beta = 0^\circ, 30^\circ, 65^\circ$  and  $90^\circ$ ). The cores were then cut and lapped to obtain specimens that met the tolerance limits suggested in ISRM (1981). The length to diameter ratio ( $l/d$ ) used for Brazilian tests was 0.5, whereas for axial and diametral point load strength tests, the ratio was 1. Uniaxial compressive strength tests were carried out on specimens with  $l/d = 2$ , to eliminate any effect of the specimen length on the strength and to decrease the possibility of buckling. After preparation, the specimens were first oven dried at  $105 \pm 1^\circ\text{C}$  for 24 h and cooled in a desiccator; while some specimens could be immediately tested for dry strength, some were soaked in water for 8 weeks before testing for saturated strength. Some others were equilibrated at particular relative humidities to achieve different moisture contents or degrees of saturation.

Aqueous solutions of sulphuric acid (LANGE, 1967) were used to maintain the relative humidities. The specimens were kept in air-tight desiccators of 250 mm diameter at desired humidities, (i.e. 0, 35, 60, 80, 95 and 100%) at a constant temperature of  $22 \pm 0.5^\circ\text{C}$  and equilibrated for at least 8 weeks. The equilibrium moisture contents were determined in grams of water per gram of dry rock. Simultaneously, the density of sulphuric acid in each desiccator was determined to obtain the relative humidity. The control of specimen saturation was made by periodic weighings. A specimen was usually considered to have reached a given degree of saturation when periodic weighings showed a constant weight for at least three consecutive days.

#### *Method of Determining Pore Water Pressures Under Partial Saturation*

As stated earlier, in a saturated rock under externally applied stresses, the pore water is subject to a hydrostatic pressure ( $\bar{u}_w$ ) due to its inability to drain

SANDSTONE STRENGTH

out and its incompressible nature. On the other hand, the pore water pressure will be negative in partially saturated rocks. Evaluation of negative pore water pressures is very tedious. With the conventional pore pressure apparatus, pressures less than minus 1 atmosphere cannot be measured, due to the cavitation of water in the measuring system at about this pressure. The axis-translation technique can only be applied when there is continuity in both the air and water phases, and this is only possible at a high degree of saturation. The only other viable alternative is to compute the value.

VENKATAPPA RAO & SRIDHARAN (1978) have given a method for evaluating negative pore water pressures using the classical capillary equation:

p = (2 T\_s cos theta) / r ..... (2)

where p = pressure deficiency in a pore of radius r,
T\_s = surface tension of fluid, and
theta = contact angle.

Negative pore water pressures can be computed using this equation if the pore size distribution of the material is known. The method of determining the pore size distribution of porous materials is outlined below.

Pore Size Distribution

Pore size distribution studies have become progressively more important in understanding the physico-chemical behaviour of porous materials. Three methods are reported in the literature to measure the pore size distribution: (i) the mercury injection method (WASHBURN, 1921; RITTER & DRAKE, 1945); (ii) the water vapour sorption method (BRUNAUER et al, 1967); and (iii) the resin impregnation method (PATSOULES & GRIPPS, 1982). Due to limitations in methods (i) and (iii) regarding their application to rocks, the water sorption method has been adopted in this study. This method involves the concept of capillary condensation in the pores. It is based on Kelvin's capillary condensation equation and the multi-layer adsorption theory of BRUNAUER et al (1948). Following BRUNAUER et al (1967), the pore volume and surface distributions are determined as functions of hydraulic radii. The hydraulic radius, r\_h, of a pore or a group of pores is defined as:

r\_h = V / S ..... (3)

where  $V$  = volume of pore or pore system, and  
 $S$  = surface area of pore walls.

This definition applies to pores of any shape. Values of  $V$  and  $S$  are obtained from adsorption or desorption isotherms. The details of the calculation methodology have been presented in detail by VENKATAPPA RAO & REKHI (1979).

#### *Testing Programme*

Physical properties such as water absorption, specific gravity, saturated and dry densities, absolute and effective porosities, and sonic wave velocity of four sandstones were determined. Uniaxial compression, Brazilian and point load strength tests (axial and diametral) were also carried out on dry, partially and fully saturated specimens. For each condition, more than four specimens were tested. Axial ( $\epsilon_a$ ) and diametral ( $\epsilon_d$ ) strains were measured in uniaxial compressive strength tests using 'Bakelite' backed electrical resistance strain gauges.

### TEST RESULTS

#### *General Characteristics of Sandstones*

Mean values of the physical properties of the rocks tested are presented in Table 3. It was observed that the Jhingurda Sandstone had the maximum porosity (36%) and water absorption (13.43%) among the four rocks tested, followed by the Singrauli and Kota sandstones. Jamrani Sandstone had the least porosity (6.4%) and water absorption (2.2%). Further, Jhingurda Sandstone exhibited the least sonic wave velocity in the dry state, confirming the earlier observation about its highly porous nature. For all four rocks, the sonic wave velocity is higher for saturated specimens than for dry specimens.

#### *Strength Indices*

The mean values of a minimum of four results of uniaxial compression, Brazilian, axial and diametral point load strength tests ( $\sigma_c$ ,  $\sigma_{lb}$ ,  $\sigma_{la}$  and  $\sigma_{ld}$ , respectively) are depicted in Table 4. It is evident from this table that the Kota Sandstone exhibits the highest strength, followed by the Jamrani and Singrauli sandstones, with the lowest being Jhingurda Sandstone. The variation in tangent modulus ( $E_t$ ) at 50% of ultimate strength for these rocks is similar to that observed in strength. The Poisson's ratio ( $\nu$ ) of these sandstones fall in a narrow range, varying from 0.21 to 0.29. The data, when presented

*SANDSTONE STRENGTH*

**Table 3. Physical Properties of Sandstones Tested.**

Rock Type	Water Absorption (%)	Specific Gravity	Density (g/cm <sup>3</sup> )		Porosity (%)		Sonic Wave Velocity (km/sec)	
			Dry	Saturated	Absolute	Effective	Dry	Saturated
Kota Sandstone	3.26	2.63	2.31	2.38	13.87	7.11	3.09	3.71
Singrauli Sandstone	6.64	3.20	2.31	2.46	26.65	16.69	2.43	2.77
Jhingurda Sandstone	13.34	2.63	1.67	1.93	36.30	25.19	1.90	1.99
Jamrani Sandstone	2.21	2.65	2.48	2.53	6.41	5.86	2.83	3.07



on DEERE & MILLER's (1966) chart, reveals that all four sandstones generally fall within the envelope proposed for arenaceous rocks. Using this chart, the classifications of the Kota, Jamrani, Singrauli and Jhingurda sandstones are CL, DL, DL and EM, respectively.

**Table 4. Typical Strength Index Properties of Sandstones Tested.**

Rock Type	Index Properties					DEERE & MILLER (1966) Classification	
	$\sigma_c$ (kg/cm <sup>2</sup> )	$\sigma_{tb}$ (kg/cm <sup>2</sup> )	$\sigma_{ta}(50)$ (kg/cm <sup>2</sup> )	$\sigma_{td}(50)$ (kg/cm <sup>2</sup> )	$E_t \times 10^5$ (kg/cm <sup>2</sup> )		$\nu$
Kota Sandstone	801.28	77.78	60.67	56.31	1.428	0.214	CL
Jamrani Sandstone	431.02	44.48	37.10	36.75	0.537	0.217	DL
Singrauli Sandstone	242.68	32.91	15.98	17.19	0.440	0.291	DL
Jhingurda Sandstone	58.13	12.68	6.11	5.20	0.290	0.250	EM

*Pore Size Distributions*

Figure 2 shows the adsorption isotherms (equilibrium water contents as a function of relative humidity) obtained for the four sandstones. These have been analysed using the method proposed by BRUNAUER et al (1967) and discussed previously.

The pore size distributions obtained are presented in Figure 3. In this figure, the volume desorbed is plotted as a cumulative curve, the volume decreasing from the largest pores on the right to the smallest pores on the left. The total pore volume is indicated by the horizontal bars on the ordinate, thus making obvious the extent to which pores have not been described by this procedure. For observing more clearly the differences in pore size distribution, the pore spectra are presented as bar charts in Figure 4.

From these figures, it is clearly seen that the pore sizes that could be conveniently measured with the present procedure range from 0.005 to 0.4  $\mu\text{m}$  (50 Å to 4000 Å) for these sandstones. It is clear from Figure 4 that in the Jamrani and Kota sandstones, pores of 0.1 to 0.4  $\mu\text{m}$  diameter are less whereas the pores of diameter 0.004 to 0.1  $\mu\text{m}$  are more in volume. In the case of the Singrauli and Jhingurda sandstones, pores of diameter greater than 0.4  $\mu\text{m}$  are more and those 0.004 to 0.1  $\mu\text{m}$  diameter are less in volume.



SANDSTONE STRENGTH

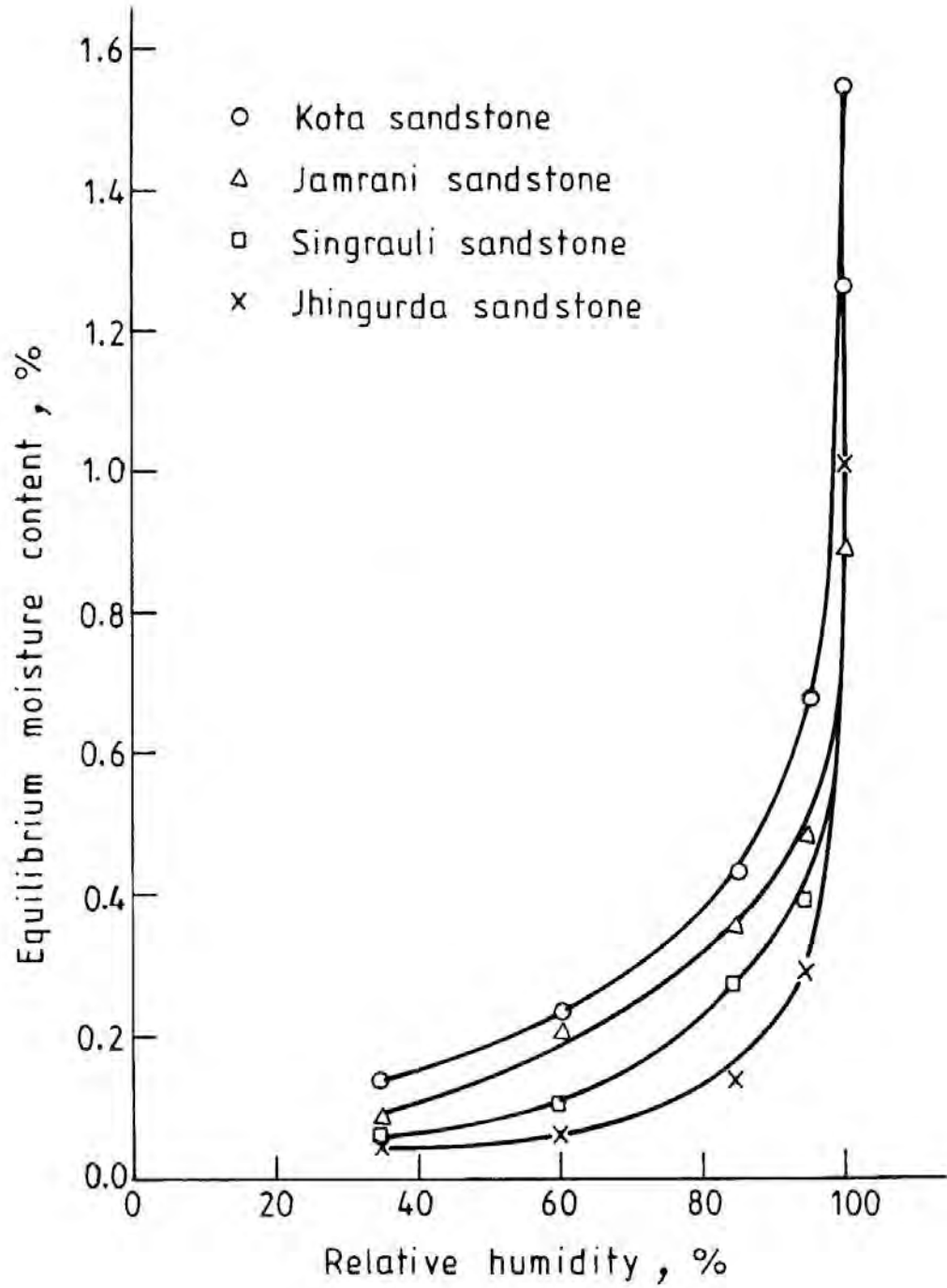


Fig. 2. Water Vapour Sorption Isotherms.

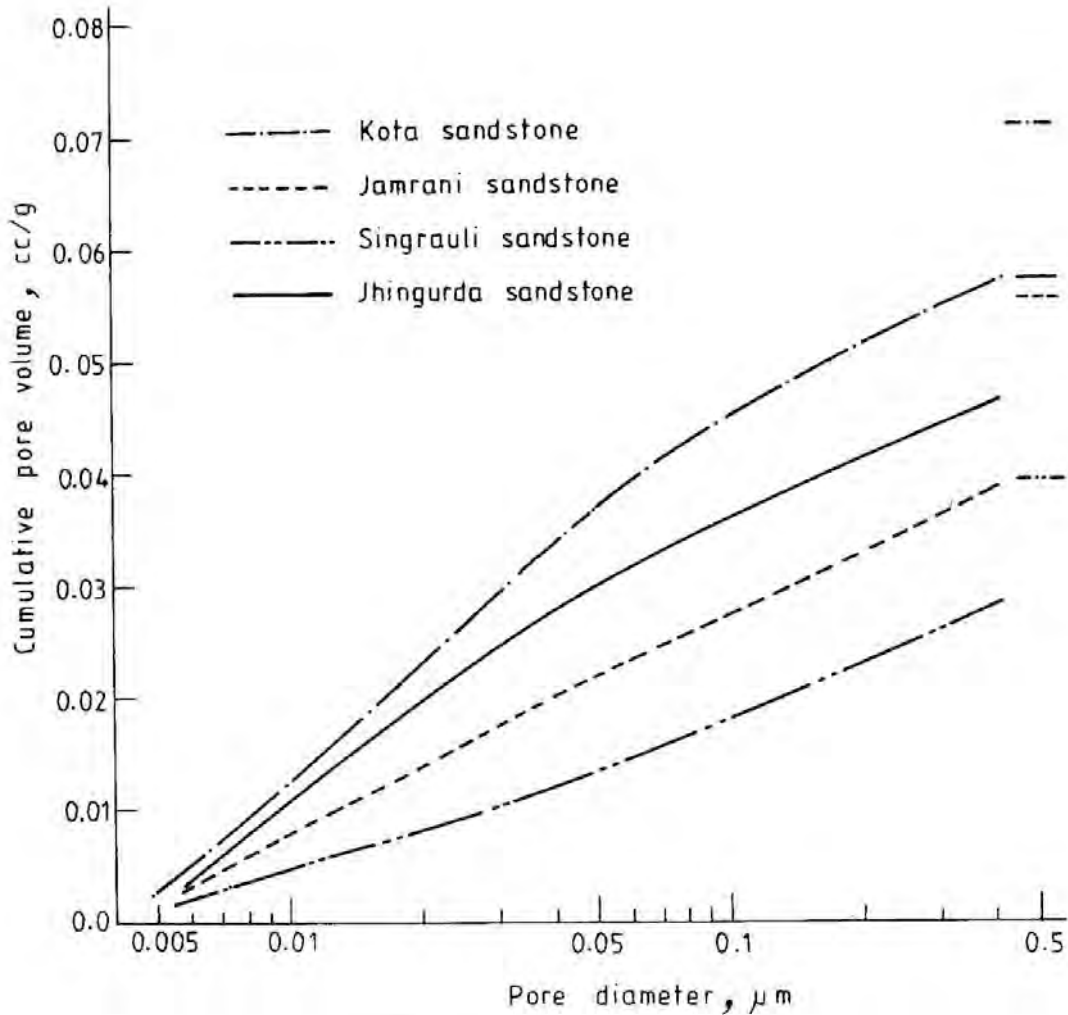


Fig. 3. Pore Size Distribution Curves.

*Effective Negative Pore Water Pressure*

As already discussed, the capillary model can be used for determining negative pore water pressures in rocks. Assuming cylindrical pores, the capillary pressure may be calculated by equation 2, with the value of the wetting angle ( $\theta$ ) assumed to be equal to zero, as in soil-water systems (AITCHISON, 1961; OLSON & LANGFELDER, 1965). At a constant temperature, surface tension ( $T_s$ ) for water is a constant. Hence, the capillary pressure is an inverse function of the pore radius. The effective pore diameter, i.e. the portion available for capillary pressure to act on, is the

112

**SANDSTONE STRENGTH**

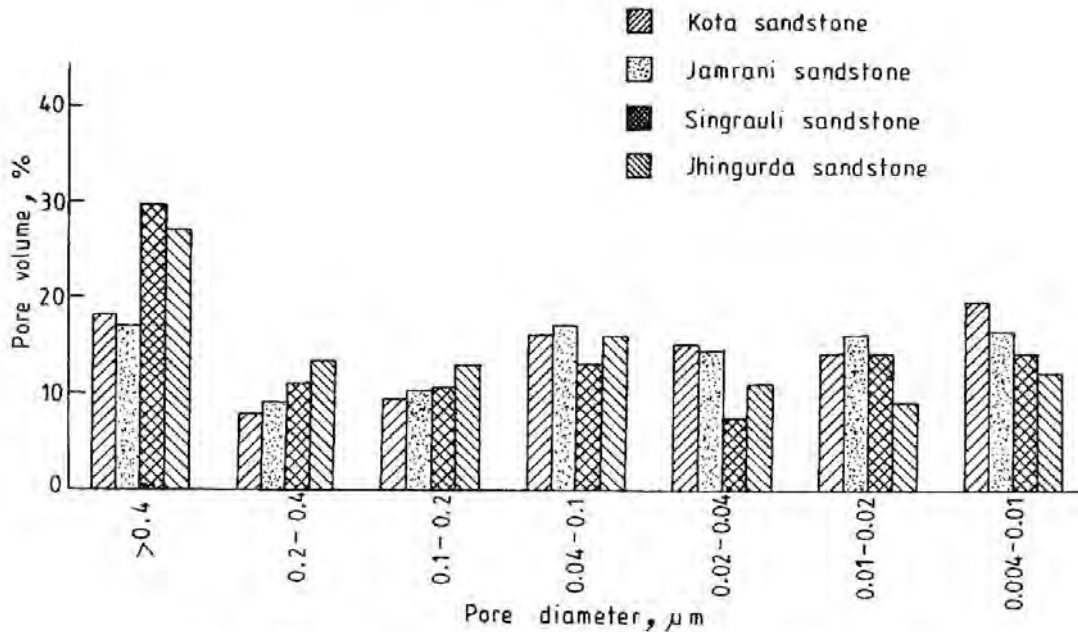


**Fig. 4. Pore Volume vs Pore Diameter for Sandstones Tested.**

diameter of the pore excluding the thickness of the adsorbed water. In this analysis, the thickness of the adsorbed water is obtained using a t-curve (HAGYMASSY et al, 1969), instead of assuming a constant thickness for the whole range of saturation.

The effective pore water pressure ( $\bar{u}_w$ ) can be determined only if the unit area through which the negative pore water pressure is transmitted between the minerals ( $a_w$ ) is known. This should be directly proportional to the percentage of the total pore volume that is filled with water at a particular water content, and since the relation between water content and percentage of filled pore volume is known,  $a_w$  can be calculated. Thus,

$$\begin{aligned}
 a_w &= \frac{\text{Pore volume filled at any water content}}{\text{Total pore volume}} \\
 &= \frac{\text{Total water content (cc)} - \text{Adsorbed water in unfilled pores (cc)}}{\text{Total pore volume}} \\
 &= \frac{V_w - V_{aw}}{V_v} = \frac{V_w}{V_v} - \frac{V_{aw}}{V_v} \\
 &= S_r - \frac{V_{aw}}{V_v} \dots\dots\dots (4)
 \end{aligned}$$

where  $S_r$  = degree of saturation.

The results of the computed effective negative pore pressures for the four sandstones are presented in Figure 5. The data indicate that there is an 'optimum' degree of saturation at which the effective negative pore pressure is a maximum. This maximum occurs when the product of  $a_w$  and the capillary pressure ( $p$ ) peaks. Thus, it is clearly dependent on the pore size distribution. It is also interesting to note that the maximum effective negative pore pressure decreases with an increase in void ratio. With a void ratio of 0.022, Jamrani Sandstone shows a maximum value of about 33.05 kg/cm<sup>2</sup>, whereas Jhingurda Sandstone with a void ratio of 0.128 exhibits a value of only 1.30 kg/cm<sup>2</sup>. The values for the other rocks vary between these two limits. It may be observed from Figure 5 that, for the Jamrani and Kota sandstones, the negative pore water pressure decreases rapidly with increasing moisture content, after an initial peak. The decreases in  $\bar{u}_w$  for Singrauli and Jhingurda sandstones are very much less. Since this approach takes into consideration the adsorbed water, and since adsorbed water is directly related to the surface area, the surface area of the rock is an important factor. This figure also shows that at high degrees of saturation, the magnitude of the effective negative pore water pressure is very small.

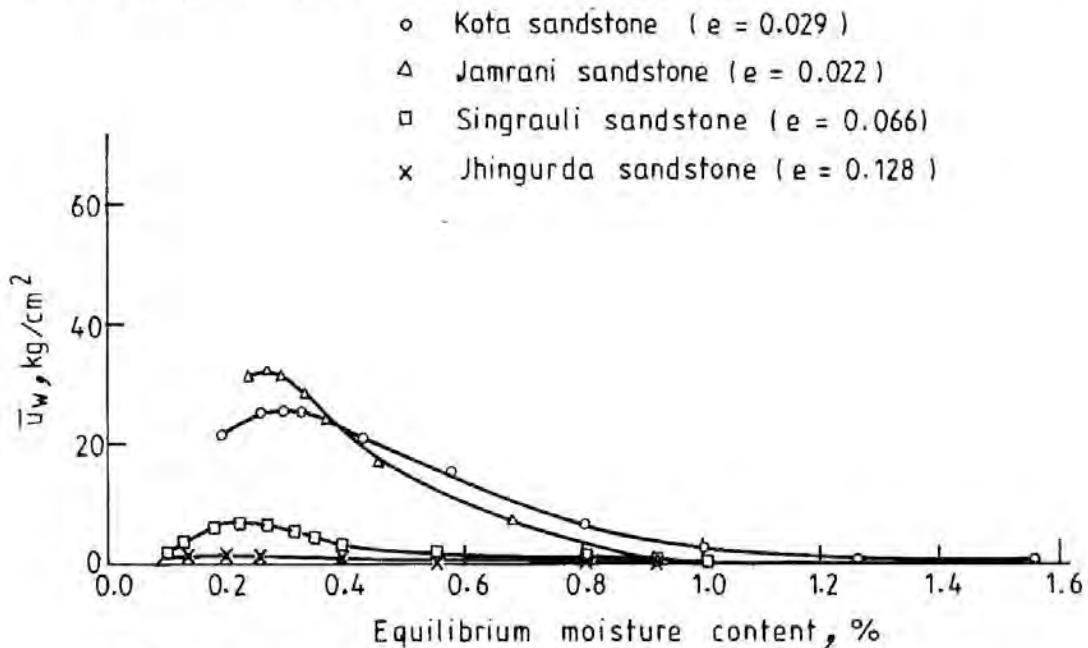


Fig. 5. Variation of Negative Pore Water Pressure with Moisture Content.

*Stress-Strain Behaviour*

Figure 6 shows typical stress-strain (axial and diametral) curves for Kota Sandstone at different relative humidities. It is seen that these curves are

SANDSTONE STRENGTH

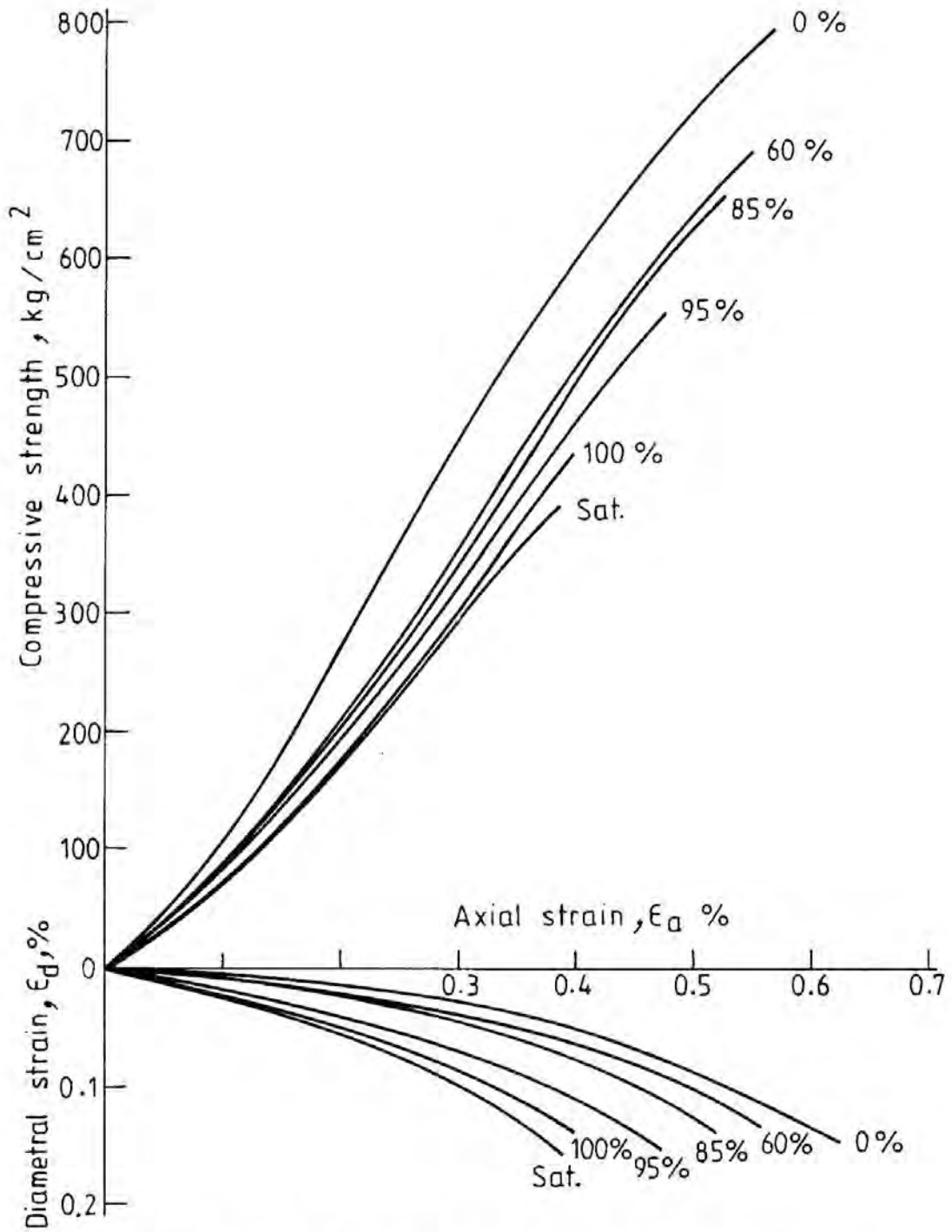


Fig. 6. Stress-strain Curves for Kota Sandstone at Different Humidities.

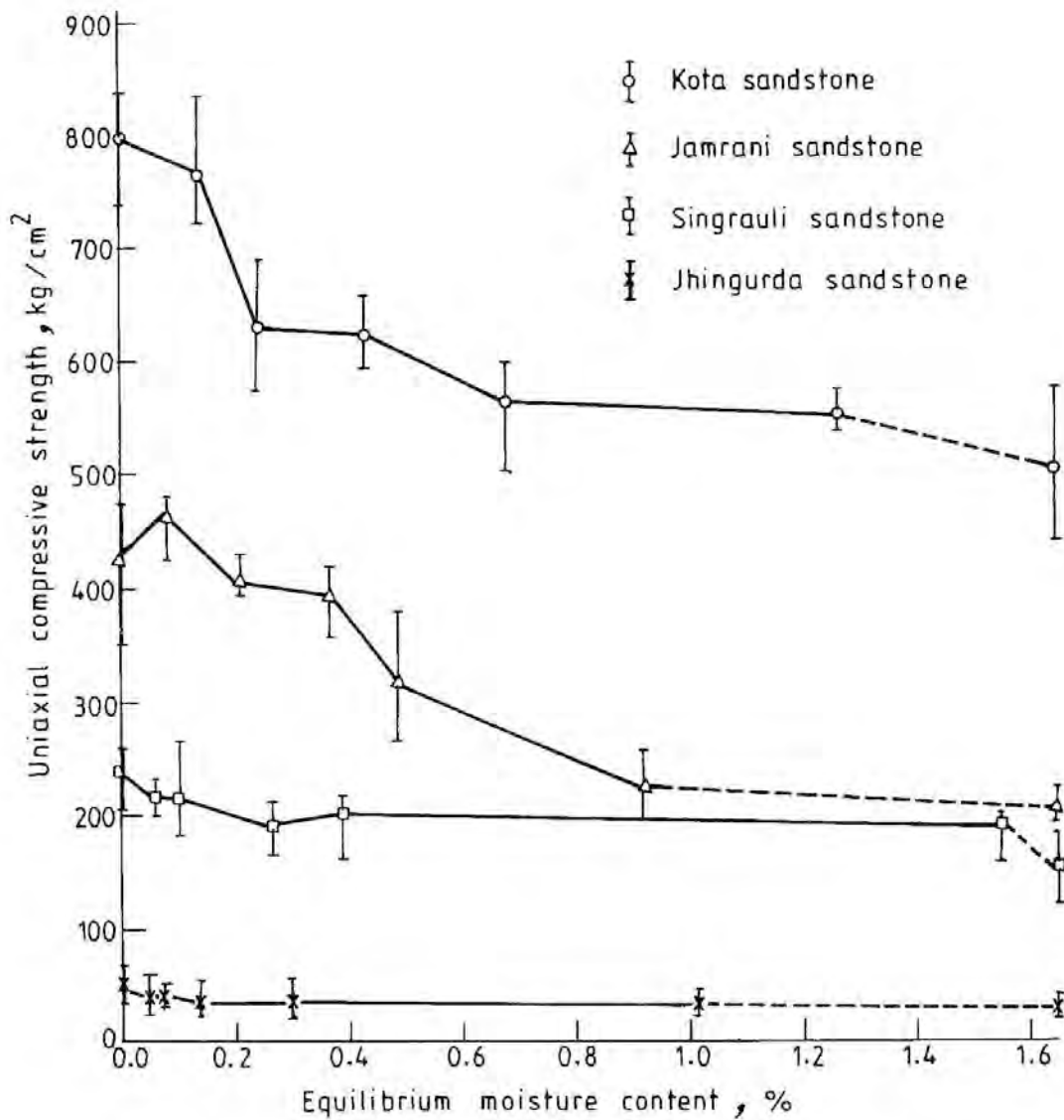


Fig. 7. Variation of Uniaxial Compressive Strength with Moisture Content.

nonlinear, with a concave upward portion up to about one quarter of peak strength. Similar behaviour was observed for the other three sandstones. In all cases, peak strengths decreased with an increase in moisture content, with the saturated condition giving the least strength.

The uniaxial compressive strengths for all four rocks tested at varying relative humidities are presented in Figure 7. The strengths of saturated specimens are also given at the right side of the figure. The vertical bars



### SANDSTONE STRENGTH

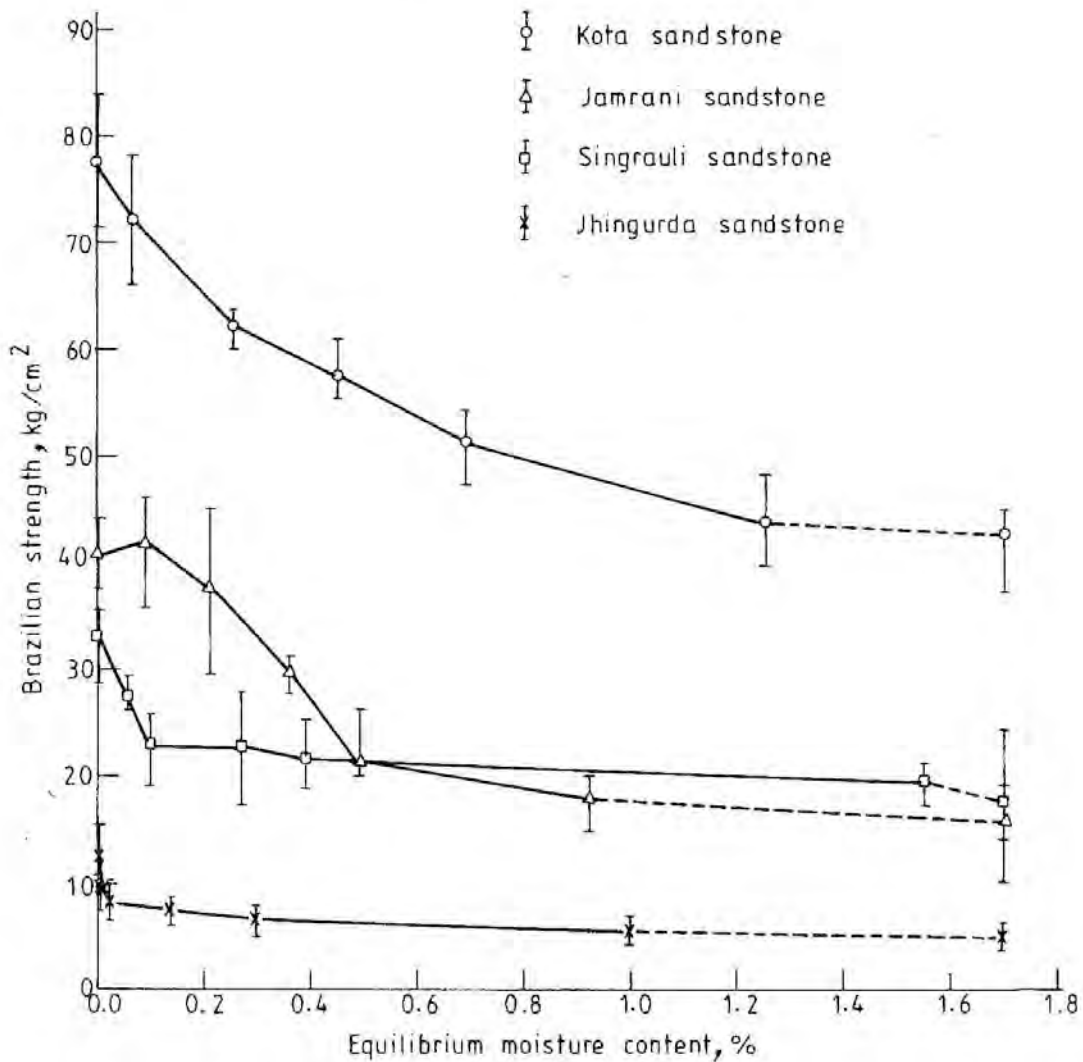


Fig. 8. Variation of Brazilian Strength with Moisture Content.

show the extent to which a variation of strength occurs at each humidity. At a given relative humidity, the maximum strength is exhibited by the Kota Sandstone, followed by the Jamrani and Singrauli Sandstones, with the least for the Jhingurda Sandstone. Jamrani Sandstone shows the steepest decrease in compressive strength with increasing equilibrium moisture content. By comparing the values of the dry and saturated uniaxial compressive strengths, it can be seen that saturation causes a reduction in strength of 52, 48, 37 and 33% for the Jamrani, Jhingurda, Kota and Singrauli Sandstones, respectively. This variation falls within the range observed by earlier investigators (PRICE, 1960; COLBACK & WIID, 1965; VAN EECKHOUT, 1976).

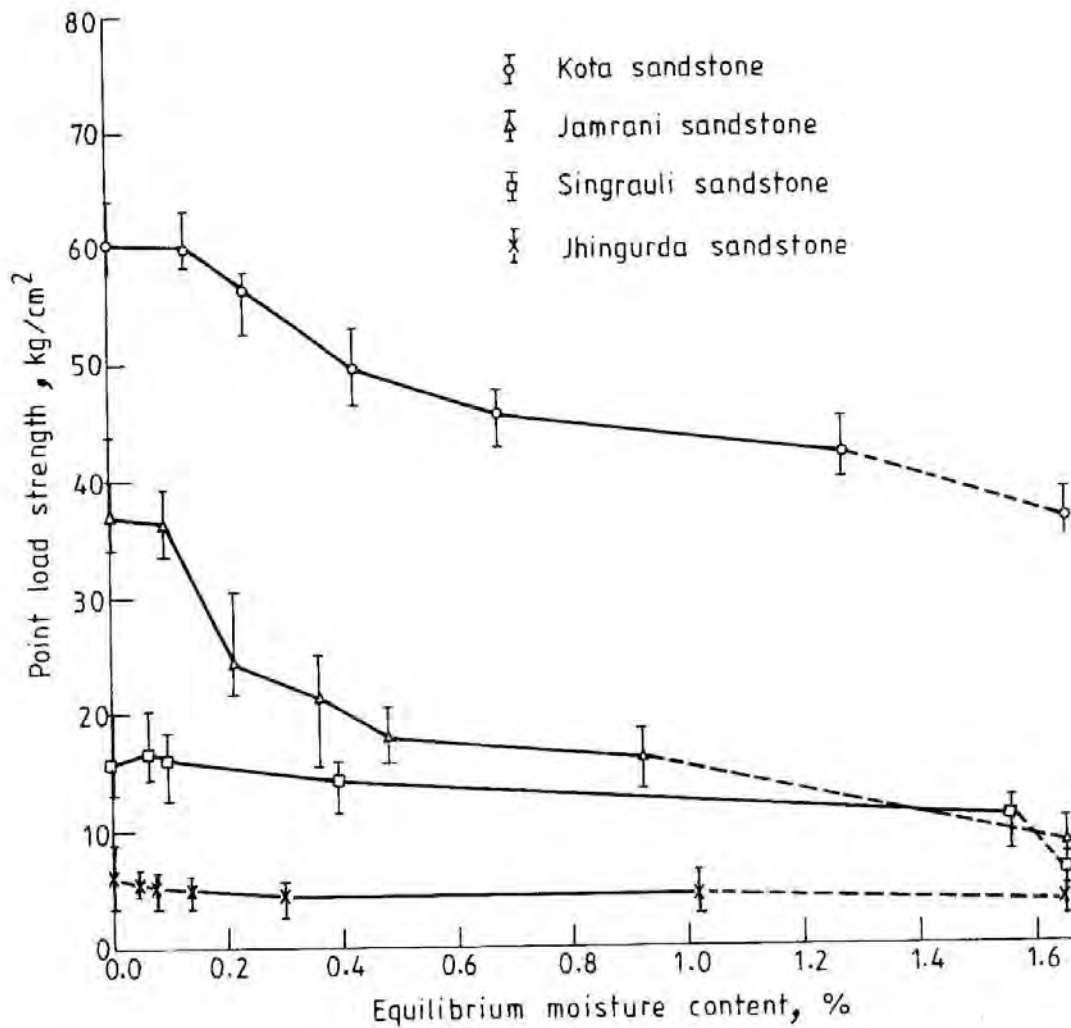


Fig. 9. Variation of Axial Point Load Strength with Moisture Content.

Close scrutiny of Figure 7 reveals that, whereas the variation in strength is minor beyond an equilibrium moisture content of 0.6%, the changes up to 0.6% are quite significant. While there appears to be a general increase in strength on reduction of moisture content below this limit, the actual variation seems to depict certain second order peaks. For instance, the Kota and Jamrani sandstones appear to show second order peaks around an equilibrium moisture content of 0.4%, and for the other two rocks this value is 0.1%.

The variation in Brazilian strength with equilibrium moisture content is shown in Figure 8 for all the sandstones. Similar variations in axial and diametral point load strength indices are presented in Figures 9 and 10.

### SANDSTONE STRENGTH

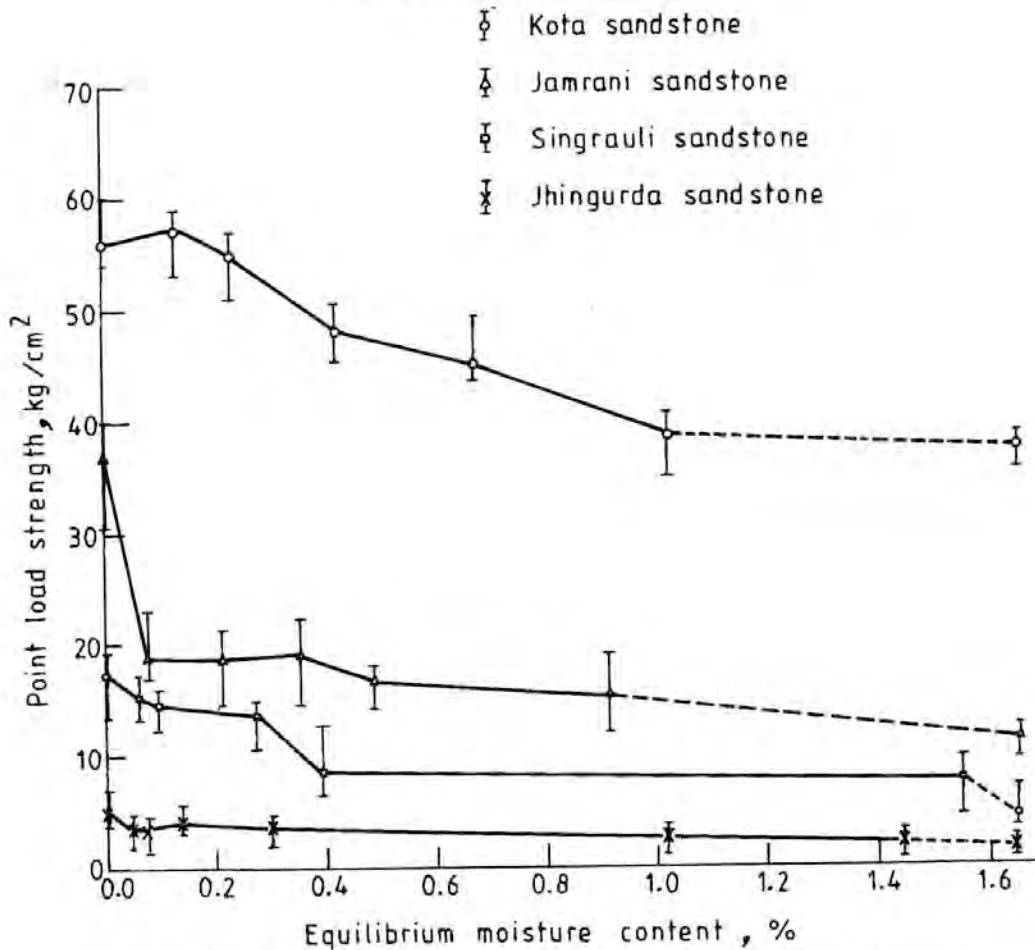


Fig. 10. Variation of Diametral Point Load Strength with Moisture Content.

In general, it is seen that the decrease in strength is rather sharp up to a moisture content of about 0.4%, and from there onwards the decrease is gradual (a phenomenon already observed in the uniaxial compressive strength). Furthermore, in all these cases the reduction on saturation is greatest for the Jamrani Sandstone, followed by the Jhingurda Sandstone. The second order peaks mentioned in the case of the uniaxial compressive strength are again evident, particularly in Figure 10 (diametral point load strength).

#### Elastic Constants

Values of modulus of elasticity ( $E_t$ ) and Poisson's ratio ( $\nu$ ) calculated at 50% of failure stress are given in Table 5 for all the rocks tested at different humidities. It is shown that  $E_t$  decreases with an increase in water content,

giving a minimum under saturated condition for all sandstones. The variation of Poisson's ratio with relative humidity is not as uniform as  $E_t$ , but in general, there is an increase in  $\nu$  with an increase in relative humidity.

Table 5. Variation of  $E_t$  and  $\nu$  with Humidity for the Sandstones Tested.

Relative Humidity (%)	Kota Sandstone		Jamrani Sandstone		Singrauli Sandstone		Jhingurda Sandstone	
	$E_t \times 10^5$ (kg/cm <sup>2</sup> )	$\nu$	$E_t \times 10^5$ (kg/cm <sup>2</sup> )	$\nu$	$E_t \times 10^5$ (kg/cm <sup>2</sup> )	$\nu$	$E_t \times 10^5$ (kg/cm <sup>2</sup> )	$\nu$
0	1.5304	0.0784	0.546	0.2857	0.440	0.1364	0.3053	0.1316
35	1.8250	0.1250	0.546	0.2461	0.4583	0.1250	0.2174	0.1087
60	1.1896	0.1034	0.4106	0.2500	0.4255	0.1489	0.1864	0.1818
85	1.1123	0.1579	0.3879	0.4697	0.3654	0.1154	0.1842	0.1579
95	1.0370	0.2407	0.3539	0.4444	0.4250	0.1542	0.2100	0.3000
100	0.9505	0.2667	0.3193	0.4386	0.3091	0.2545	0.1524	0.2400
Saturated	0.9091	0.3182	0.2724	0.5345	0.2633	0.3167	0.1154	0.2309

## DISCUSSION OF RESULTS

### *Mechanisms of Strength Reduction*

From the effective stress equation (equation 1), two parameters are stated to be responsible for the changes in rock strength that occur with variations in moisture content (apart from stresses due to externally applied loads), as discussed below.

*Negative Pore Water Pressure.* The pore water pressure in unsaturated rocks is negative, the variation of which has already been presented in Figure 5 for the rocks under study. It should be borne in mind that curves such as those presented in Figure 5 were obtained after making several assumptions regarding the shape of pores, the continuity of pore structure and the physico-chemical nature of the rock surface before fracture. Due to this, one can at best use these curves in a qualitative way for comparison purposes.

*Inter-Particle Forces/Surface Energy.* It was brought out in the literature review that the interparticle forces (electrical attractive and repulsive forces) can be visualised as arising from two components. The primary component is due to mineralogy and/or cementing material, which may be taken as constant for a given rock type. The other component arises from surface forces. An increase in equilibrium moisture content is known to result in

**SANDSTONE STRENGTH**

a decrease in surface energy. The surface energy of dry sandstone may be assumed to be the same as that of quartz, 640 erg/cm<sup>2</sup> (BRACE & WALSH, 1962), which on exposure to a relative humidity of 100%, reduces to 240 erg/cm<sup>2</sup> (BOYD & LIVINGSTONE, 1942). From Griffith's crack theory, strength is expected to be a function of  $(E\gamma)^{\frac{1}{2}}$  and assuming that the reduction in surface energy is proportional to the change in relative humidity, a computation can be made to verify the validity of Griffith's concept. In such an analysis, one may include the variations that arise in E due to changes in moisture content.

In the following, a critical appraisal is made of the influence of the change in pore water pressure and surface energy on the strength of rocks.

From the dry state up to a moisture content of 0.1%, it can easily be concluded that surface energy forces dominate strength mobilization, because there is not yet enough water in the specimen to cause any negative pore water pressure. The sharp decrease in strength with moisture content commonly observed in this range can thus be attributed to a change in surface energy such as seen in the typical curves of  $(\gamma/\gamma_{dry})^{\frac{1}{2}}$  in Figure 11 (see also

**Table 6. Test Results for Kota Sandstone.**

Property	Relative Humidity (%)						
	0	35	60	85	95	100	Saturated
Moisture content (%)	0	0.137	0.238	0.427	0.677	1.264	2.992
$\sigma_c$ (kg/cm <sup>2</sup> )	801.28	750.60	633.40	625.90	564.30	554.60	544.20
$E_t \times 10^5$ (kg/cm <sup>2</sup> )	1.5304	1.825	1.1896	1.1123	1.0370	0.9505	0.9091
$\gamma_{dry}$ (erg/cm <sup>2</sup> )	640	595	565	505	425	240	—
$(\gamma/\gamma_{dry})$	1.0	0.929	0.883	0.789	0.664	0.375	—
$(E\gamma/E_{dry} \gamma_{dry})$	1.0	1.108	0.686	0.574	0.449	0.233	—
$(\sigma_c/\sigma_{c \text{ dry}})$	1.0	0.937	0.790	0.781	0.704	0.692	0.679
$(\sigma_{tb}/\sigma_{tb \text{ dry}})$	1.0	0.973	0.832	0.772	0.691	0.584	0.571
$(\sigma_{ta}/\sigma_{ta \text{ dry}})$	1.0	1.006	0.943	0.825	0.760	0.708	0.613
$(\sigma_{td}/\sigma_{td \text{ dry}})$	1.0	1.012	0.977	0.852	0.799	0.684	0.675
$(\gamma/\gamma_{dry})^{0.5}$	1.0	0.964	0.939	0.888	0.815	0.612	—
$(\gamma/\gamma_{dry})^{0.45}$	1.0	0.968	0.945	0.899	0.832	0.643	—
$(E\gamma/E_{dry} \gamma_{dry})^{0.5}$	1.0	1.053	0.828	0.757	0.671	0.483	—
$(E\gamma/E_{dry} \gamma_{dry})^{0.3}$	1.0	1.032	0.893	0.846	0.787	0.646	—

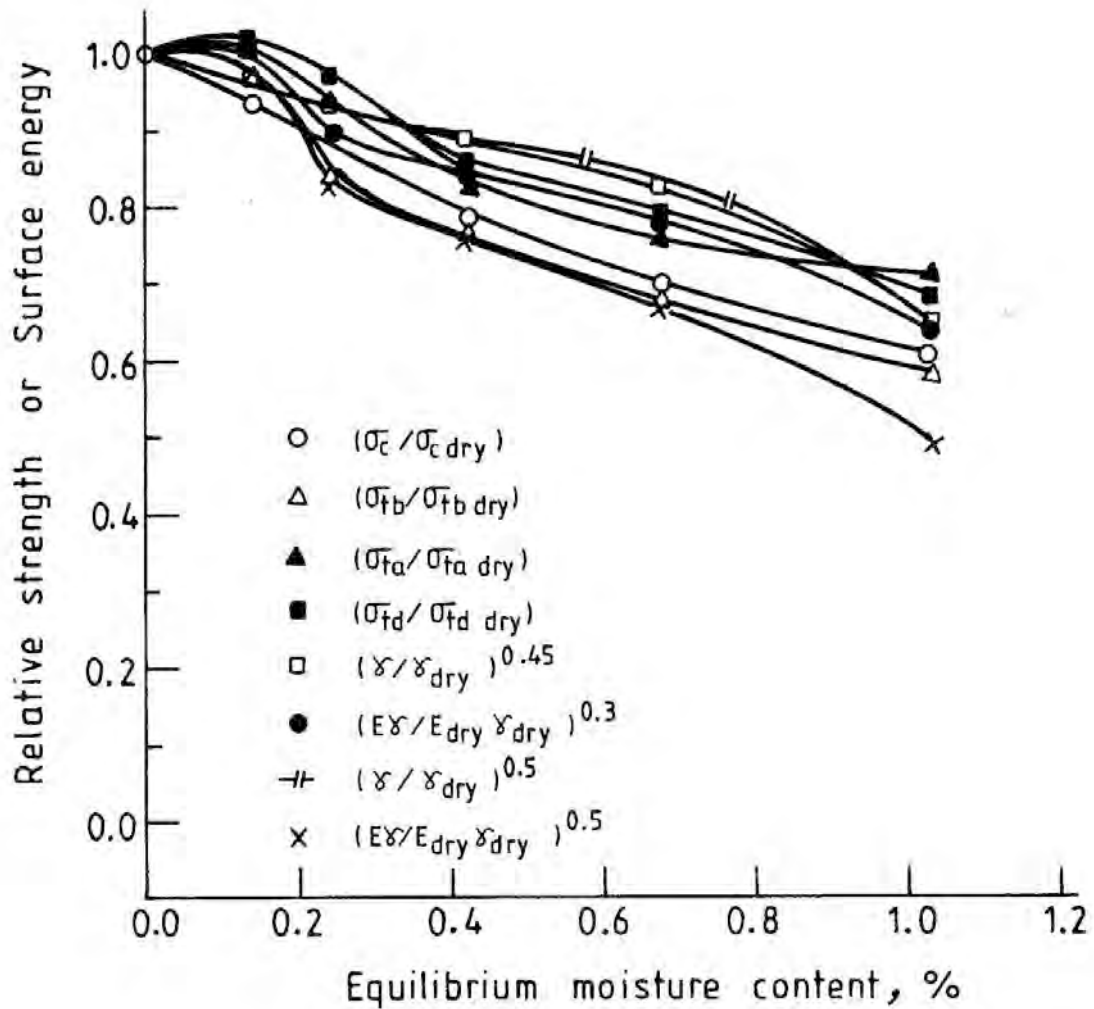


Fig. 11. Variation of Relative Strength or Surface Energy with Moisture Content for Kota Sandstone.

Table 6). Beyond this limit, both surface energy and negative pore pressure come into play. Because of a continuous decrease in the value of  $v$ , and the typical variation of  $\bar{u}_w$  (showing a peak around moisture content of 0.2%), the variation in strength can easily be expected to follow the trend already



## SANDSTONE STRENGTH

observed. This expectation is further reinforced by the observation that the second order peaks in the strength variation nearly match with the observed peaks in  $\bar{u}_w$ . A reasonably good match is observed in the diametral point load index and the uniaxial compressive strength.

Figure 11 presents the variation of  $(\gamma/\gamma_{dry})^{\frac{1}{2}}$  and  $(E\gamma/E_{dry}\gamma_{dry})^{\frac{1}{2}}$  with equilibrium moisture content, along with the variations in the relative strength indices  $(\sigma_c/\sigma_{c\ dry})$ ,  $(\sigma_{tb}/\sigma_{tb\ dry})$ ,  $(\sigma_{ta}/\sigma_{ta\ dry})$  and  $(\sigma_{td}/\sigma_{td\ dry})$ , for Kota Sandstone. It appears that while the variation with moisture content in all cases is of the same nature, there does not seem to be any agreement between predicted and observed variations. However, by changing the exponent 0.5 (as obtained from Griffith's theory) to other values, better matching is possible. Figure 11 presents curves for exponents of 0.45 and 0.30 for  $(\gamma/\gamma_{dry})$  and  $(E\gamma/E_{dry}\gamma_{dry})$ , respectively. Similar computations have also been made for the remaining three rocks, with results similar to the Kota Sandstone. A summary of the exponents chosen for reasonably good correlation between experimental and predicted results is given in Table 7. This table reveals that the exponents differ with rock type, but seem to be related to the strength reduction which occurs on saturation.

**Table 7. Optimal Exponents for Sandstones Tested.**

Exponent 'n' value	Rock Type			
	Jamrani Sandstone	Jhingurda Sandstone	Kota Sandstone	Singrauli Sandstone
$(\gamma/\gamma_{dry})^n$	0.71	0.70	0.45	0.30
$(E\gamma/E_{dry}\gamma_{dry})^n$	0.25	0.41	0.30	0.17
$(\sigma_{c\ sat}/\sigma_{c\ dry}), \%$	52	48	37	33

### SUMMARY AND CONCLUSIONS

A detailed experimental programme was carried out on four types of sandstone to determine strength changes with a variation in moisture content. It was observed that the strength in all test modes, as well as the modulus of elasticity, decreased with an increase in moisture content with saturated specimens yielding the smallest values.

These changes in engineering properties with moisture content has been evaluated from a physico-chemical view point using the effective stress concept. This concept has been used to demonstrate the unification of the

existing strength reduction mechanisms. The major changes which occur in rock with an increase in moisture are, firstly, changes in negative pore pressure, and secondly, changes in interparticle forces/surface energy. By analysing water vapour adsorption isotherms, the pore size distributions of the rocks have been estimated. From these, negative pore pressures were computed. It has also been shown that a net decrease in electrical forces/surface energy occurs with increases in moisture content up to saturation.

Starting from the dry condition, with increases in moisture content, the negative pore pressure initially exhibits a peak and then shows a drastic reduction, whereas surface energy steadily decreases. Accordingly, the strength variation is the resultant or combination of these two factors although the relative contributions are difficult to ascertain. However, close scrutiny of both the variations of negative pore pressure and strength with moisture content has clearly revealed the zones wherein pore pressure does seem to be significant. The initial drastic reduction in strength that occurs between 0 and about 0.2% moisture content is seen to be solely caused by decreased surface energy (which decreases steadily with moisture content). Furthermore, strength is expected to be a function of  $(E\gamma)^{0.5}$  from Griffith's crack theory. Assuming that the reduction in surface energy is proportional to the change in relative humidity, a computation has been made of the variation of  $(E\gamma)^{0.5}$ . These variations have been compared with actual strength changes, and though there is broad agreement, the matching has been poor. On the other hand, by changing the exponent of this quantity to other values, better correlations have been obtained. Interestingly, these exponents were found to be a function of rock type.

#### REFERENCES

- AITCHISON, G.D. (1961). Relationships of Moisture Stress and Effective Stress Functions in Unsaturated Soils. *Proceedings of the Conf. on Pore Pressure and Suction in Soils*, London, p. 150.
- BOOZER, G.D., HILLER, K. & SERDENGECTI, S. (1962). Effects of Pore Fluids on the Deformation Behaviour of Rocks Subjected to Triaxial Compression. *Proc. of the 5th Symp. on Rock Mech.*, Pergamon, pp. 579-625.
- BOYD, G.E. & LIVINGSTON, H.K. (1942). Adsorption and the Energy Changes at Crystal-line Solid Surfaces. *J. Am. Chem. Soc.*, vol. 64, pp. 2383-2388.
- BRACE, W.F. & WALSH, J.B. (1962). Some Direct Measurements of the Surface Energy of Quartz and Orthoclase. *Am. Mineralogist*, vol. 47, pp. 1111-1122.
- BROCH, E. (1979). The Influence of Water on some Rock Properties. *Third Int. Cong. of the Int. Soc. Rock Mech.*, Denver, vol. IIA, pp. 33-38.
- BROCH, E. & FRANKLIN, J.A. (1972). The Point Load Strength Test. *Int. J. Rock Mech. and Min. Sci.*, vol. 9, pp. 669-697.

## SANDSTONE STRENGTH

- BRUNAUER, S., EMMETT, P.H. & TELLER, E. (1948). Adsorption of Gases in Multimolecular Layers. *J. Am. Chem. Soc.*, vol. 60, pp. 309-319.
- BRUNAUER, S., MIKHAIL, R.S.H. & BODOR, E.E. (1967). Pore Structure Analysis without a Pore Shape Model. *J. Colloid and Interface Science*, vol. 24, pp. 451-463.
- CHAMBERLAIN, P.G., NECKHOUT, & PODNIEKS, E.R. (1976). Four Factors Influencing Observed Rock Properties. *Soil Specimen Preparation for Laboratory Testing, ASTM STP 599*, pp. 21-36.
- COLBACK, P.S. & WIID, B.L. (1985). Influence of Moisture Content on the Compressive Strength of Rocks. *Proc. 3rd Canadian Symp. Rock Mech.*, Toronto, pp. 65-83.
- DEERE, D.U. & MILLER, R.P. (1966). Engineering Classification and Index Properties for Intact Rock. *Tech. Rept. No. AFWL-TR-65-116*, Air Force Weapons Lab., New Mexico.
- FEDA, J. (1966). The Influence of Water Content on the Behaviour of Sub-Soil Formed by Highly Weathered Rocks. *Proc. 1st Cong. Int. Rock Mech.*, Lisbon, vol. 1, pp. 283-288.
- HAGYMASSY, J., BRUNAUER, S. & MIKHAIL, R.S.H. (1969). Pore Structure Analysis of Water Vapour Adsorption, 1-t Curves for Water Vapour. *J. Colloid and Interface Science*, vol. 29, pp. 483-491.
- HANDIN, J., HAGER, R.V., FRIEDMAN, M. & FEATHER, J.N. (1963). Experimental Deformation of Sedimentary Rocks under Confining Pressure : Pore Pressure Effects. *Bull. Am. Assoc. Petrol. Geol.*, vol. 47, pp. 717-755.
- HEARD, H.C. (1960). Transition from Brittle Fracture to Ductile Flow in Solenhofen Limestone as a Function of Temperature, Confining Pressure, and Interstitial Fluid Pressure. *Rock Deformation*, Griggs & Handin (Eds.), Geol. Soc. Am., Memoir 79, pp. 193-226.
- ISRM(1981). *Rock Characterisation, Testing and Monitoring*, Brown, E.T. (Ed.), Pergamon Press, Oxford, pp. 211.
- JAEGER, J.C. (1966). Brittle Fracture of Rocks. *8th Symp. Rock Mech. on Failure and Breakage of Rock*, Univ. Minnesota, pp. 3-57.
- LAMBE, T.W. (1960). A Mechanistic Picture of Shear Strength of Clay. *Proc. of the Res. Conf. on Shear Strength of Cohesive Soils, ASCE*, Colorado, pp. 555-580.
- LANGE, N.A. (ed.) (1967). *Handbook of Chemistry*. McGraw-Hill, New York, p. 1435.
- OLSON, R.E. & LANGFELDER, L.J. (1965). Pore Water Pressures in Unsaturated Soils. *J. Soil Mech. Found. Div., ASCE*, vol.91, SM 4, pp. 127-150.
- PATSOULES, M.G. & CROPPS, J.C. (1982). The Application of Resin Impregnation to the 3-dimensional Study of Chalk Pore Geometry. *Engng. Geol.*, vol.19, pp. 15-27.
- PRICE, N.J. (1960). The Compressive Strength of Coal Measure Rocks. *Collieray Engineering*, vol. 37, pp. 283-292.
- PUGH, S.F. (1967). The Fracture of Brittle Material. *Br. J. Appl. Phys.*, vol. 18, pp. 129-162.
- RAMAMURTHY, T. & GOEL, S.C. (1973). Strength of Sandstones in Triaxial Compression. *Proc. of the Symp. Rock Mech. & Tun. Prob.*, Kurukshetra, vol. 1, pp. 204-209.
- RITTER, H.L. & DRAKE, L.C. (1945). Pore-size Distribution of Porous Materials. *Industrial and Engineering Chemistry, Anal. Ed.*, vol.17, no.12, pp. 782-786.
- RAO, K.S. (1984). *Strength and Deformation Behaviour of Sandstones*. Ph.D. Thesis, Indian Institute of Technology, Delhi, 279 p.
- RAO, K.S., RAO, G.V. & RAMAMURTHY, T. (1981). Effect of Moisture on Strength of Intact Rocks. *Proceedings of GEOMECH-81*, Hyderabad, vol. 1, pp. 245-254.

- SKEMPTON, A.W. (1961). Effective Stresses in Soils, Concrete and Rocks. *Conf. on Pore Pressure and Suction in Soils*, London, pp. 4-16.
- SRIDHARAN, A. (1968). *Some Studies on the Shear Strength of Partly Saturated Clay*. Ph.D. Thesis, Purdue Univ., Indiana, USA.
- SRIDHARAN, A. & RAO, G.V. (1973). Mechanisms Controlling Volume Change of Saturated Clays and the Role of the Effective Stress Concept. *Geotechnique*, vol. 23, pp. 359-382.
- SRIDHARAN, A. & VENKATAPPA RAO, G. (1971). Effective Stress Theory of Shrinkage Phenomena. *Can. Geotech. J.*, vol. 8, pp. 503-513.
- SRIDHARAN, A. & RAO, G.V. (1979). Shear Strength Behaviour of Saturated Clays and the Role of the Effective Stress Concept. *Geotechnique*, vol.29, no.2, pp.177-193.
- TERZAGHI, K. (1936). The Shearing Resistance of Saturated Soils. *Proc. 1st Int. Conf. Soil Mech. Found. Engg.*, vol.1.
- VAN EECKHOUT, E.M. (1976). The Mechanism of Strength Reduction due to Moisture in Coal Mine Shales. *Int. J. Rock Mech. Min. Sci and Geomech. Abstr.*, vol. 13, pp. 61-67.
- VENKATAPPA RAO, G. & SRIDHARAN, A. (1978). Strength Behaviour of Partially Saturated Clays. *Proc. Conf. on Geotech. Engg.*, New Delhi, vol.1, pp. 124-129.
- VENKATAPPA RAO, G. & REKHI, T.S. (1979). Pore Structure Analysis of a Silt with Additives. *Ind. Geotech. J.*, vol.9, pp. 328-343.
- VENKATAPPA RAO, G., PRIEST, S.D. & KUMAR, S.S. (1983). *Effect of Moisture on Strength of Intact Rocks and the Role of Effective Stress Principle*. Project Report, I.I.T., Delhi, p. 62.
- VUTUKURI, V.S., LAMA, R.D. & SALUJA, S.S. (1974). *Handbook on Mechanical Properties of Rocks, Vol. I-IV*, Trans. Tech. Publications.
- WASHBURN, E.W. (1926). *International Critical Tables of Numerical Data, Physics, Chemistry Technology*. McGraw-Hill, New York.
- WIID, B.L. (1970). The Influence of Moisture in the Pre-rupture Facturing of two Rock Types. *Proc. II Cong. Int. Soc. Rock Mech.*, Belgrade, vol.2, pp. 239-245.

APPENDIX — NOTATION

A	net inter-particle electrical attractive forces
$a_m$	mineral-to-mineral unit contact stress
$\bar{\sigma}_c$	effective contact stress
E	modulus of elasticity
$E_t$	modulus of elasticity at 50% of ultimate stress
e	void ratio
$\gamma$	surface energy
R	net inter-particle electrical repulsive forces
r	pore radius
$r_h$	hydraulic radius
n	exponent
t	thickness of adsorbed water film

### *SANDSTONE STRENGTH*

$u$	pore pressure
$u_a$	pore air pressure
$u_w$	pore water pressure
$\bar{u}_w$	effective pore water pressure
$\bar{u}_a$	effective pore air pressure
$V_v$	volume of voids
$V$	volume of the pore or pore system
$\nu$	Poisson's ratio
$\epsilon_a$	axial strain
$\epsilon_d$	diametral strain
$\sigma_c$	uniaxial compressive strength
$\sigma_{ta}$	axial point load strength
$\sigma_{tb}$	Brazilian strength
$\sigma_{td}$	diametral point load strength
$\sigma$	normal stress
$\bar{\sigma}$	mineral -to-mineral contact stress
$S$	surface area of pore walls
$S_r$	degree of saturation

---

## ERRATUM

---

Page 235, Volume 17, Number 2 (December 1986) should begin as follows :

MODEL PILE SKIN FRICTION IN CALCAREOUS SAND

H.G. POULOS & K.F. CHAN

The Printer apologises for This error.



---

## CONFERENCE NEWS

---

**6th International Conference on Structural Design of Asphalt Pavements**, Ann Arbor, Michigan, July 13-16, 1987. All enquiries to : G.W. Ring III, Transportation Research Board, 2101 Constitution Avenue N.W., Washington D.C. 20418, U.S.A.

**VIII Asian Regional Conference on Soil Mechanics and Foundation Engineering**, Kyoto, Japan, July 20-24, 1987. All enquiries to : 8ARC SMFE, c/o Kyoto International Conference Hall, Takara-ike, Sakyo-ku, Kyoto, 606, Japan.

**International Workshop on Constitutive Equations for Granular Non-Cohesive Soils**, Cleveland, Ohio, July 22-24, 1987. All enquiries to : Prof. A.S. Saada, Dept. of Civil Engineering, Case Western Reserve University, University Circle, Cleveland, Ohio 44106, U.S.A.

**Erosion and Sediment Transport in Pacific Rim Mountainous Lands**, Corvallis, Oregon, August 3-7, 1987. All enquiries to : College of Forestry, Oregon State University, Corvallis, Oregon 97331, U.S.A.

**Geotechnical Engineering of Soft Soils**, Mexico City, Mexico, August 12-13, 1987. All enquiries to : Manuel J. Mendoza, Instituto de Ingenieria-Unam, Apdo, Postal 70-472, 04510, Mexico.

**4th International Conference on Low-Volume Roads**, Ithaca, New York, August 16-20, 1987. All enquiries to : N.F. Hawks, Transportation Research Board, 2101 Constitution Avenue N.W., Washington D.C. 20418, U.S.A.

**8th Panamerican Conference on Soil Mechanics and Foundation Engineering**, Cartagena, Colombia, South America, August 16-21, 1987. All enquiries to : J. Montero-Olarte, P.O. Box 057045, Bogota, D.E. Columbia.

**6th International Congress on Rock Mechanics**, Montreal, Canada, August 30-September 3, 1987. All enquiries to : ISRM Congress 1987, 400-1130 Sherbrooke St. W., Montreal, H3A 2M8, Quebec, Canada.

**Ninth European Conference on Soil Mechanics and Foundation Engineering**, Dublin, Ireland, August 31-September 3, 1987. All enquiries to : Dr. Trevor Orr, Secretary General, IX ECSMFE, Civil Engineering Department, Trinity College, Dublin, 2, Ireland.

**Carboniferous Stratigraphy and Geology**, Beijing, China, August 31-September 4, 1987. All enquiries to : Prof. Yang Jing-zhi, Nanjing Institute of

Geology and Palaeontology, 39 East Beijing Road, Chi-Ming-Ssu, Nanjing, P.R. China.

**International Symposium on Terminal Precambrian and Cambrian Geology**, Yichang, China, September 8-14, 1987. All enquiries to : Dr Wang Xiao-feng, Yichang Institute of Geology and Mineral Resources, P.O. Box 502, Yichang City, Hubei Province, P.R. China.

**Engineering Geology of Underground Movements**, Nottingham, UK, September 13-17, 1987. All enquiries to : Dr. F.G. Bell, Alwinton, Blyth Hall, Blyth, Notts S81 8HL, U.K.

**The Origin of Granites**, Edinburgh, Scotland, September 14-16, 1987. All enquiries to : The Royal Society of Edinburgh, 22-24 George Street, Edinburgh EH2 2PQ, Scotland, U.K.

**9th African Regional Conference on Soil Mechanics and Foundation Engineering**, Lagos, Nigeria, September 15-18, 1987. All enquiries to : 9 ARC, Nigerian Geotechnical Association, P.O. Box 2100, Lagos, Nigeria.

**Fourth International Conference on Polypropylene Fibers and Textiles**, Nottingham, U.K., September 23-25, 1987. All enquiries to : M.D. Shuttleworth, The Plastics and Rubber Institute, 11 Hobart Place. London SW1W 0HL, U.K.

**Exploration '87**, Toronto, Canada, September 27- October 1, 1987. All enquiries to : Exploration '87, c/o 222 Snidercroft Rd, Conford, Ontario L4K 1B5, Canada.

**Microcomputer Applications to Geotechnique**, Regina, Saskatchewan, October 22-23, 1987. All enquiries to : D. Charleson, Saskatchewan Highways and Transportation, 1855 Victoria Avenue, Regina, Saskatchewan S4P 4V5, Canada.

**Second International Conference on Education, Practice and Promotion of Computational Methods in Engineering using Small Computers**, Guangzhou, China, November 27 - December 1, 1987. All enquiries to : Secretariat EPMESC, c/o Office of Foreign Affairs, South China Institute of Technology, Guangzhou, (Canton), China.

**Sixth International Conference on Expansive Soils**, New Delhi, India, December 1-3, 1987. All enquiries to : Mr K.R. Saxena, Central Board of Irrigation and Power, Malcha Marg, Chanakyapuri, New Delhi 110021, India.

**9th Southeast Asian Geotechnical Conference**, Bangkok, Thailand, December 7-12, 1987. All enquiries to : 9th SEAGC, c/o Division of Geotechnical and

Transportation Engineering, Asian Institute of Technology GPO Box 2754, Bangkok 10501, Thailand.

**Asian Mining '88**, Kuala Lumpur, Malaysia, March 8-11, 1988. All enquiries to : The Institution of Mining and Metallurgy, 44 Portland Place, London W1N 4BR, England.

**Sixth International Conference on Numerical Methods in Geomechanics**, Innsbruck, Austria, April 11-15, 1988. All enquiries to : ICONMIG 88, Kongresshaus Innsbruck, Rennweg 3, A-6020 Innsbruck, Austria.

**Tunnelling '88**, London, England April 17-22, 1988. All enquiries to : The Institution of Mining and Metallurgy, 44 Portland Place, London W1N 4BR, England.

**International Conference on Centrifuge Testing**, Paris, France, April 25-27, 1988. All enquiries to : Mr J.F. Corte, c/o Laboratoire Central des Ponts et Chausees, Centre de Nant B.P. 19, Bouguenais, France.

**4th International Conference on Tall Buildings**, Hong Kong and Shanghai, China, April/may 1988. All enquiries to : P. Lee, Department of Civil and Structural Engineering, University of Hong Kong, Hong Kong.

**Second International Conference on Case Histories in Geotechnical Engineering**, St. Louis, Missouri, June 1-3, 1988. All enquiries to : S. Prakash, Civil Engineering Department, University of Missouri-Rolla, Rolla, Missouri 65401-0249, U.S.A.

**Penetration Testing in The UK 1988**, Birmingham, UK, July 6-8, 1988. All enquiries to : Mrs. P.J. Ross, Institution of Civil Engineers, 1-7 Great George Street, London SW1P 3AA, U.K.

**Vth International Symposium on Landslides**, Lausanne, Switzerland, July 10-15, 1988. All enquiries to : Cristophe Bonnard, P.O. Box 83, CH-1015, Lausanne 15, Switzerland.

**ASCE Specialty Conference on Hydraulic Fill Structures**, Fort Collins, Colorado, August 7-10, 1988. All enquiries to : W.D. Carrier III, Bromwell & Carrier, Inc., P.O. Box 5467, Lakeland, Florida, U.S.A.

**International Conference on Engineering Problems on Regional Soils**, Beijing, China, August 11-15, 1988. All enquiries to : Mr. Du Xibin, China Civil Engineering Society, P.O. Box 2500, Beijing, China.

**Fifth ANZ Conference on Geomechanics**, Sydney, Australia, August 22-26,

1988. All enquiries to : Prof. H.G. Poulos, School of Civil and Mining Engineering, The University of Sydney, Sydney 2006, Australia.

**International Geotechnical Symposium on Theory and Practice of Earth Reinforcement**, Fukuoka City, Japan, October, 1988. All enquiries to : Prof. N. Miura, Dept. of Civil Engineering, Saga University, Saga 840, Japan.

**28th International Geological Congress**, Washington D.C., U.S.A., July, 1989.

**12th International Conference on Soil Mechanics and Foundation Engineering**, Rio de Janeiro, Brazil, 1989. All enquiries to : P.A. Neme, Associacao Brasileira de Mecanica dos Sols, P.O. 7141. Sao Paulo 01000, SP, Brazil.

---

## ANNOUNCEMENTS

---

### **Eighth Asian Regional Conference on Soil Mechanics and Foundation Engineering**

The Eighth Asian Regional Conference on Soil Mechanics and Foundation Engineering will be held in Kyoto, Japan, July 20-24, 1987. The object of the conference is to provide an opportunity for engineers and scientists working in the field of soil mechanics and foundation engineering to meet and present new ideas, achievements and experiences. There will be a special emphasis on practical applications, and papers dealing with engineering practice. The conference themes are the following:

- 1) Development of theory and practice in geotechnical engineering
- 2) Problems of regional soils
- 3) Soil dynamics and geotechnical aspects of earthquake engineering
- 4) Tunneling and excavation in soils
- 5) Deep and shallow foundations
- 6) Embankments and slope stability

The official languages of the conference will be English and Japanese. Simultaneous translation will be provided for oral presentations. The papers submitted should, however, be written in English. All correspondence regarding the conference should be directed to:

T. Adachi, Secretary of the 8th ARCSMFE  
Kyoto International Conference Hall  
Takara-ike, Sakyo-ku, Kyoto 606  
JAPAN

During the week preceding the conference a short course on "Construction in Soft Ground" will be held at the Kobe Convention Center in Kobe, Japan on July 17-18, 1987.

### **Ninth Southeast Asian Geotechnical Conference**

The Ninth SEAGC is to be held December 7-12, 1987 at Bangkok, Thailand in conjunction with the 20th anniversary celebration of the Southeast Asian Geotechnical Society. The Conference theme is "Geotechnical Engineering in Southeast Asia" with specific emphasis on:

- (i) Engineering Behaviour of Soils and Rocks
- (ii) Site Investigation and Insitu Tests



- (iii) Ground Improvement
- (iv) Shallow and Deep Foundations
- (v) Settlement of Structures
- (vi) Earth and Earth Supported Structures

Papers relating to this theme are invited. Summaries of papers, not exceeding 300 words in length, should be sent to the Hon. Secretary by July 30, 1986. All enquiries should be addressed to:

The Hon. Secretary, 9th SEAGC,  
c/o Division of Geotechnical &  
Transportation Engineering,  
Asian Institute of Technology,  
P.O. Box 2754  
Bangkok 10501,  
Thailand.

## **XII International Conference on Soil Mechanics and Foundation Engineering**

The Brazilian Society of Soil Mechanics, on behalf of the International Society of Soil Mechanics and Foundation Engineering, takes pleasure in inviting the members of the International Society, their companions, and others who are interested, to attend the XII International Conference on Soil Mechanics and Foundation Engineering to be held in Rio de Janeiro, Brazil in 1989. Bulletins containing information on conference themes, submission of papers, and the conference program will be distributed through the National Societies during the 1986-1989 period. The official languages of the International Society are English and French. At all sessions, simultaneous translation will be provided in English and French. An interesting and exciting social program is being organized. The official travel agent is preparing packages with the purpose of offering to the participants the opportunity to see some of the most interesting attractions of Brazil. In connection with the conference, an exhibition will be arranged to display recent developments in geotechnical engineering equipment and techniques. Brazil is a country of continental dimensions with an area of more than 8.5 million square kilometers. Its population is over 130 million. Rio de Janeiro was founded in 1565 and served as the capital of Brazil from 1763 to 1960 when the seat of government moved to Brasilia. More information can be obtained from:

Organizing Committee  
XII ICSMFE, Caixa Postal 1559  
2000 Rio de Janeiro, RJ  
BRAZIL



## **Golden Jubilee Commemorative Volume of the Southeast Asian Geotechnical Society**

**Geotechnical Engineering in Southeast Asia**, a commemorative volume of the Southeast Asian Geotechnical Society, is now available from Balkema Publishers. This volume contains 11 contributions from Southeast Asia ranging from the behaviour of piles in soft organic clays to landslides and their control. It also includes bibliographies of books, journals, conference publications, theses, etc (c. 2,200 titles) and a directory of consultants and contractors in Southeast Asia. This 352 page document (US\$ 40) can be obtained from:

A.A.Balkema Book Distributors  
P.O. Box 1675, NL-3000 BR Rotterdam  
Netherlands

## **General Committee Members of SEAGS**

The Governing Committee of the Southeast Geotechnical Society for the period 1985-1987 is as follows:

Prof. A.S. Balasubramaniam (President)  
Dr. Ting Wen Hui (Immediate Past President)  
Dr. E.W. Brand (Past President)  
Dr. Za-Chieh Moh (Founder President)  
Dr. Tan Swan Beng (Past President)  
Prof. Chin Fung Kee (Past President)  
Mr. D.R. Greenway (Editor)  
Prof. Seng Lip Lee  
Mr. G.W. Lovegrove  
Dr. Ooi Teik Aun  
Mr. Yu Cheng  
Mr. Jose Rolando R. Santos

## **SEAGS Newsletter**

All correspondence related to the SEAGS Newsletter should be addressed to:

Southeast Asian Geotechnical Society  
c/o Division of Geotechnical and Transportation Engineering,  
Asian Institute of Technology,  
P.O. Box 2754  
Bangkok, Thailand 10501.

## SI UNITS AND SYMBOLS

The following list of quantities, SI (Système International) units and SI symbols, are recommended for use in Geotechnical Engineering.

Quantities	Units	Symbols
Length	kilometre	km
	metre	m
	millimetre	mm
	micrometre	$\mu\text{m}$
Area	square kilometre	$\text{km}^2$
	square metre	$\text{m}^2$
	square millimetre	$\text{mm}^2$
	cubic metre	$\text{m}^3$
Volume	cubic millimetre	$\text{mm}^3$
	tonne	t
Mass	kilogramme	kg
	gramme	g
	tonne per cubic metre	$\text{t/m}^3$
Density $\rho$ (mass density)	kilogramme per cubic metre	$\text{kg/m}^3$
Unit weight $\gamma$ (weight density)	kilonewton per cubic metre	$\text{kN/m}^3$
	Force	MN
Pressure	kilonewton	kN
	newton	N
	megapascal	MPa
	kilopascal	kPa
Energy	megajoule	MJ
	kilojoule	kJ
	joule	J
	Coefficient of volume compressibility or swelling $m_v$	1/megapascal
1/kilopascal		$\text{kPa}^{-1}$
Coefficient of consolidation or swelling $c_v$	square metre per second	$\text{m}^2/\text{s}$
	square metre per year	$\text{m}^2/\text{year}$
Hydraulic conductivity $k$ (formerly coefficient of permeability)	metre per second	$\text{m/s}$

NOTES: The term specific gravity is obsolete and is replaced by relative density. The former term relative density  $(e_{\text{max}} - e)/(e_{\text{max}} - e_{\text{min}})$  is replaced by the term density index,  $I_D$ .